2017

Density-Dependent Foraging in Caenorhabditis Elegans

Joshua Greene

DENSITY-DEPENDENT FORAGING IN *CAENORHABDITIS ELEGANS*

A Thesis Presented to the Faculty of

The Rockefeller University

in Partial Fulfillment of the Requirements for

the degree of Doctor of Philosophy

by

Joshua S. Greene

June 2017

DENSITY-DEPENDENT FORAGING IN *CAENORHABDITIS ELEGANS*

Joshua S. Greene, Ph.D.

The Rockefeller University 2017

Game theory has long predicted that the density of competitors and their behaviors should affect foraging, and moreover suggests that multiple strategies can evolve and co-exist within a single species. I show that both of these predictions are met by foraging *Caenorhabditis elegans*. In Chapter 2, I show that animals alter their foraging behavior in response to population density, that certain pheromones induce this behavioral change, and that different wild isolates vary in response to the potent ascaroside icas#9. I use QTL mapping to find a major locus responsible for this variation, and map it to an icas#9 receptor, *srx-43.* Reduced expression of this gene in the sensory neuron ASI contributes to naturally occurring insensitivity to icas#9. Remarkably, I find that the QTL falls in a high-diversity region that exists in two distinct haplotypes in *C. elegans* populations around the world. This pattern of diversity is consistent with a locus under balancing selection, and through competition experiments, I show that indeed the two haplotypes result in differential fitness depending on icas#9 and food distribution. In Chapter 3, I extend these findings by showing that a second chemoreceptor, *srx-44,* is also a component of the initial QTL. A gain-in-function in *srx-44* contributes to reduced icas#9 sensitivity in the wild isolates that have reduced expression of *srx-43*. Through the use of transgenic animals and

CRISPR/Cas9-mediated mutagenesis, I identify a polymorphism in the promoter of this gene causing increased expression in the sensory neuron ASJ, in which *srx-44* acts to suppress icas#9 response. In Chapter 4, I examine pheromone regulation of foraging behavior in animals lacking specific neurotransmitters or neurotransmitter receptors. This screen identified GABA as broadly necessary for ascaroside-suppression of roaming. Through cell specific rescue and inhibition experiments, I show that GABA release from the unpaired AVL neuron is both necessary and sufficient for this behavior. Taken together, these experiments provide insight into the genetics and neural circuitry underlying social communication and foraging behavior.

ACKNOWLEDGEMENTS

My years in graduate school have been some of the most fun and happy years of my life. I am grateful for having had the opportunity to think about neuroscience and conduct experiments under the guidance of a brilliant mentor and amongst a caring community. I am deeply indebted to this support.

Over the years, I have grown a deeper appreciation of Dr. Cori Bargmann's capacity as a scientist and as a mentor. I came into the lab aware of her ability to lead thorough, thoughtful, and creative research projects. I have since become aware that her contribution to neuroscience far exceeds this. One essential talent is her ability to identify patterns across wide ranging experiments throughout the lab and the field at large; from these patterns emerge general principles by which genes and neural circuits operate. Importantly, Cori also invests heavily in the future of science, going to great lengths to teach future generations of scientists including myself. It was comforting knowing that Cori's door was always open. She was consistently around – even often late at night or on the weekend – to help analyze data, design experiments, and provide encouragement after failures. In addition to all of this, Cori has fostered a collegial and curious laboratory environment full of many wonderful postdocs and students.

Two postdocs in the laboratory have been instrumental in shaping my thesis. Dr. Steven Flavell took me on when I was a rotation student in the lab, and continued to guide me throughout the early years of my graduate work. His grace as an experimentalist continues to astound me - his experiments were so

well thought out, that any result inevitably was informative. He didn't seem to waste a movement. I still aspire to design experiments in Steve, and thankfully have learned a lot from working with him. Dr. Patrick McGrath not only influenced the thoughts behind my project - first bringing to my awareness the fingerprints balancing selection left throughout the genome and that were enriched in our QTL, but he also provided essential assistance analyzing the genomic data and conducting the QTL analysis. These were fields of science that I had absolutely no experience in, but thanks to Patrick, I now feel comfortable navigating.

One great benefit of the collaborative approach to science of the Bargmann lab has been our relationship to Dr. Rebecca Butcher, who initially identified icas#9, the pheromone at the center of this thesis project. Not only has Dr. Butcher facilitated analysis of icas#9 production by wild strains, but she has synthesized all the ascarosides that we have used to conduct our assays.

I would like to thank my thesis committee, Dr. Songhai Shi, Dr. Shai Shaham, and Dr. Marc Tessier-Levigne, for taking the time to critically assess my thesis at regular points throughout this project, asking challenging question, and providing essential direction. In addition, I am grateful for Dr. Matt Rockman's participation on my thesis committee as the external examiner.

I am thankful for a great network of friends both within and outside of the laboratory environment. Among the lab, I have enjoyed sharing a bay with Margaret Ebert and Alejandro Lopez, and working adjacent to Xin Jin. The conversations we have had about science and otherwise have made my time in the laboratory fly by. Outside of the laboratory, friends including Dahlia Perez,

Juliet Zhang, Brian Haley, Andrew Levine, and Josh Salvi, have provided support in rough times and added to the joy in good times.

Finally, I would like to thank my family. My parents, Les, Judy, and Norm, and also, Isaac, Sarah, Lincoln and Quinn, who have helped make these last few years such a great experience.

TABLE OF CONTENTS

LIST OF FIGURES

LIST OF TABLES

Chapter 1:
Introduction

Chemosensation, the ability to detect chemicals in the environment, is essential to all living organisms. Yet despite its ancient origins, the molecular basis of chemosensation is not universal and instead varies dramatically among different organisms. In contrast with opsins, a superfamily of light-sensitive proteins found in all animals possessing sight[1], chemoreceptors are diverse and whole superfamilies of chemosensors have been gained and lost repeatedly over evolution. Within a given species, chemoreceptor genes typically belong to families and superfamilies that diversify; chemoreceptors undergo duplication and pseudogenization rapidly compared to other genes[2,3]. Moreover, the number of distinct chemoreceptor proteins within a species tends to far surpass the number of primary receptor proteins in other sensory systems. The vast and shifting repertoire of chemoreceptors can be understood through their function. Whereas light differs primarily in frequency and amplitude, chemicals have countless shapes and properties. Moreover, the chemicals needing detection change as most are produced by organisms that evolve themselves. Diverse and dynamic chemical signals necessitate an equally complex and evolvable molecular basis for detection. The evolvability of chemoreceptors underlies their importance as a target of natural selection, facilitating the development of ever-changing sensory capacities and behaviors.

One indication of the diversity and rapid evolution of chemoreceptor genes is the number of chemoreceptor superfamilies that have evolved from distinct precursors. We are likely only aware of a subset of the chemoreceptor

superfamilies that exist, as a new superfamily has just been discovered in mice[4], an extensively characterized model organism. Moreover, there may be undiscovered chemoreceptors that are not members of easily identified large superfamilies[5]. Further shrouding the identification of chemoreceptors is that many are expressed where you would not expect them: Some estimates place the expression of as many as 20% of chemoreceptors in tissues besides chemosensory neurons[2,6-9]. One such unusual site is the gut, where chemoreceptors regulate endocrine systems in response to food intake[10]. From what we do know about chemoreceptors, it is clear that they have evolved repeatedly. For instance, nematodes, insects, and vertebrates use entirely distinct classes of genes for the detection of volatile odors, which likely reflects these branches of life leaving the ocean and confronting airborne chemicals on separate occasions[2]. Clearly nature possess a striking capacity to evolve chemosensors from many molecular starting points.

Chemosensors also demonstrate high levels of variation within each superfamily of receptor genes. One example of this variation is the changes in the number of odorant receptors across species. Mice have approximately 900 odorant receptor genes, while humans only have approximately 350[11]. In some cases, large changes in odorant receptor number are associated with changes in habitat or behavior that suggest explanations. For instance, humans and Old World monkey have evolved trichromatic color-vision systems; these primates also have low numbers of presumed functional chemoreceptors, and genomic evidence suggests that purifying selection has been relaxed on many of the

chemoreceptors that remain. This paring leads to the hypothesis that increased reliance on vision could underlie the decreased number of odorant receptors in primates[3,12], although other explanations can be made. One alternative hypothesis is that with higher brain function, a greater olfactory ability can be achieved with a smaller number of odorant receptors[3,13]. We currently lack empirical evidence that can strongly differentiate between these possibilities. A more plausible connection can be drawn between the reductions in odorant receptor numbers with the return of land animals to aquatic or semi-aquatic life, as volatile odors do not exist underwater. Both toothed whales and platypuses have lost many odorant receptors[3,14-18]. Interestingly, in both of these cases, the changes in lifestyle are also associated with the advent or major retooling of a sensory system: whales have developed echolocation, and platypuses rely on a special sense in their bills that combines electroreception and mechanoreception[19]. These examples demonstrate the broad flexibility of sensory systems and their importance as targets of evolutionary change.

Even within species, there can be considerable variation in odorant receptors. *Caenorhabditis elegans* possess 22 families of chemoreceptor genes comprising 8 distinct superfamilies (Table 1). The reference genome has approximately 1,300 chemoreceptors and about 400 related “pseudogenes” (Table 1) [20]. However, most of these pseudogenes have just one apparent defect, suggesting that they may have only recently been lost in the reference genome. An analysis of 31 of these pseudogenes revealed that at least 10 have functional alleles in one or more wild *C. elegans* isolate[21]. What selective

pressures could underlie such dynamic within-species variation in chemoreceptors? The gray pawn hypothesis provides one possible explanation[20]. It suggests that individually chemoreceptors are insignificant and can be lost with little consequence, but that as a group, chemoreceptors are required to cover a broad ligand space. Thus while selection does not strongly maintain any single chemoreceptor, selective pressure creates a large and diverse repertoire of chemoreceptors through duplication and elaboration countering the effect of pseudogenization. An alternative possibility is that selection is acting on many of these chemoreceptor genes individually, driving their loss in some lines and preservation in others. Although this hypothesis entails selective pressures acting on hundreds of chemoreceptors that vary within a population, some findings support this alternative to the gray pawn hypothesis. In unpublished work, our collaborator Dr. Patrick McGrath has shown that regions of the genome containing chemoreceptors are disproportionately likely to have a very high or a very low Tajima's D score, indicating that genetic intervals containing chemoreceptors are likely to be under balancing or positive selection respectively.

Table 1-1 *C. elegans* chemoreceptor families

Superfamily	Family	Genes	Pseudogenes	%pseudogenes
str	*srh*	217	91	30
	str	192	75	28
	sri	60	18	23
	srd	64	12	16
	srj	39	18	32
	srm	5	1	17
	srn	1	0	0

Table 1-1 (cont.) *C. elegans* chemoreceptor families

Superfamily	Family	Genes	Pseudogenes	%pseudogenes
	all Str	578	215	27
sra	*sre*	51	5	9
	sra	32	7	18
	srab	22	5	19
	srb	14	5	26
	all Sra	119	22	16
srg	*srx*	94	44	32
	srt	59	15	20
	srg	59	9	13
	sru	39	9	19
	srv	30	6	17
	srxa	17	2	11
	all Srg	298	85	22
Solo	*srw*	100	45	31
Solo	*srz*	64	39	38
Solo	*srbc*	71	13	15
Solo	*srsx*	37	3	8
Solo	*srr*	9	1	10
	total	1276	423	25

adapted from[22]

Another compelling example of active selection that violates the gray pawn hypothesis involves the chemoreceptors underlying gustation in vertebrates. I own a rather large cat, and as is the case with many domestic cats, he has a voracious and wide-ranging appetite. Yet, while my cat will quickly devour most foods left unguarded, from bread to edamame, when it comes to sweets he abstains. A lack of attraction to compounds that taste sweet to humans is a distinguishing feature of the taste preferences of domestic cats and their wild cousins. While feline indifference towards sweets has been known in the scientific literature since 1977[23] (and I suspect much longer to observant cat owners), its molecular basis was only determined in 2005[24].

In vertebrates, sweet and savory ("umami") tastes are mediated largely by a class of G-protein coupled receptors termed T1Rs. Most vertebrates have three T1R's, T1R1-3. A heterodimer of T1R1 and T1R3 detects savory amino acids (principally glutamate and related compounds), whereas a heterodimer of T1R2 and T1R3 detects sweet compounds (carbohydrates and artificial sweeteners). A mutation deactivating T1R2 is found in domestic cats and all other wild felines, indicating that this mutation goes back to a common ancestor[24]. The loss of sweet receptors is strongly correlated to a carnivorous diet. An analysis of 12 non-feline carnivore species identified 7 obvious loss-of-function mutations in T1R2, and 6 of these 7 were distinct mutations, indicating that the loss of the sweet receptor occurred repeatedly[25]. Sea lions provide a particularly striking example, as they are missing both T1R2 (sweet) and T1R1 (savory) receptors; It has been speculated that this loss of taste is linked to the predilection of sea lions to swallow their food without chewing[25]. This hypothesis is supported by the separate loss of both T1R2 and T1R1 in dolphins, which independently evolved similar dietary practices[15,25]. This relation between carnivorous diet and the loss of sweet receptors extends to bats: those dieting on fruit retain T1R2, whereas in vampire bats this gene is pseudogenized[26-28]. Conversely, giant pandas lack T1R1 (savory) receptors; Pseudogenization of this gene can be traced back to the point that their diet switched to bamboo[28], which is not a rich source of amino acids.

T1R2 receptors are absence from reptile lineages, including birds[29,30]. This represents a secondary loss as T1R2 receptors are present in the more

evolutionarily ancient fish. Studies of gustation in birds reveal the dangers of inferring behaviors such as taste preference from genomic information alone. As expected, many birds that lack T1R2 also show no preference for sugar. Chickens are one such example[31,32]. However, hummingbirds lack T1R2 but diet entirely on nectar. Moreover, they show a strong preference for sugar solution over water in controlled laboratory settings[30]. A recent study has shown that this preference stems from sequence change in the T1R1-T1R3 savory receptor that make it competent to detect sugar[30]. The very evolvability of chemosensory systems necessitates caution when inferring the causes of change.

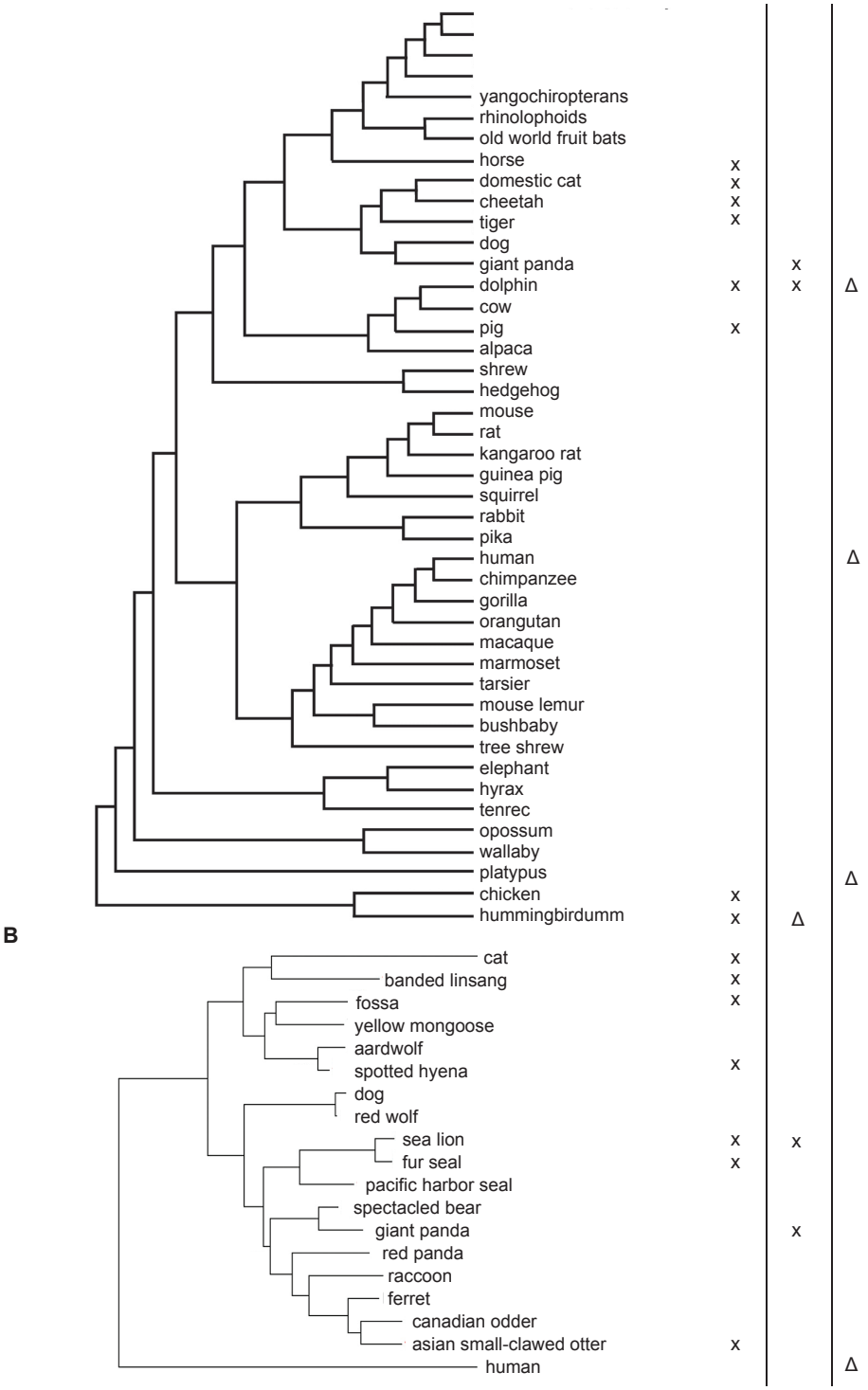

Figure 1.1: The loss of sweet and umami taste receptors

Taste receptors repeatedly lost over evolution. a) loss of taste receptors in vertebrates[25] b) loss of sweet receptors among Carnivora[24]. X indicates known loss of function mutation. Δ indicates major change in number or function. Phylogenies adapted: 24, 25.

A familiar example further illustrating this point involves phenylthiocarbamide (PTC), a compound some humans taste as bitter[3]. Three eminent evolutionists, R. A. Fisher, E. B. Ford, and J. Huxley, proposed that variation in the ability to taste PTC was caused by balancing selection. It had recently been discovered that humans and apes share the same blood groups. As this indicates that the blood group alleles have persisted among humans and apes since their common ancestor without drifting to fixation, it was assumed that balancing selection must be maintaining multiple alleles of this gene. While discussing this possibility at the International Congress of Genetics at Edinburgh in 1939, the three evolutionists realized that a parallel study could be conducted with tasting PTC. It had been well characterized that a subset of humans can taste this compound, but no one knew whether apes could. So they ran off to the Edinburgh zoo, and to their delight, discovered that apes showed similar perception of PTC as humans. Not only were a similar fraction of apes tasters of PTC, but the PTC concentrations apes tasted reflected PTC concentrations humans detect. The evolutionists deduced that alternative abilities to taste PTC were as ancient as blood groups[33].

Only decades later was this line of reasoning debunked by the characterization of the molecular basis of PTC sensitivity in humans and apes. Variable PTC tasting in humans stems from two common alleles of *TAS2R38.* The different alleles encode taste receptors with different affinities for PTC. In apes, variation in PTC taste sensitivity also stems from variation in *TAS2R38,* but the two common alleles in apes are entirely distinct from the two alleles in

humans[34]. Variability in PTC sensitivity is not ancient, but instead has evolved twice!

As it turns out, Fisher et al may still be right, just for the wrong reasons. Genomic analyses have confirmed the presence of balancing selection at the *TAS2R38* locus[35,36]. The picture now is of convergent evolution (variability in PTC tasting evolving twice) followed by more recent balancing selection (maintaining the variable PTC tasting in human and ape populations). Why selection would have repeatedly produced and then subsequently maintained variable PTC tasting in apes and humans remains unclear. One possibility stems from the observation that the PTC receptor also recognizes goitrin[36]. Gotirin is abundant in certain classes of nutritious vegetables, and can worsen hypothyroidism caused by low iodine intake[37]. Therefore depending on the local prevalence of dietary iodine, goitrin should or should not be avoided. But as is now abundantly clear, such hypotheses about the nature of selection leading to present traits need to be empirically tested.

The challenge of understanding the 'goal' of evolution by looking at what has evolved was famously illustrated with the metaphor of spandrels in a critique written by Gould and Lewontin of "adaptationism" in 1979[38,39]. The adaptationist research program was based on a belief in the power of selection to optimize, and involved partitioning organisms into traits and proposing an adaptive story for each trait separately. All traits were viewed as the perfect end product of selection; anything apparently suboptimal reflected a necessary trade-off. Gould and Lewontin describe the four main spandrels of St. Mark's Cathedral in Venice.

These spandrels are large triangular structures surging upwards from four columns sitting bellow the main dome. The spandrels are elaborately decorated with Christian iconography, with each spandrel depicting one of the four biblical rivers. Given the detail of the art and the clever relation of imagery to structure, one might be tempted to assume that aesthetics was a central goal of the master architect when designing the spandrels, and not - as was actually the case - that the spandrels were the result of engineering necessity; the spandrels provide needed support for the dome[39]. Meaning is often hidden under the surface.

TRP channels, many of which serve as chemoreceptors, may be biology's best example of a spandrel; the hidden relationships between these enigmatic genes can be inferred by their sequence homology as their functions diversify. One example of the evolvability of TRP channels is their use in infrared vision. Venomous pit vipers use infrared radiation to detect warm-blooded prey[40]. This form of vision is not mediated by their eyes, but rather by a specialized loreal pit organ that is located on each side of the viper's face between the eye and nostril. The molecular sensors of the infrared signal are TRPA1 channels, which detect the subtle heating of a thin membrane within the pit. While certain TRP channels have known sensitivities to heat, this had been controversial with TRPA1, variously suggested to detect heat, cold, or neither temperature. Rather, in several vertebrate species ranging from mammals to fish, TRPA1 functions as a receptor for environmental irritants. TRPA1 channels detect the pungent allyl isothiocyanate (AITC) found in wasabi and mustards as well as other electrophillic irritants through an unusual gating mechanisms: reactive

compounds open the channel by covalently modifying a cytosolic cysteine residue. The rattlesnake TRPA1 receptors retain only moderate response to AITC while showing exquisite sensitivity to temperature compared to mammalian counterparts[40,41]. Clearly, TRPA1 function cannot simple be deduced from homology.

Like snakes, vampire bats have also evolved infrared sensation, but they elaborated an infrared detector from a different starting point. Vampire bats use TRPV1 to detect infrared[42]. TRPV1 is heat-sensitive in other animals, but not suited for infrared detection. Whereas in most mammals TPV1 is activated around 39°C, in bats the thermal activation threshold of TRPV1 is reduced to about 30°C through alternative splicing that results in a channel with a truncated carboxy-terminal cytoplasmic domain. This isoform is expressed exclusively in the trigeminal ganglia, allowing bats to elaborate an infrared detector from TRPV1 without altering TRPV1 function as a noxious heat detector in somatic afferents[42]. The evolution of infrared detection in snakes and bats provide yet another example of dramatic changes in sensory systems being linked to novel behavior, lifestyles, and diets.

A central question of evolutionary biology is the predictability of evolution. Will the same selective pressures reliably yield the same result? In opposition to this possibility, olfaction evolved in nematodes, insects, and vertebrates from different molecular starting points. Similarly infrared detection was elaborated from different starting points in snakes and bats. Perhaps these cases are

unusual as they involve the evolution of an entirely new sensory system. In many other cases, it appears that evolution repeats itself. Variation in ability to taste PTC has evolved independently in both humans and apes through changes in the same receptor. Carnivores have repeatedly lost the ability to taste sugar on many separate occasions through the psuedogenization of T1R2. We cannot be certain whether the loss of the sweet receptor was a driver of taste preference or the result. However, 'use it or lose it' is a simple refrain that could explain many observed changes in chemosensation.

While the specific receptors under selection vary, a common theme is that changes underlying adaptation occur at the sensory level. Studies with *C. elegans* provide several striking examples. Culturing *C. elegans* at high densities has lead to deletions in the same *srg* genes encoding G protein-coupled ascaroside receptors on two separate occasions[43]. On a third occasion, similar culturing conditions led to a spontaneous deletion of the *C. briggsae* ortholog of the same *srg* genes. By failing to detect dauer promoting ascarosides, the selected strains were apparently able to avoid developmental arrest as dauers, and thereby outcompeted wild-type strains in the lab cultures[43]. Unintentional selection during laboratory cultivation has also promoted *C. elegans* strains with a relaxed preference for low oxygen levels. This has occurred through selection of mutant alleles of *glb-5* and *npr-1*[44-46]. *glb-5* acts directly in oxygen sensing neurons to alter their response, and *npr-1* acts in neurons that integrate multiple sensory inputs, leading to changes in sensory neuron signaling. Although these examples involve cases of artificial selection, similar findings have emerged from

C. elegans studies of natural variation. Changes in lawn leaving rates among natural isolates reflects variations in *tyra-3,* a catecholamine receptor expressed in sensory neurons[47]. One benefit of using *C. elegans* to study the evolution of behavior is the ability to test fitness effects of polymorphisms through competition experiments in controlled laboratory settings. Through such approaches we can complete the circle linking the causes and mechanisms of selection.

I set off on my thesis project with the goal of exploring natural variation in social communication using *C. elegans*. It is no surprise that I soon found myself studying chemoreceptors and their role in shaping behavior.

C. elegans relies primarily on chemosensation to navigate through its environment, to find food or mates, and to avoid pathogens or toxic conditions[48]. The first candidate chemoreceptors in *C. elegans* were identified in 1995[6]. Their function was largely deduced based on transgene expression patterns in known chemosensory neurons, the large size of the divergent gene families, and their similarity to G protein-coupled receptors. A year later, the first *C. elegans* chemoreceptor was de-orphaned: *odr-10* was shown to encode a diacetyl receptor[49]. With the sequencing of the *C. elegans* genome, relatives of *odr-10* were identified forming the *str* and related *sri, srj* and *srh* families[50-52]. Additional families were added incrementally[9,53,54]; now there are 22 recognized families of *C. elegans* chemoreceptor genes comprising 8 superfamilies described in Table 1. This represents an immense level of molecular diversity; mice have only 6

families of chemoreceptors forming 2 distinct superfamilies[4,55]. Interestingly, *C. elegans* chemoreceptor genes are not spread out evenly throughout the genome, but instead are both locally clustered and heavily enriched on the arms of chromosome V[22]. The exact significance of this pattern remains unclear, but it may relate to the propensity of genes located on chromosome arms to undergo local duplication events[56-58]. Chemoreceptor clustering might also be functional, similar to what has been proposed in other *C. elegans* gene classes[59].

Chemosensation in *C. elegans* stems largely from the activity of eleven pairs of amphid sensory neurons[48]. The neurons extend cilia through the cuticle to gain access to the environment, and each has specialized chemoreceptors, G proteins, and signal transduction pathways (table 2). Each neuron has characteristic functions, some partially overlapping with other neurons, and many neurons mediate more than one biological function. For example, ASH functions principally as a nociceptor, detecting bitter, harsh chemical signals, as well as osmotic stresses and physical touch that elicit escape behavior[60-65]. Interestingly this neuron also serves a role in aggregation, which is more frequent in noxious conditions[66]. A set of neurons, ASI, ASG, and ADF promote formation of the developmental dauer stage, but have distinct functions in adult food-sensing and plasticity; ASJ antagonizes dauer formation but promotes recovery from the dauer to the adult[48]. Clearly the extensive repertoire of chemosensors in *C. elegans* facilitates the sophisticated chemosensory behaviors and physiological functions achieved through their few chemosensory neurons.

Table 2 *C. elegans* chemosensory neurons

Neuron	Function	Receptors	Signal transduction
ASE	Water-soluble chemotaxis	guanylate cyclases	*tax-4, tax-2, daf-11*, cGMP
AWC	Volatile chemotaxis, Lifespan, Navigation	*str-2,* other GPCRs *nb Bibi identified about ten total AWC chemoreceptors, and odr-3 is a G protein*	*odr-3, tax-4, tax-2, daf-11, odr-1, odr-4, odr-8,* cGMP
AWA	Volatile chemotaxis, Lifespan (minor)	*odr-10,* other GPCRs	*odr-3, osm-9, ocr-2, fat-3*, PUFA, *odr-4,odr-8*
AWB	Volatile avoidance	GPCRs	*tax-4, tax-2, daf-11, odr-1,* cGMP
ASH	Nociception: Osmotic avoidance, Nose touch avoidance, Chemical avoidance, Social feeding	GPCRs	*odr-3, osm-9, ocr-2, fat-3,* PUFA, *qui-1*(chemical only), *osm-10* (osmo only), *odr-4*
ASI	Dauer formation, Chemotaxis(minor), Navigation, Dwelling/roaming	*srg-36, srg-37, str-3,* other GPCRs	*tax-4, tax-2, daf-11,* cGMP, *odr-1,odr-4*
ADF	Dauer formation, Chemotaxis (minor), Pathogen learning	GPCRs	*osm-9, ocr-2, odr-4*
ASG	Dauer formation (minor), Lifespan, Chemotaxis (minor)	GPCRs	*tax-4, tax-2,* cGMP, *odr-4*
ASJ	Dauer formation and recovery, Chemotaxis (minor), Lifespan	GPCRs	*tax-4, tax-2, daf-11, daf-21,* cGMP,*odr-1, odr-4*
ASK	Amino acid chemotaxis, Pheromone attraction, Lifespan, Navigation	*srbc-64, srbc-6,* other GPCRs	*tax-4, tax-2,* cGMP, *odr-1, daf-11,odr-4*

Table 2 (cont.) *C. elegans* chemosensory neurons

Neuron	Function	Receptors	Signal transduction
ADL	Pheromone avoidance, Social feeding	GPCRs	*osm-9, ocr-2, odr-4*
URX, AQR,PQR (not amphid)	Oxygen/aerotaxis, Social feeding, Regulation of fat stores and body size	Soluble guanylate cyclases:: *gcy-35, gcy-36;* GPCRs	*tax-4, tax-2,* cGMP
PHA, PHB (not amphid)	Avoidance (antagonistic)	GPCRs	*osm-9, ocr-2, odr-4*

Adapted from[48]

Chapter 2:
Balancing selection affecting a pheromone receptor regulates density-dependent foraging strategies

INTRODUCTION

Game theory suggests that the benefit of a particular foraging strategy varies in part based on the behavior of competitors, and therefore that balancing selection can favor the co-existence of multiple strategies within a species[67,68]. The pioneering example of strategic competition is natural genetic variation at the *foraging* (*for*) gene in *Drosophila melanogaster* larvae[69-71]. Larvae with high-activity for^R (rover) alleles have active foraging behaviors, while larvae with low-activity for^S (sitter) alleles are more sedentary. Frequency-dependent balancing selection can maintain both alleles by selecting against larvae with the more common foraging strategy[72]. The *for* example is a genetic polymorphism, but suggests that animals could benefit from detecting and responding to competitors in real time, and modifying foraging behavior accordingly. However, little is known about the genes and neural circuits that incorporate information about conspecifics into foraging strategies.

An opportunity to address this question is provided by the nematode *C. elegans,* an animal with well-characterized foraging circuits and intraspecific pheromone signaling. *C. elegans* foraging on bacterial food spontaneously alternates between an exploratory behavior called roaming and a less active behavior called dwelling, each of which persists for several minutes per episode[73,74]. Transitions between roaming and dwelling are regulated by distributed neuromodulatory systems that link internal cues such as nutritional status to locomotion circuits[74,75]. *C. elegans* senses population density using a family of secreted pheromones called ascarosides, which control the

developmental decision to enter the starvation-resistant dauer larva stage[76] as well as regulating behavioral responses such as aggregation and male attraction to hermaphrodites[77,78]. G protein-coupled receptors for the ascarosides ascr#2 and ascr#5 have been identified based on their effects on dauer larva formation, and are members of large multigene families[43,79,80]. These receptors can be highly selective, indicating that animals detect the diversity of pheromones, not just the total pheromone amount. Here we show that physiological levels of ascarosides regulate foraging by suppressing roaming behaviors. By characterizing differences in pheromone sensitivity in natural *C. elegans* isolates, we identify a pheromone receptor that shapes alternative foraging strategies and affects fitness depending on the structure of the food environment.

RESULTS

Ascaroside pheromones regulate foraging behavior

The effects of ascaroside pheromones on *C. elegans* foraging were examined by quantifying long-term exploration of a bacterial lawn by individual wild-type N2 animals (Figure 1A). To mimic the effects of high density on these isolated animals, we conducted the assay in the presence of natural pheromone extracts. The pheromones strongly suppressed exploration (Figure 1B), as did several pure synthetic ascarosides at concentrations at or below those that induced dauer larva development: ascr#2 (10 nM), and ascr#3 (10 nM), ascr#8 (1 nM), and icas#9 (1 nM) (Figure 1C, 1D). However, ascr#5, a potent regulator of dauer development, only suppressed exploration at concentrations above 100 nM

(Figure 1D). Thus a subset of ascarosides can regulate foraging behavior at biologically relevant concentrations.

The exploration assay is an indirect measure of the relative time *C. elegans* spends in roaming and dwelling behavioral states. Roaming and dwelling were examined directly in video recordings, monitoring the high locomotion speed with infrequent turning that characterizes roaming and the slow locomotion speed with frequent turning that characterizes dwelling[74,75]. The potent ascarosides icas#9 or ascr#8 decreased the fraction of time roaming (Figure 1E) by decreasing the duration of roaming states (Figure 1F), but had no significant effect on the duration of dwelling states (Figure 1G). The detailed behavioral features of roaming and dwelling states were only slightly affected by ascarosides (Figure S1), suggesting that their primary effect is on roam state duration.

Natural *C. elegans* isolates vary in their sensitivity to icas#9

A behavioral screen of genetically diverse wild-type *C. elegans* strains demonstrated that all of them responded to ascarosides with a suppression of exploration, like the control N2-like strain CX12311[44] (Figure 2A). CX12311 bears ancestral alleles of the *npr-1* and *glb-5* genes, which affect oxygen sensitivity and are mutated in the N2 laboratory strain[44]; behavior in CX12311 and all naturally isolated strains was scored at their preferred 8% O_2 conditions. Among the wild strains, the German strain MY14 failed to respond to 10 nM icas#9 in the exploration assay, while responding normally to ascr#2, ascr#3, and ascr#8

(Figure 2A). Video recordings of roaming and dwelling states confirmed the icas#9-resistance of MY14 (Figure S2). Coupled alterations in pheromone signaling and detection can contribute to reproductive isolation during incipient speciation[81]. However, MY14 and CX12311 were found to produce similar levels of icas#9 and 16 other tested ascarosides (Figure S3), indicating that the change in the icas#9 response in MY14 was independent of its production.

To determine the genetic basis of icas#9-insensitivity, 94 Recombinant Inbred Lines (RILs) were generated from intercrosses between MY14 and CX12311. A continuous distribution of icas#9 sensitivity was observed in exploration behavior of the RILs (Figure 2B) suggesting that two or more loci contribute to icas#9-sensitivity. The 94 RILs were genotyped at ~185 kb resolution across the genome by low-coverage whole-genome sequencing[82]. Quantitative trait locus (QTL) analysis identified a single significant QTL at genome-wide significance, which will be called *roam-1* (Figure 2C). *roam-1* accounted for 34.9% of the variance among the RILs, and mapped to Chromosome V in the interval between 14.2 and 18.0 Mb (Figure 2C). Covariate analysis failed to find additional QTLs that were either additive or interactive (Figure S4). These results show that the *roam-1* QTL accounts for substantial variation in icas#9 sensitivity between MY14 and CX12311, along with additional loci of smaller effect size.

The impact of *roam-1* on foraging was confirmed by creating near-isogenic lines (NILs) with small genetic regions substituted between the strains. The QTL was narrowed to 2.5 Mb (V:14.3-16.8 Mb) by examining 14 high-confidence

phenotypically extreme RILs and this region was exchanged between CX12311 and MY14. The two resulting NILs were intermediate in icas#9-sensitivity compared to the parental strains (Figure 2Di). Thus the *roam-1* region accounts for some but not all of the difference between the two starting strains, and can be detected in both CX12311 and MY14 strain backgrounds.

To simplify further mapping, the *roam-1* region from MY14 (*kyIR139)* was crossed into the N2 laboratory strain. The resulting NIL was resistant to icas#9 at 21% ambient O_2 (*kyIR144,* Figure 2Dii), facilitating further mapping with N2 that localized *roam-1* to 182 kb (Figure 2Dii). High-density mapping was then performed by genotyping 2600 F2 progeny of a cross between N2 and the NIL *kyIR147* to find recombinants in the 182 kb region (Methods). Characterizing the behavioral phenotypes of the 12 informative recombinants mapped the *roam-1* QTL to 37 Kb on chromosome V between 16.006 Mb and 16.043 Mb (Figure 2Diii).

A chemoreceptor gene in the *roam-1* QTL is required for icas#9 response and is functionally polymorphic in N2 and MY14

The 37 kb *roam-1* region contained sixteen protein-coding genes, including five genes that encoded predicted G protein-coupled receptors in the *srx* or *str* chemoreceptor gene families (Figure 3A). We hypothesized that one or more of the chemoreceptors could be icas#9-receptor(s) that had reduced activity in MY14. With this in mind, N2-derived sequences overlapping the chemoreceptor genes were introduced into the *roam-1*$_{MY14}$ N2 NIL and the resulting strains were

tested for icas#9-sensitivity. N2-derived transgenes covering *srx-43* conferred icas#9-sensitivity to *roam-1*$_{MY14}$ (Figure 3B), but transgenes with nonsense mutations disrupting the coding region of *srx-43* were inactive (Figure 3B).

The function of *srx-43* was examined further with loss of function (*lf*) mutations. In N2, a nonsense allele was derived from a mutagenesis screen. In a *roam-1*$_{MY14}$ N2 NIL, CRISPR Cas9 was used to make multiple independent insertion/deletion alleles that disrupted reading frame and lead to a premature stop codon. *srx-43(lf)* mutants were profoundly insensitive to icas#9 in both N2 and *roam-1*$_{MY14}$ genetic backgrounds (Figure 3C). icas#9 insensitivity in the *srx-43*(*lf*) mutant was rescued by an N2 *srx-43* transgene (Figure 3C). These results indicate that *srx-43* is necessary for the icas#9 response, and essential for the behavioral difference between N2 and MY14 strains.

The activity of the N2 and MY14 *srx-43* genes was compared by targeting a single copy of *srx-43* from each strain to a defined locus using the Mos1 transposase, in an *srx-43(lf)* mutant so that the single-copy transgene was the sole source of *srx-43*. Targeted insertion of N2 or MY14 *srx-43* genomic sequences resulted in different levels of icas#9 sensitivity: the N2 *srx-43* gene fully rescued the icas#9 response, whereas the MY14 gene did not (Figure 3D). The differential effects of single-copy transgenes indicate that MY14 *srx-43* has reduced activity compared to N2 *srx-43*.

SRX-43 is a chemoreceptor for icas#9 whose expression differs among natural isolates

Reporter genes with N2 or MY14 *srx-43* promoters driving GFP were expressed selectively in the ASI sensory neurons (Figure 3E), which promote roaming behavior[71,75]. A genomic clone with GFP fused to the C-terminus of the SRX-43 protein was enriched in ASI sensory cilia, the site of sensory transduction (Figure 3E). These properties suggest that SRX-43 is a chemoreceptor. We investigated effects of icas#9 on ASI activity using *in vivo* calcium imaging, but failed to observe a response. This negative result is consistent with studies of dauer formation, where ascarosides regulate gene expression in ASI and not acute ASI calcium levels[43,79,83,84].

To ask whether SRX-43 could be an icas#9 receptor, *srx-43* cDNAs were ectopically expressed in the ASH sensory neurons, which are normally insensitive to ascarosides[43] (Figure S5), and ascaroside-induced calcium flux was monitored using genetically-encoded calcium indicators[43,85]. ASH neurons expressing SRX-43 responded with calcium transients to 10 nM icas#9 but not to ascr#2, ascr#3, or ascr#8 ascarosides or to indole (Figure 3F).

Although the MY14 strain was largely insensitive to icas#9 in foraging assays, an *srx-43* cDNA clone from MY14 appeared to encode a functional receptor, detecting icas#9 when expressed in ASH (Figure 3G). The MY14 *srx-43* promoter was also active, as it could drive a GFP reporter gene in ASI (Figure 3E), but its expression appeared weaker than the N2 GFP reporter. To ask which sequences distinguished N2 and MY14 *srx-43* activity, their promoter and coding regions were exchanged and tested as Mos1-mediated Single Copy Insertion (MosSCI) *srx-43* transgenes. A transgene with the N2 promoter region and MY14

coding region rescued icas#9 sensitivity in *srx-43(lf)* mutants but the converse did not, localizing the difference to the *srx-43* promoter (Figure 3H). Returning to the N2 and *roam-1*$_{MY14}$ NIL strains, quantitative measurements of endogenous *srx-43* mRNA levels using digital PCR demonstrated that *srx-43* was expressed at a five-fold lower level in *roam-1*$_{MY14}$ than in N2 (Figure 3I). Therefore, natural variation in the activity of the *srx-43* promoter between N2 and MY14 impacts *srx-43* gene expression and behavioral sensitivity to icas#9.

ASI, the cellular sight of variable *srx-43* expression, couples ascaroside detection to development into dauer larva through suppressing the transcription of secreted TGF-β-related peptide, *daf-7*. Loss-of-function mutants of *daf-7* have reduced levels of roaming, like animals treated with ascarosides. This raises the possibility that ascarosides suppress roaming in N2 by down-regulating *daf-7.* To test this, the effect of icas#9 on *daf-7* expression was determined with a *daf-7::GFP* reporter. In all assay conditions *daf-7::GFP* was found only in ASI, and icas#9 lead to a significant reduction in *daf-7::GFP* in N2 but not *roam-1*$_{MY14}$ animals (Figure 3J). The substantial reduction in exploration induced by *daf-7(lf)* prevents accurate assessment of icas#9 impact on foraging behavior. However, the importance of *daf-7* regulation for icas#9 foraging response can be tested by examining *daf-7 daf-3* double knock outs, as *daf-7* canonically acts through antagonizing *daf-3*, a co-SMAD protein. While N2 *daf-7(lf) daf-3(lf)* animals explore control plates comparably to WT animals, the double knock outs responded significantly less to icas#9 (Figure 3K). These results suggest that in N2, *srx-43* detection of icas#9 reduces exploration in part through inhibiting *daf-7*

transcription. In coupling icas#9 detection to *daf-7* regulation, *srx-43* could influence behavior without altering ASI calcium signals, and this mechanism would provide an explanation for the slow time course of icas#9 action on foraging behavior (Figure S6) as canonical *daf-7* signaling pathways involve several steps of transcriptional regulation. To test whether altered *daf-7*/daf-3 signaling contributes to the *roam-1*$_{MY14}$ phenotype, we tested the icas#9 sensitivity of *roam-1*$_{MY14}$ *daf-7(lf) daf-3(lf)*. The pheromone response of *roam-1*$_{MY14}$ *daf-7(lf) daf-3(lf)* resembled that of *roam-1*$_{MY14}$ (Figure 3K). The absence of an additive effect suggests that attenuated regulation of *daf-7* in *roam-1*$_{MY14}$ contributes to reduced icas#9 sensitivity.

Balancing selection at the *roam-1* foraging locus

To understand the population genetics of *roam-1*, we examined the genomic sequence of a 20 kb region centered around *srx-43* in 39 additional wild *C. elegans* isolates sequenced by the Million Mutation Project[86]. Two discrete and highly divergent haplotypes for the *roam-1* region were found, one resembling N2 and present in 34 strains, and the other resembling MY14 and present in seven strains isolated at multiple sites on two continents (Figure 4A, S8). The N2 and MY14 haplotypes over the 20 kb *roam-1* region differed at 2.64% of all positions, 12 times the average across the genome[87]. As these data derive from Illumina sequencing that can fail to align highly divergent sequences, we Sanger sequenced the *srx-43* gene and promoter from both strains, finding that MY14 actually differed from N2 sequence at 19.7% of all positions (Figure S8). This

variability did not stem from relaxed constraint on *srx-43,* as *srx-43* coding regions had a low ratio of nonsynonymous to synonymous changes (dN/dS = 0.048) indicating purifying selection. The seven strains sharing the MY14-like *roam-1* haplotype resided on several distinct branches of *C. elegans* phylogenetic tree (Figure 4B), and all MY14-like strains were relatively resistant to icas#9 compared to N2-like strains (Figure 4C). These results suggest that naturally occurring icas#9 resistance is associated with a highly divergent *roam-1* haplotype including *srx-43*.

A possible explanation for the two highly divergent *roam-1* haplotypes is balancing selection acting on *roam-1*, raising the possibility that this locus influences fitness. Therefore, we designed competition experiments to compare the relative fitness of N2 and *roam-1*$_{MY14}$ strains. Experiments were conducted under high-density conditions to permit the accumulation and detection of endogenously produced icas#9, and competition was applied by growing cultures past the point of starvation, i.e. with limiting food.

The first competition experiments were conducted on a standard lawn of OP50 *E. coli* bacteria. A population founded by 20 N2 and 20 *roam-1*$_{MY14}$ age-matched adults was grown to starvation (4 days) and held for an additional 48 hours. 20% of the population (~5000 animals) was transferred to a new plate with food for another cycle, and the remainder harvested for quantitative DNA analysis (Figure 5A). In two succeeding cycles, the larger starting population depleted food within 48 hours and was held for an additional 48 hours. These conditions led to a consistent growth advantage for the N2 genotype over *roam-*

1$_{MY14}$ in the first cycle of competition and an increasing advantage in the subsequent cycles (Figure 5B).

The two tested strains differ in a 182 kb region encompassing the *roam-1* QTL and a total of 81 genes. To ask if the competitive advantage required *srx-43,* the experiment was repeated using N2 *srx-43(lf)* and *roam-1*$_{MY14}$ *srx-43(lf)* strains. The competitive N2 advantage disappeared in this setting, identifying the icas#9 receptor SRX-43 as an essential element of the difference between strains (Figure 5C).

The role of endogenous pheromones in the selective advantage was assessed by repeating the competition experiments with N2 and *roam-1*$_{MY14}$ strains mutant for the gene *daf-22*, which is required for the secretion of short-chain ascarosides including icas#9. *daf-22* mutations eliminated the competitive advantage of the N2 strain over *roam-1*$_{MY14}$ (Figure 5D). A selective advantage of N2 *daf-22* was partially recovered when the competition experiment was repeated in the presence of exogenous 10 nM icas#9 (Figure 5D). These results show that selection on the *roam-1* locus depends on the presence of pheromones.

The increased roaming of *roam-1*$_{MY14}$ at high density might be expected to cause greater exploration of a patchy food environment. In a second competition design, 20 N2 and 20 *roam-1*$_{MY14}$ adults were used to seed a patchy environment consisting of 15 small bacterial lawns (Figure 5A). In these conditions the N2 advantage was lost, and instead a moderate but significant selection favored *roam-1*$_{MY14}$ over N2 animals (Figure 5E). Together, these results demonstrate

that *roam-1* can affect fitness bidirectionally depending on *srx-43,* pheromone production, and food distribution.

DISCUSSION

Conspecific animals are informative and highly relevant features of an animal's natural environment, in part because they compete for resources. Although population density has long been predicted to affect foraging[67,68], direct evidence for its interpretation by biological mechanisms has been elusive. Our results demonstrate that conspecific pheromones alter long-term foraging strategies, and additionally provide evidence that selection on these traits can generate natural variation in foraging behavior within a species.

In *C. elegans,* ascaroside pheromones indicate the density of competitors, and can predict the overpopulation bust in the boom-and-bust cycle that is thought to represent its typical lifestyle[88-90]. The formation of starvation-resistant dauer larvae is one consequence of ascaroside density signals. Our results show that a shift in foraging strategy toward dwelling is another consequence that is preferentially triggered by a different group of ascarosides. Other behavioral responses to ascarosides include rapid attraction for mating, rapid avoidance, increased olfactory adaptation, and induction of aggregation, each with its own chemical specificity[77,78,88,91]. The suite of ascarosides produced by animals varies with their sex, age, and feeding status[92,93], and the specificity of receptors such as SRX-43 provides a mechanism by which this information can be detected by the nervous system to regulate different behaviors. *srx-43* is expressed in ASI

sensory neurons, which are also targets of internal neuromodulators that regulate roaming and dwelling[75], providing a site of integration of internal and external influences on foraging behavior.

Natural isolates are differentially sensitive to icas#9 due to variation at the *roam-1* locus, and an essential component of this behavioral variation results from altered expression of the icas#9 receptor SRX-43. Secreted icas#9 is present in dense culture supernatants at concentrations 100-fold above those that suppress roaming. Although we do not know the suite of pheromones that are produced by *C. elegans* in the wild, the prevalence and high potency of icas#9 in the exploration assay suggest that it is a relevant regulator of foraging, and that altered sensitivity to this molecule could affect animals' overall sensitivity to secreted ascarosides.

The highly polymorphic *roam-1* region has sequence features of an area under balancing selection[94,95]. It is present in two distinct forms in multiple isolates from two continents, with a distribution distinct from overall strain divergence. The level of polymorphism near *srx-43* is exceptionally high, and comparable to that of the *srbc-46* chemoreceptor, part of a haplotype under balancing selection that causes genetic incompatibility between wild *C. elegans* strains[94]. Following the hypothesis that food distribution and population density could interact to determine the optimal foraging strategy, we were able to identify conditions that favored either the N2 or MY14 *roam-1* QTL in competition experiments. While *srx-43* is an essential part of *roam-1*, it may not be the only gene in this QTL or the only gene under balancing selection, as the haplotype

extends for 20 kb to include several other genes. Moreover, the behavior identified here need not be the most important one in natural settings; it may represent one of several behavioral and physiological responses that facilitate adaptation to different environments.

Balancing selection acting on a locus for a prolonged duration increases the local density of SNPs, as seen for the *roam-1* locus. A recent report identified 61 such regions of high diversity segregating among wild strains of *C. elegans*[87]*.* Among these are alleles under balancing selection, for example at the *glc-1* gene[96], which resides 200 kb from *roam-1.* Selection for the linked *glc-1* genotype is unlikely to explain the divergent *roam-1* alleles, as phylogenetic and SNP analysis of *glc-1* and the sequences between *glc-1* and *roam-1* indicated substantial recombination between them in wild strains (Figure S7). Our results instead suggest that multiple regions of diversity in the *roam-1/glc-1* region are associated with balancing selection. The composition of these regions is not random but rather biased towards particular gene classes including chemoreceptors[87], which may act as hotspots of evolution.

At a conceptual level, behavioral genetics in animals and humans is dominated by evidence for gene-environment interactions[97,98]. Our results take this abstraction to a concrete level, showing that natural trait variation acts explicitly at the intersection of innate circuits and environment cues, with genetic changes allowing differential incorporation of environmental information into innate foraging behaviors.

Figure 2.1 Ascaroside pheromones suppress exploratory foraging behavior

A) Exploration assay. Tracks left by an individual animal are examined after 16 hours on a uniform 35 mm bacterial lawn. Scoring grid has 86 squares.

B) Wild-type N2 response to crude pheromone extract, showing exploration scores in the presence and absence of pheromone (each dot represents one animal), and a pheromone response index generated by subtracting exploration scores in pheromone from scores in controls. Data represented as mean ± SEM.

C) Structures and names of selected ascarosides.

D) Wild-type N2 response to individual ascarosides at a range of concentrations expressed as mean ± SEM. ***P<0.001, **P<0.01 by ANOVA with Dunnett correction; ns, not significant.

E) Roaming and dwelling behaviors scored from video analysis, in wild-type N2 animals in the presence or absence of 10 nM pheromone. n=96-134 tracks per data point.

F and G) Cumulative distribution of roaming (F) and dwelling (G) state durations for animals in (E). Roaming states are shortened in ascarosides. ***P<0.001 by log rank test; ns, not significant.

Figure 2.1

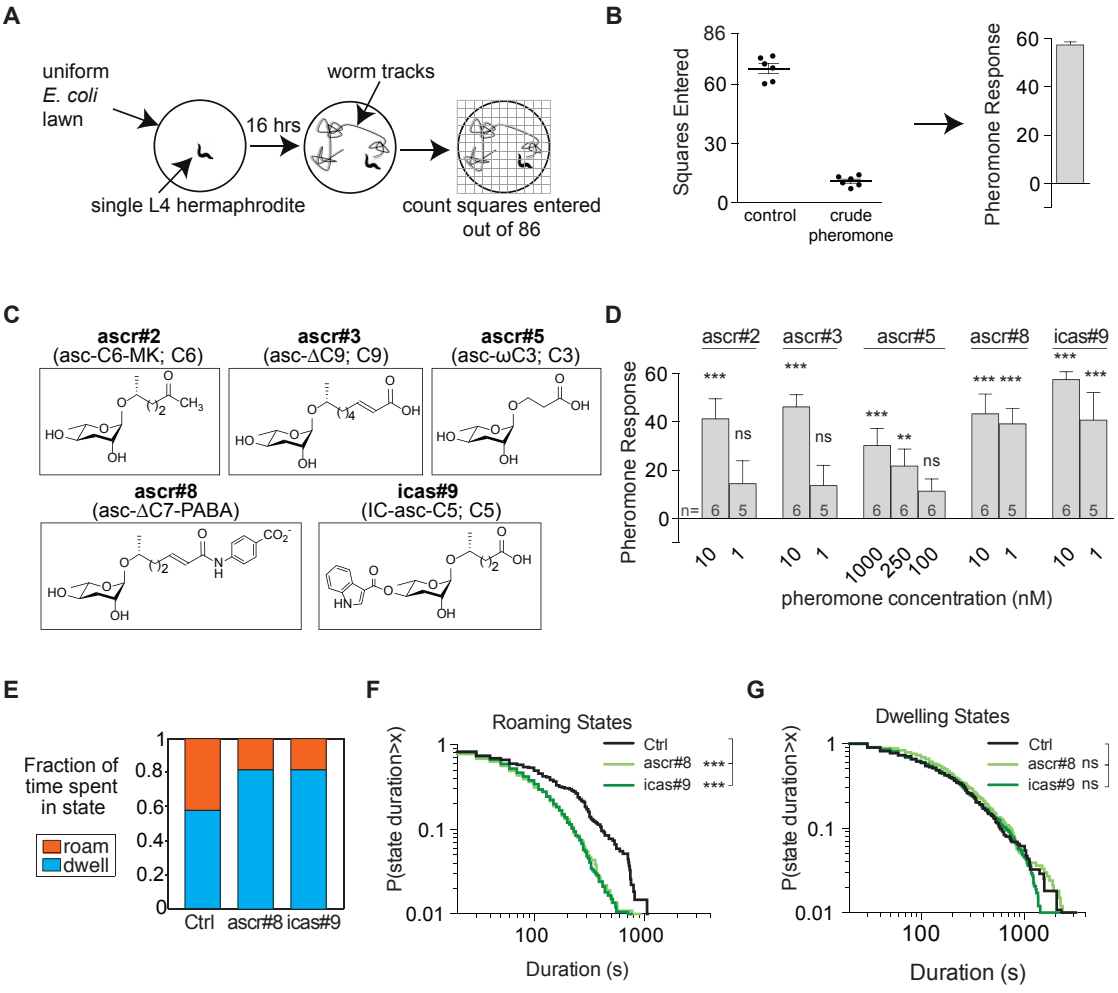
A
uniform
E. coli
lawn
16 hrs
worm tracks
single L4 hermaphrodite
count squares entered
out of 86
B
Squares Entered
86
60
30
0
control
crude
pheromone
Pheromone Response
60
40
20
0
C
ascr#2
(asc-C6-MK; C6)
ascr#3
(asc-ΔC9; C9)
ascr#5
(asc-ωC3; C3)
ascr#8
(asc-ΔC7-PABA)
icas#9
(IC-asc-C5; C5)
D
ascr#2
ascr#3
ascr#5
ascr#8
icas#9
Pheromone Response
60
40
20
0
***
ns
**
n=
6
5
10
1
1000
250
100
pheromone concentration (nM)
E
Fraction of
time spent
in state
roam
dwell
1
0.8
0.6
0.4
0.2
0
Ctrl
ascr#8
icas#9
F
Roaming States
P(state duration>x)
1
0.1
0.01
Ctrl
ascr#8 ***
icas#9 ***
100
1000
Duration (s)
G
Dwelling States
P(state duration>x)
1
0.1
0.01
Ctrl
ascr#8 ns
icas#9 ns
100
1000
Duration (s)

Figure 2.2 Natural genetic variation in pheromone sensitivity

A) Response of a panel of natural *C. elegans* isolates to synthetic ascarosides in the exploration assay. Strains were tested in 8% ambient O_2, where natural isolates and CX12311 have low levels of roaming behavior. Data presented as mean ± SEM. ***P<0.001 by ANOVA with Dunnett correction.

B) icas#9 response of 94 CX12311-MY14 recombinant inbred lines (RILs) and parental strains, presented as mean ± SEM. Color shows genotype at the *roam-1* locus (Red = homozygous N2; Blue = homozygous MY14; black = heterozygous).

C) QTL analysis of the RILs shown in B, showing a major peak on chromosome V. The horizontal line denotes P<0.05 genome-wide significance threshold. LOD, log likelihood ratio.

D) icas#9 response of Near Isogenic Lines (NILs) used for mapping the chromosome V QTL. i) Reciprocal NILs with 2.5 Mb introgressions in CX12311 and MY14 backgrounds. ii) Initial recombination mapping in N2 NILs. iii) Key results of dense recombination mapping in N2 NILs. Colors of the top bars indicate the strain background; colors of the middle bars indicate genotype in the *roam-1* region. Pheromone response in exploratory assay represented as mean pheromone response ± SEM. ***P<0.001, **P<0.01 by ANOVA with Dunnett correction; ns, not significant. Assays in A, B, and Di were conducted at 8% O_2; assays in Dii and Diii were conducted at 21% O2.

Figure 2.2

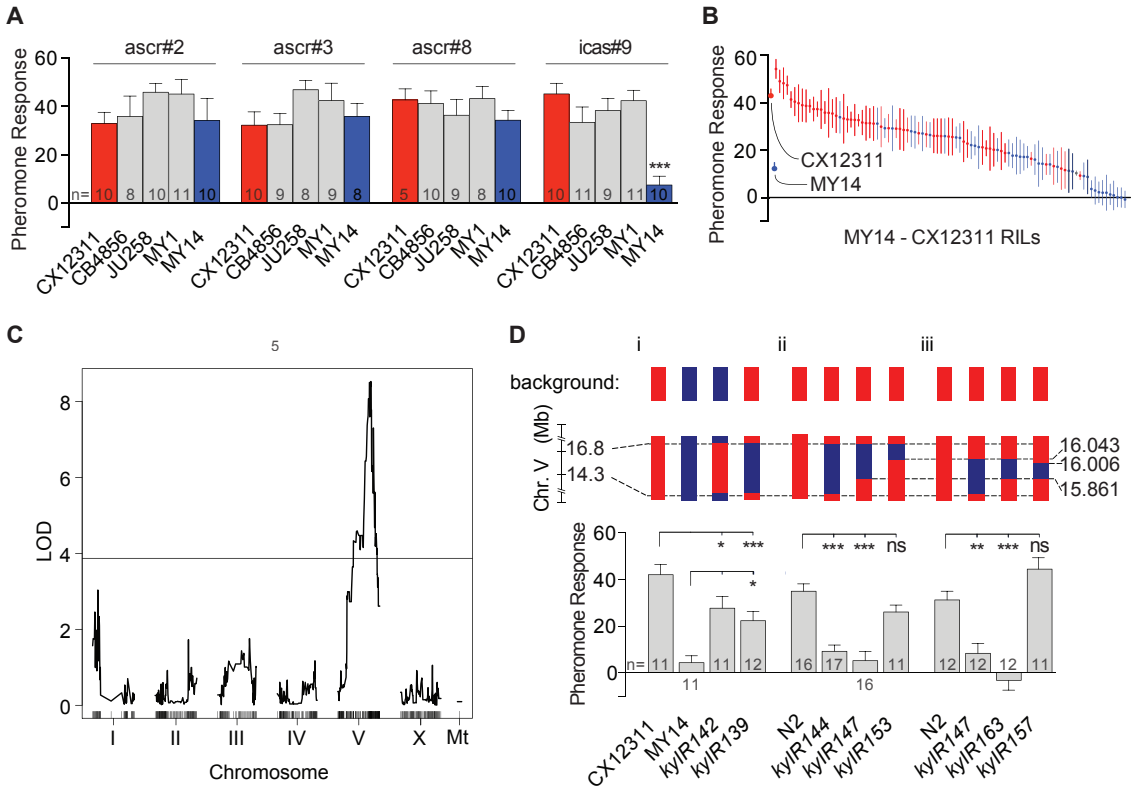
A
ascr#2
ascr#3
ascr#8
icas#9
Pheromone Response
n=
CX12311
CB4856
JU258
MY1
MY14
***
B
Pheromone Response
CX12311
MY14
MY14 - CX12311 RILs
C
LOD
Chromosome
I
II
III
IV
V
X
Mt
D
i
ii
iii
background:
Chr. V (Mb)
16.8
14.3
16.043
16.006
15.861
Pheromone Response
ns
CX12311
MY14
kyIR142
kyIR139
N2
kyIR144
kyIR147
kyIR153
kyIR163
kyIR157

Figure 2.3 The icas#9 receptor *srx-43* in the *roam-1* locus mediates pheromone sensitivity

A) The *roam-1* locus defined by QTL analysis. Bar shows region used to make transgenic strains and GFP reporters (B-E,H), and is shown at higher resolution in Figure S7B.

B) An extrachromosomal N2 *srx-43* transgene (bar in A) confers icas#9 sensitivity to the *roam-1*$_{MY14}$ NIL. A similar transgene bearing a frameshift in the coding region does not. Color indicates genotype of the *roam-1* genomic locus. ***P<0.001, by ANOVA with Dunnett correction; ns, not significant.

C) *srx-43* loss of function mutants do not respond to icas#9. ***P<0.001, **P<0.01 by ANOVA with Bonferonni correction (N2) or t test (*roam-1*$_{MY14}$); ns, not significant.

D) A Mos1-mediated Single Copy Insertion (MosSCI) *srx-43* transgene from N2, but not MY14, restores icas#9 sensitivity to the N2 *srx-43*(*lf*) strain. ***P<0.001 by ANOVA with Dunnett correction; ns, not significant.

E) Bicistronic transcript expressing the green fluorescent protein downstream of the N2 (top left) or MY14 (top right) genomic *srx-43* sequence (bar in A) is limited to the ASI sensory neurons (arrows). *srx-43-GFP* translational fusion localizes to the ASI sensory cilia (bottom; arrowhead).

F and G) Ectopic expression of N2 (F) or MY14 (G) *srx-43* coding sequence in ASH sensory neurons confers sensitivity to 10 nM icas#9 (10 s pulses,

Figure 2.3 (cont.) The icas#9 receptor *srx-43* in the *roam-1* locus mediates pheromone sensitivity

grey bars). Calcium transients were detected by fluorescence changes in GCaMP3. All ascarosides were tested at 10 nM. (F) n=23 (G) n=30.

H) MosSCI *srx-43* transgene with N2 promoter and MY14 coding sequence restores response to icas#9, but a MosSCI *srx-43* transgene with MY14 promoter and N2 coding sequence does not. ***P<0.001 by ANOVA with Dunnett correction; ns, not significant. Color indicates the genotype of the *roam-1* genomic locus.

I) Digital PCR analysis of endogenous *srx-43* mRNA levels in N2 and *roam-1*$_{MY14}$ NIL. *P<0.05 by t test. N = 3 (biological replicates).

All data are shown as mean ± SEM.

Figure 2.3

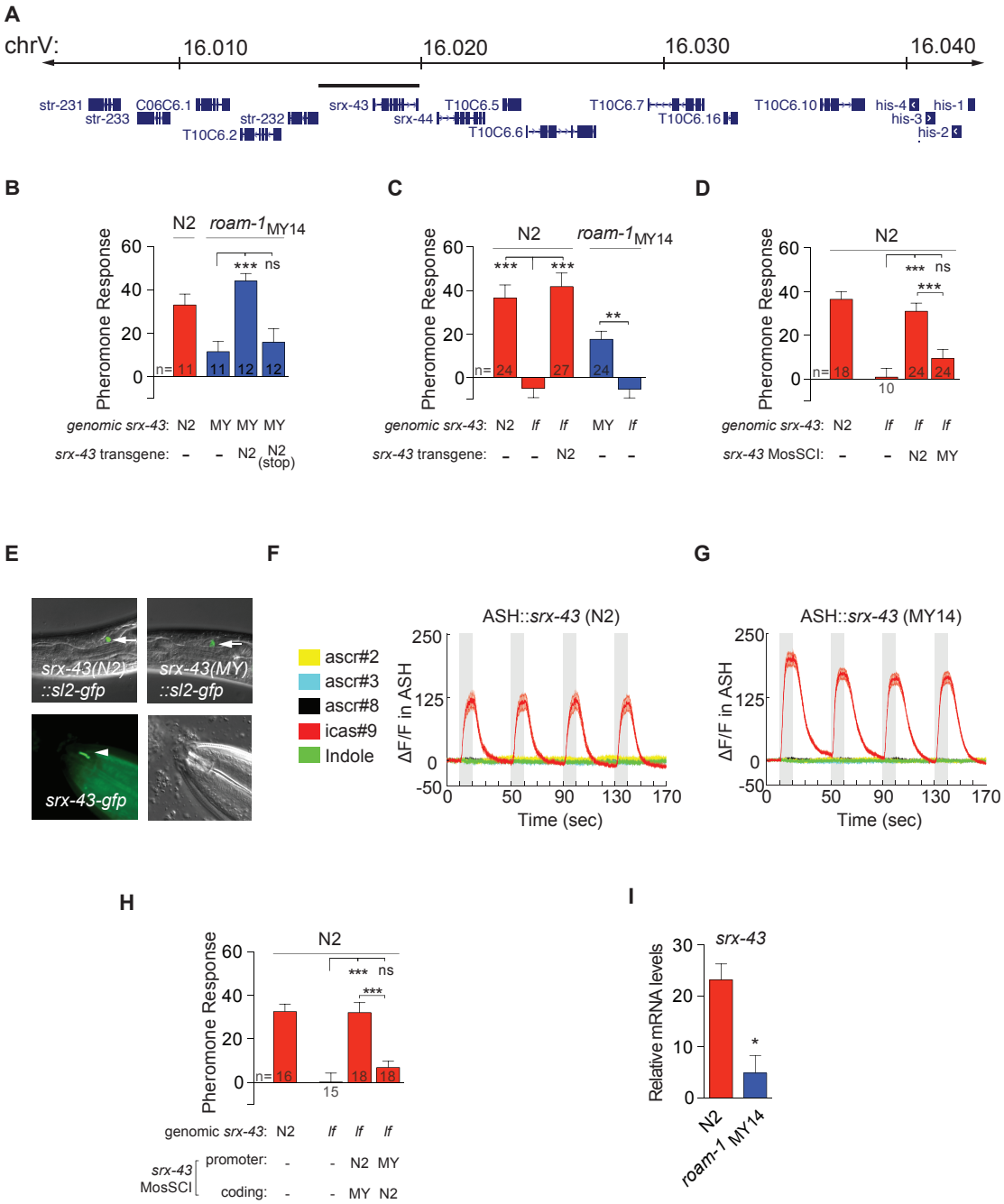
A
chrV:
16.010
16.020
16.030
16.040
str-231
C06C6.1
str-233
str-232
T10C6.2
srx-43
srx-44
T10C6.5
T10C6.6
T10C6.7
T10C6.16
T10C6.10
his-4
his-1
his-3
his-2
B
N2
roam-1MY14
Pheromone Response
genomic srx-43: N2 MY MY MY
srx-43 transgene: - - N2 N2 (stop)
C
N2
roam-1MY14
Pheromone Response
genomic srx-43: N2 lf lf MY lf
srx-43 transgene: - - N2 - -
D
N2
Pheromone Response
genomic srx-43: N2 lf lf lf
srx-43 MosSCI: - - N2 MY
E
srx-43(N2) ::sl2-gfp
srx-43(MY) ::sl2-gfp
srx-43-gfp
F
ascr#2
ascr#3
ascr#8
icas#9
Indole
ASH::srx-43 (N2)
ΔF/F in ASH
Time (sec)
G
ASH::srx-43 (MY14)
ΔF/F in ASH
Time (sec)
H
N2
Pheromone Response
genomic srx-43: N2 lf lf lf
srx-43 MosSCI promoter: - - N2 MY
srx-43 MosSCI coding: - - MY N2
I
srx-43
Relative mRNA levels
N2
roam-1 MY14

Figure 2.4 Population genetics of the *roam-1* locus and icas#9 sensitivity

A) A dendogram across 41 natural isolates representing the 20 kb *roam-1* region surrounding *srx-43.* The two major *roam-1* haplotypes from N2 and MY14 strains are indicated in red and blue respectively.

B) Whole-genome dendogram for the same strains as B, showing relationships among strains. Red and blue colors follow *roam-1* haplotypes in B.

C) icas#9 responses of natural isolates with the MY14 haplotype (blue) are consistently lower than those with the N2 haplotype (red). Pheromone response in the exploration assay shown as mean ± SEM.

Figure 2.4

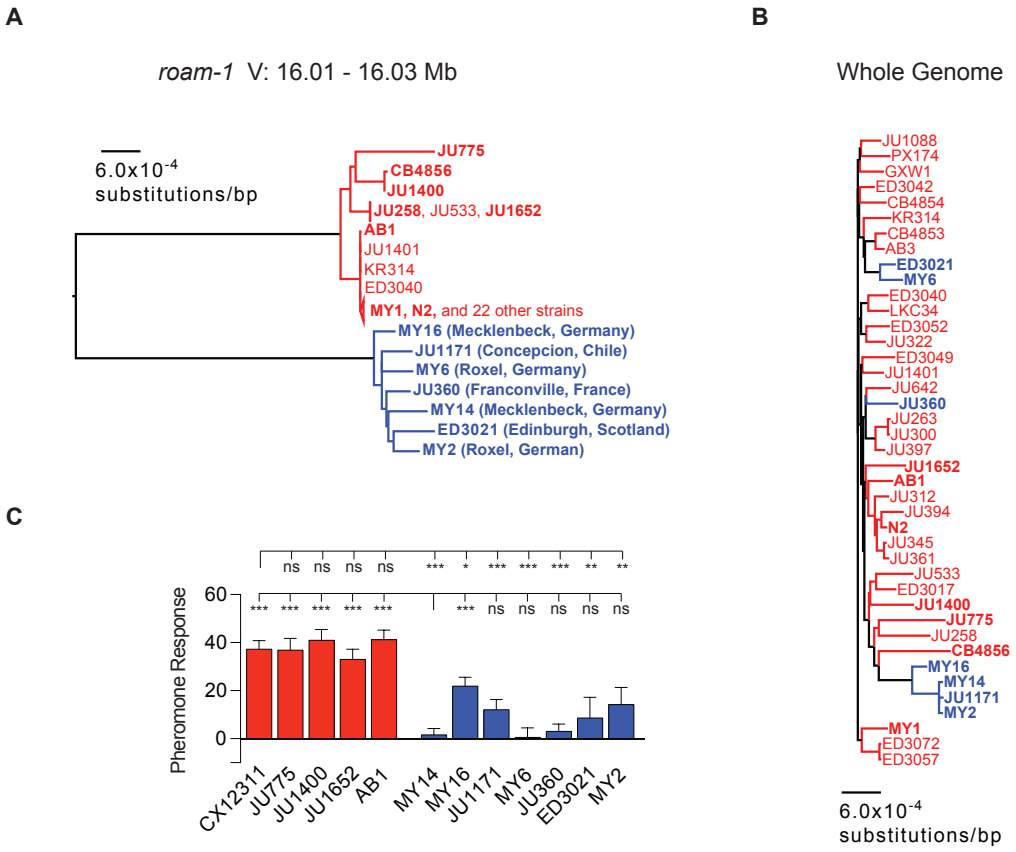
A
roam-1 V: 16.01 - 16.03 Mb
6.0x10-4
substitutions/bp
JU775
CB4856
JU1400
JU258, JU533, JU1652
AB1
JU1401
KR314
ED3040
MY1, N2, and 22 other strains
MY16 (Mecklenbeck, Germany)
JU1171 (Concepcion, Chile)
MY6 (Roxel, Germany)
JU360 (Franconville, France)
MY14 (Mecklenbeck, Germany)
ED3021 (Edinburgh, Scotland)
MY2 (Roxel, German)
B
Whole Genome
JU1088
PX174
GXW1
ED3042
CB4854
KR314
CB4853
AB3
ED3021
MY6
ED3040
LKC34
ED3052
JU322
ED3049
JU1401
JU642
JU360
JU263
JU300
JU397
JU1652
AB1
JU312
JU394
N2
JU345
JU361
JU533
ED3017
JU1400
JU775
JU258
CB4856
MY16
MY14
JU1171
MY2
MY1
ED3072
ED3057
6.0x10-4
substitutions/bp
C
Pheromone Response
60
40
20
0
ns ns ns ns *** * *** *** *** ** **
*** *** *** *** *** *** ns ns ns ns ns
CX12311
JU775
JU1400
JU1652
AB1
MY14
MY16
JU1171
MY6
JU360
ED3021
MY2

Figure 2.5 Bidirectional competitive selection at the *roam-1* locus

A) A diagram of the “boom-bust” competition experiments, initiated with equal numbers of N2 and roam-1_{MY14} animals grown to high density (thousands of animals per plate) through three transfers.
B) “Simple lawn” competition between N2 and the *roam-1*$_{MY14}$ NIL showing the ratio of each allele in the DNA harvested at transfers 1 and 3.
C) “Simple lawn” competition between N2 *srx-43(lf)* and roam-1_{MY14} *srx-43(lf)*
D) “Simple lawn” competition between N2 *daf-22(lf)* and *roam-1*$_{MY14}$ *daf-22(lf)* in the absence (left) or presence (right) of 10 nM exogenous icas#9.
E) “Patchy lawn” competition between N2 and the *roam-1*$_{MY14}$ NIL.

Grey points = individual competition experiments, red line = mean, ***P<0.001, **P<0.01, *P<0.05 compared to expected value of 0.5 by t-test with Bonferroni correction; ns, not significant.

Figure 2.5

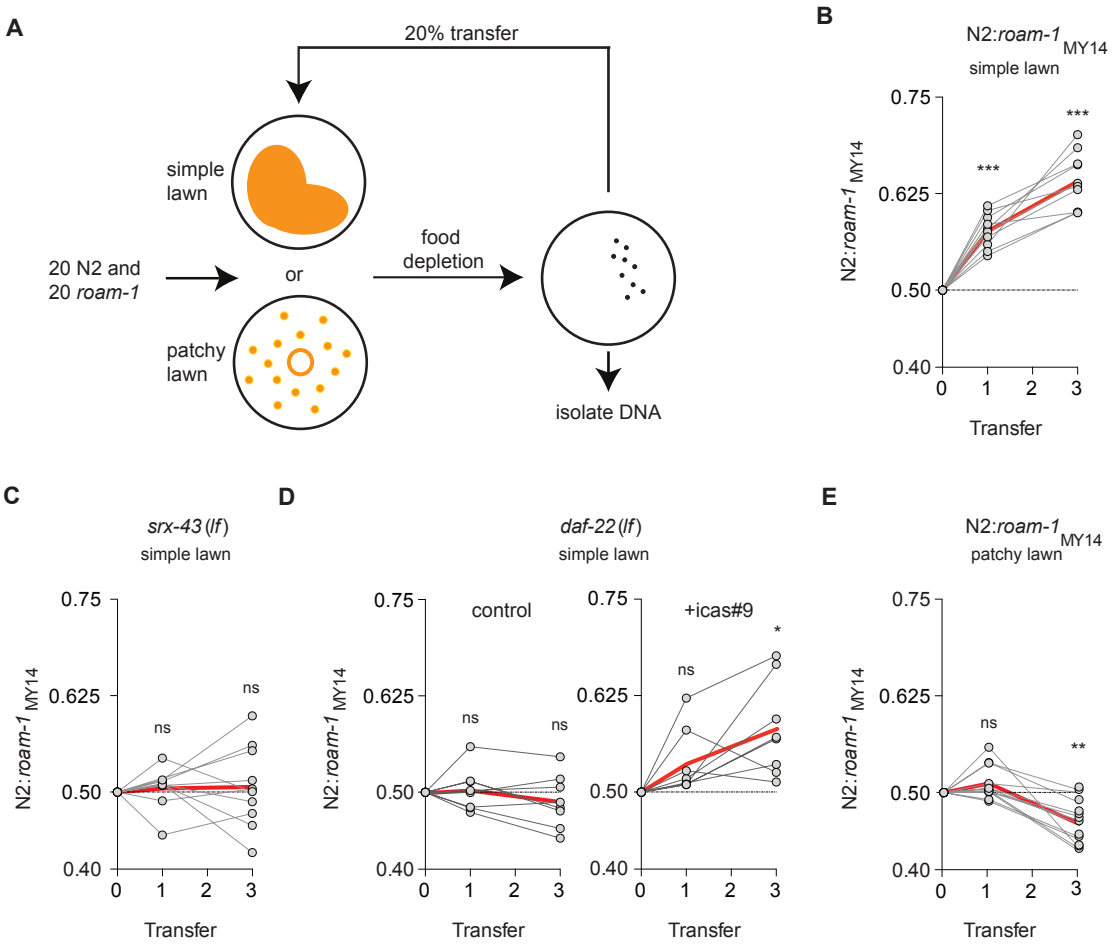
A
20% transfer
simple lawn
20 N2 and 20 roam-1
or
patchy lawn
food depletion
isolate DNA
B
N2:roam-1 MY14
simple lawn
N2:roam-1 MY14
0.75
0.625
0.50
0.40
***
***
0 1 2 3
Transfer
C
srx-43(lf)
simple lawn
N2:roam-1 MY14
ns
ns
Transfer
D
daf-22(lf)
simple lawn
control
+icas#9
ns
ns
ns
*
Transfer
E
N2:roam-1 MY14
patchy lawn
ns
**
Transfer

Figure 2.S1 Roaming and dwelling states in the presence of ascarosides

A and B) Scatter plot of average speed and angular speed (a measure of turning rate) in 10 s intervals taken from video recordings of wild-type animals in control (A) and icas#9 (B) conditions.

C and D) Speed following a reversal (C) and reversal rate (D) for roaming or dwelling wild-type animals on control, ascr#8, and icas#9-containing plates. Roaming speed is slightly slower in ascarosides (B,C).

Figure 2.S1

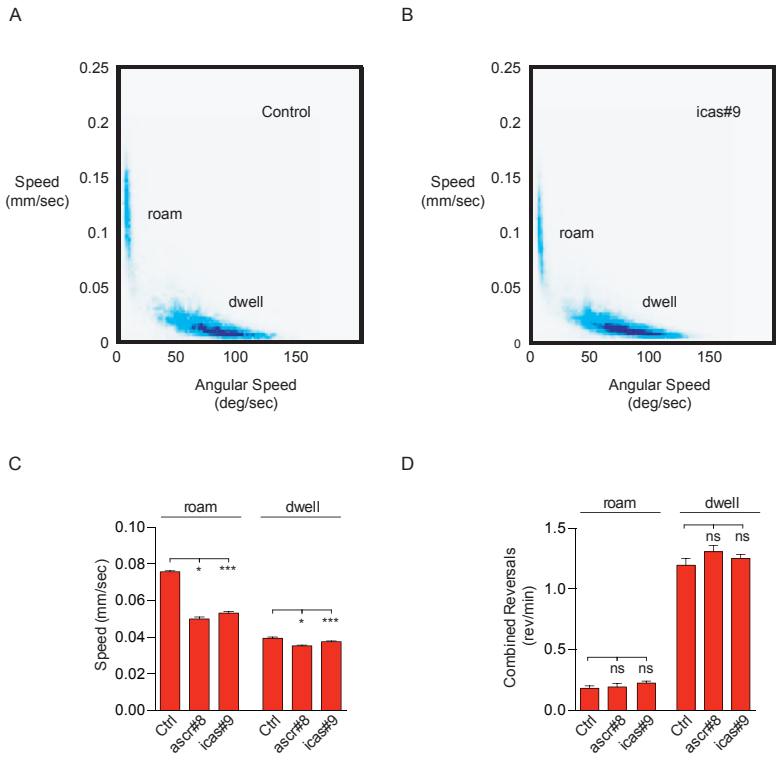
A
B
Control
icas#9
roam
dwell
Speed (mm/sec)
Angular Speed (deg/sec)
0.25
0.2
0.15
0.1
0.05
0
0
50
100
150
C
D
roam
dwell
Speed (mm/sec)
Combined Reversals (rev/min)
0.10
0.08
0.06
0.04
0.02
0.00
1.5
1.0
0.5
0.0
*
***
ns
Ctrl
ascr#8
icas#9

Figure 2.S2 Roaming and dwelling behavior of MY14

A) Fraction of time MY14 animals spend roaming or dwelling in control, ascr#8 and icas#9 conditions. n=88-109 tracks per data point. Assays were conducted in 8% O_2.

B and C) Cumulative distribution of roaming (B) and dwelling (C) state durations for MY14 animals scored in (A). Note greater shortening of roaming states in the presence of ascr#8 than in the presence of icas#9. Roaming states may be longer at baseline in the MY14 isolate than in N2 (see Fig 1).

Figure 2.S2

A

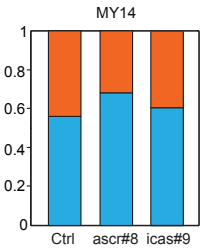

B

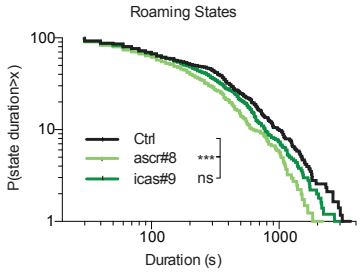

C

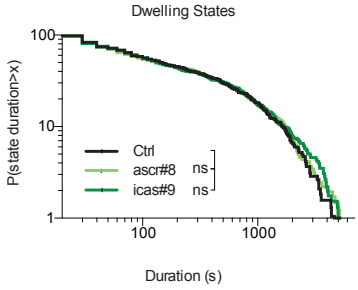

Figure 2.S3 Ascarosides produced by N2 and MY14 strains

LC-MS/MS analysis of ascarosides secreted by N2, CX12311, and MY14 strains grown on (A) OP50 or (B) HB101 bacteria. n=2-3 assays per condition.

Figure 2.S3

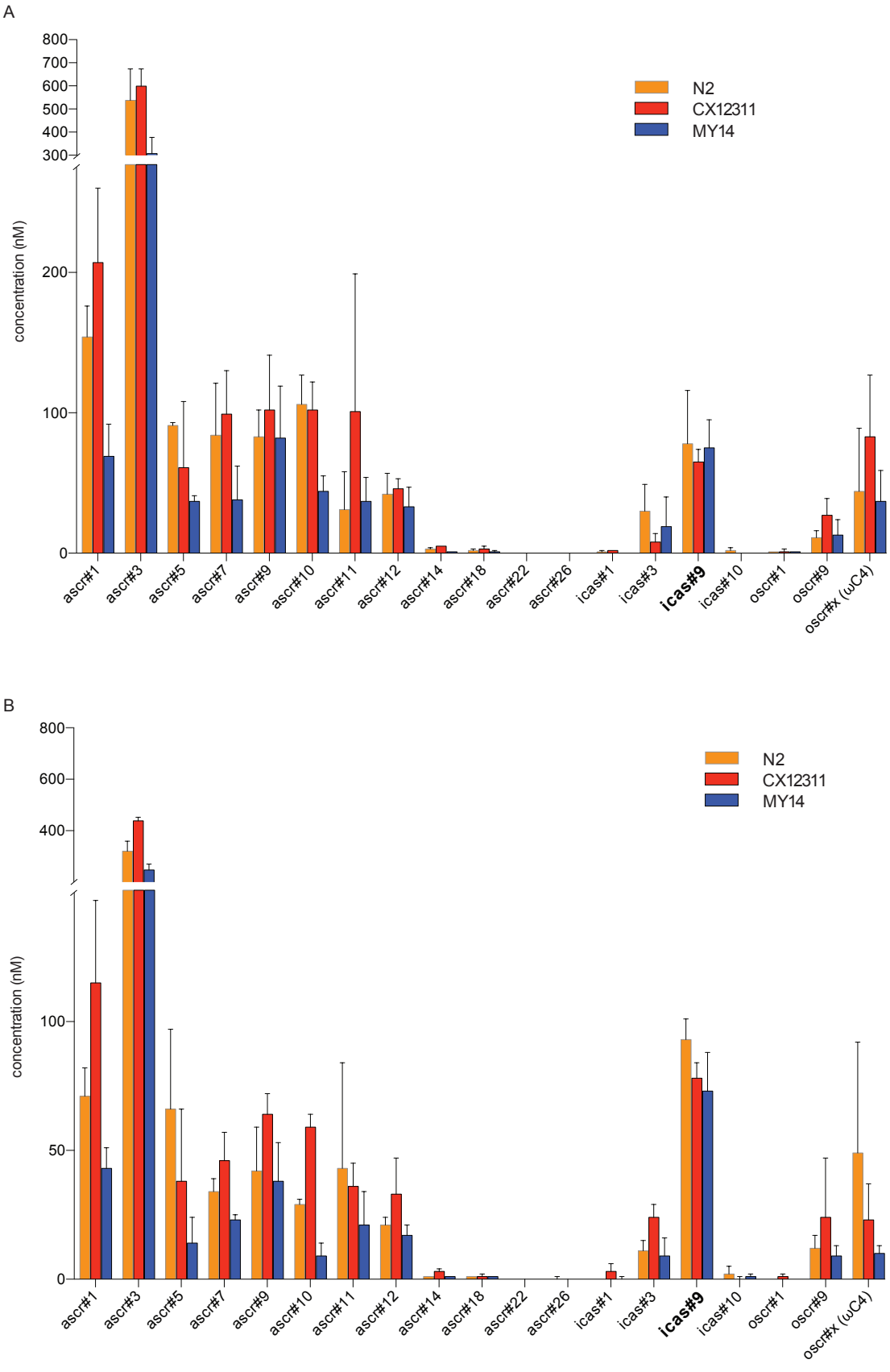
A
800
700
600
500
400
300
200
100
0
concentration (nM)
N2
CX12311
MY14
ascr#1
ascr#3
ascr#5
ascr#7
ascr#9
ascr#10
ascr#11
ascr#12
ascr#14
ascr#18
ascr#22
ascr#26
icas#1
icas#3
icas#9
icas#10
oscr#1
oscr#9
oscr#x (ωC4)
B
800
600
400
100
50
0
concentration (nM)
N2
CX12311
MY14
ascr#1
ascr#3
ascr#5
ascr#7
ascr#9
ascr#10
ascr#11
ascr#12
ascr#14
ascr#18
ascr#22
ascr#26
icas#1
icas#3
icas#9
icas#10
oscr#1
oscr#9
oscr#x (ωC4)

Figure 2.S4 Covariate analysis of 94 RILs

Covariate analysis controlling for *roam-1* genotype, testing for additive (A) or interactive (B) QTL at other loci. The horizontal line denotes the $P<0.05$ genome-wide significance threshold. LOD, log likelihood ratio.

Figure 2.S4

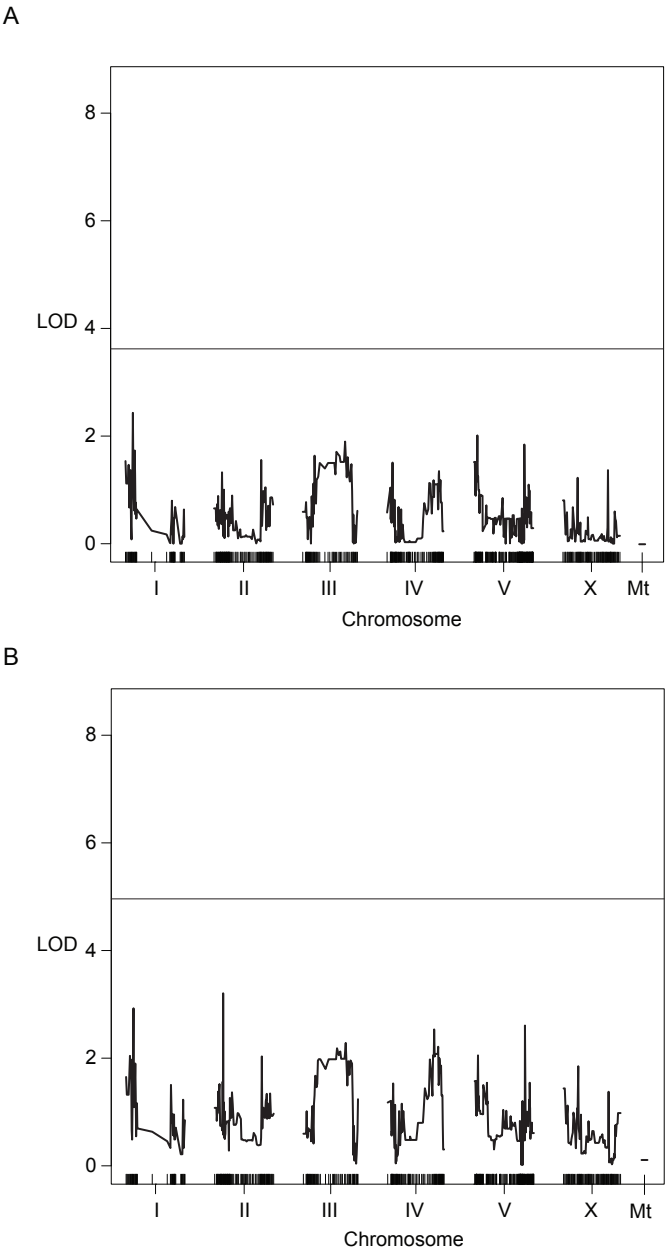
A
8
6
LOD 4
2
0
I
II
III
IV
V
X
Mt
Chromosome
B
8
6
LOD 4
2
0
I
II
III
IV
V
X
Mt
Chromosome

Figure 2.S5 ASH is insensitive to multiple ascarosides

ASH calcium imaging with GCaMP3 in control animals that do not express *srx-43* transgene, isolated as non-transgenic siblings of transgenic animals tested in Figure 3F. (n=19). Ascarosides tested at 10 nM.

Figure 2.S5

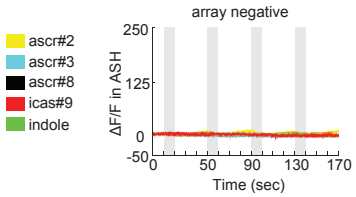
array negative
ascr#2
ascr#3
ascr#8
icas#9
indole
250
125
0
-50
ΔF/F in ASH
0
50
90
130
170
Time (sec)

Figure 2.S6 *Daf-7 (TGF-β)* involvement in pheromone response and *roam-1*

A) Regulation of *daf-7::GFP* by icas#9 occurs in N2 but not in roam-$1_{MY14.}$ Bars indicate mean fluorescence intensity ± SEM. *P<0.05 by ANOVA with Turkey's multiple comparisons test. n = # of animals, 2 neurons analyzed for all animals; experiments performed on 3 separate days.

B) Pheromone Response of *daf-3 (lf) daf-7 (lf)* is attenuated in N2 but not in *roam-*1_{MY14}. **P<0.01, ns, not significant by t test. Data represented as mean ± SEM.

C) Time course for icas#9 response. Pheromone response expressed as mean ± SEM for 2, 4, 6, 10, and 14 hours following initiation of exploration assay. ***P<0.001, ns, not significant by T test with bonferonni correction comparing squares entered in control versus 10 nm icas#9 plates. n = 12 for all time points.

Figure 2.S6

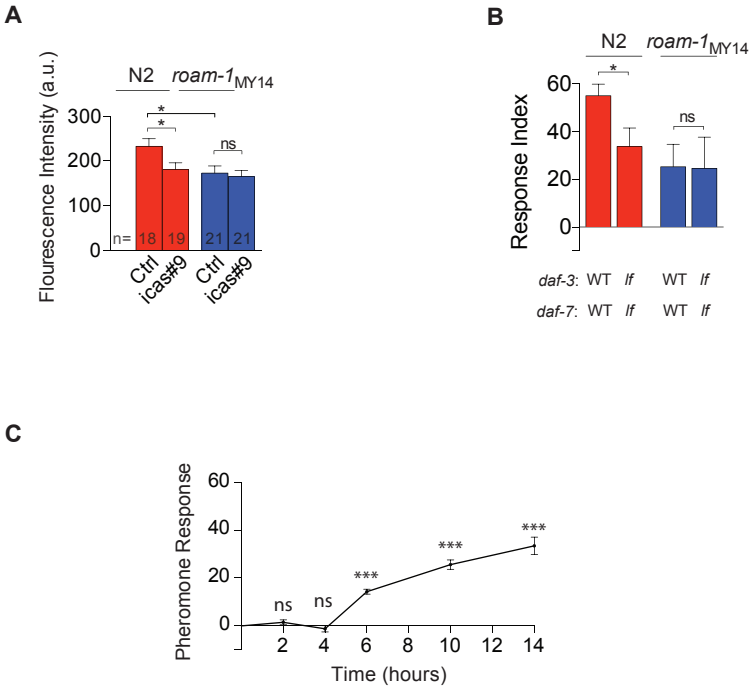
A
N2
roam-1MY14
Flourescence Intensity (a.u.)
300
200
100
0
*
*
ns
n=
18
19
21
21
Ctrl
icas#9
Ctrl
icas#9
B
N2
roam-1MY14
Response Index
60
40
20
0
*
ns
daf-3: WT lf WT lf
daf-7: WT lf WT lf
C
Pheromone Response
60
40
20
0
ns
ns
***
***
***
2
4
6
8
10
12
14
Time (hours)

Figure 2.S7 Alternative *roam-1* allele have high sequence variability

A) The *roam-1* QTL region (top). *roam-1* SNPs = SNPs with respect to the N2 reference genome that are shared by JU360, MY2, MY14, ED3021, JU1171, MY16, and MY6 and not by any other strains, according to the Million Mutation Project. Other SNPs = all other SNPs with respect to the N2 reference genome found in any of the 40 wild isolates in the Million Mutation Project.

B) Polymorphisms revealed by Sanger sequencing of *srx-43* promoter and coding region. Despite the high rate of polymorphism, there are only 4 nonsynonymous mutations in the MY14 coding sequence.

Figure 2.S7

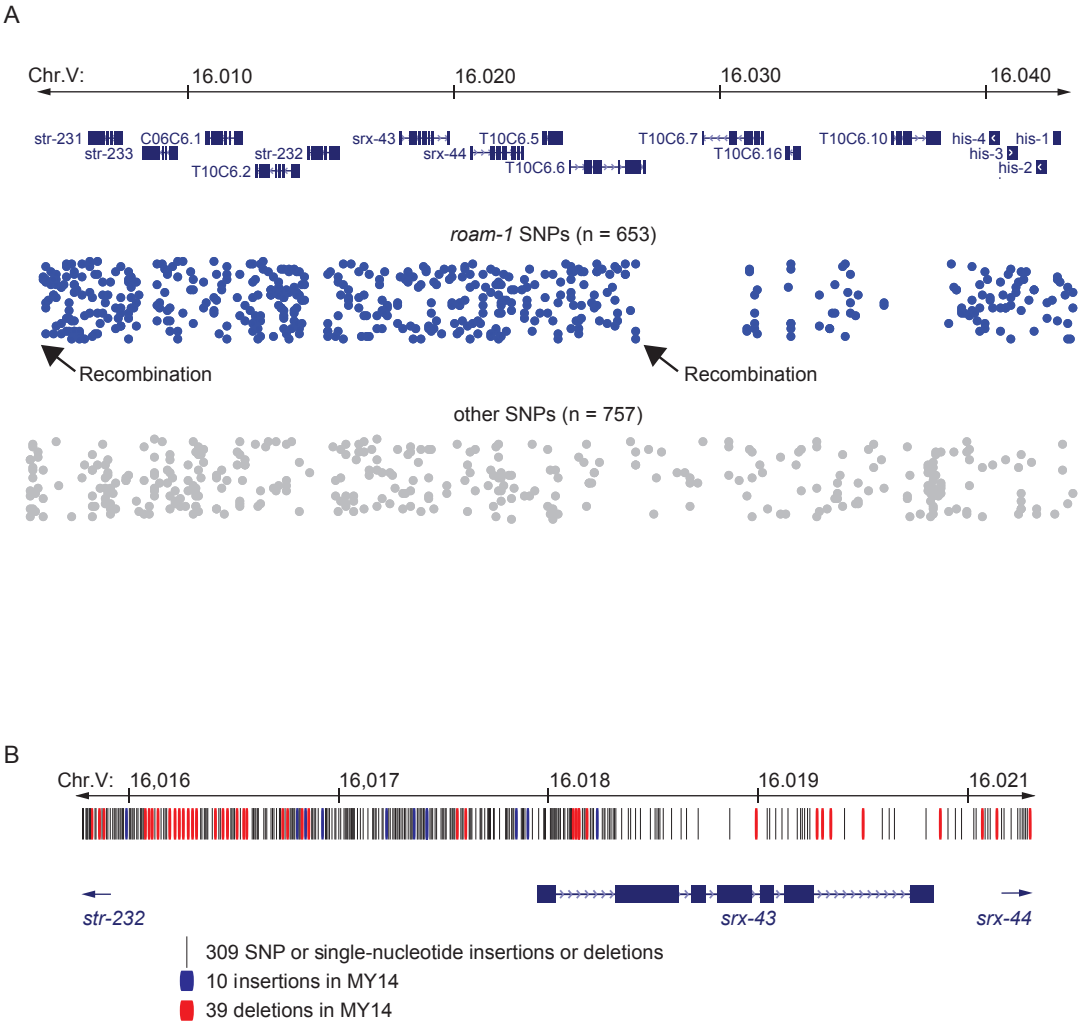
A
Chr.V:
16.010
16.020
16.030
16.040
str-231
str-233
C06C6.1
T10C6.2
str-232
srx-43
srx-44
T10C6.5
T10C6.6
T10C6.7
T10C6.16
T10C6.10
his-4
his-3
his-1
his-2
roam-1 SNPs (n = 653)
Recombination
Recombination
other SNPs (n = 757)
B
Chr.V:
16,016
16,017
16.018
16.019
16.021
str-232
srx-43
srx-44
309 SNP or single-nucleotide insertions or deletions
10 insertions in MY14
39 deletions in MY14

Figure 2.S8 Recombination between *glc-1* and *roam-1* in natural isolates

A) The *glc-1* gene has previously been shown to be under balancing selection[33], and is near *srx-43.* 76 genes are shown in the top panel. In the lower panel, blue line shows SNPs/kb for N2 and MY14 averaged over 5 kb intervals for the region spanning *srx-43* and *glc-1*. The large region of low heterozygosity between *srx-43* and *glc-1* indicates that balancing selection on *glc-1* is unlikely to account for the high heterozygosity near *srx-43.*

B) Dendogram for the *glc-1* region for strains in Figure 4A. *roam-1*$_{MY14}$ strains fall into distinct *glc-1* clades, as do *roam-1*$_{N2}$ strains.

Figure 2.S8

A

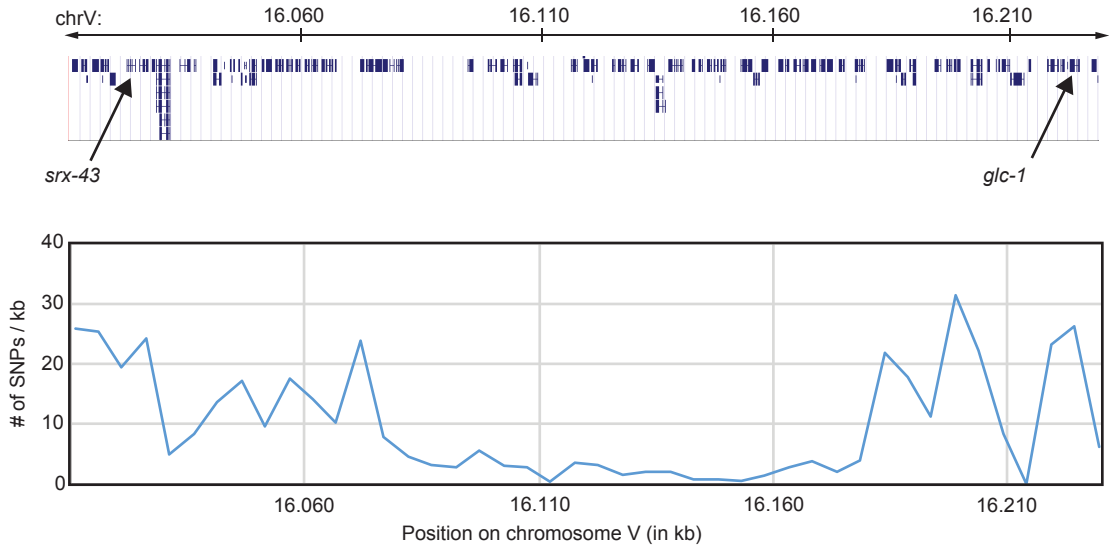

B

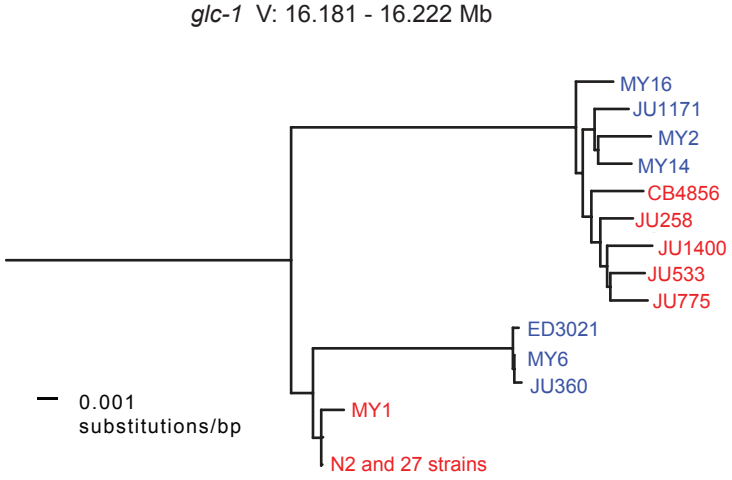

Figure 2.S9 Standard curve for dPCR experiments

Best fit line of dPCR results for known ratios of N2 to roam-1_{MY14} DNA created by mixing different ratios of genomic DNA extracted from independent N2 or *roam-1*$_{MY14}$ populations.

Figure 2.S9

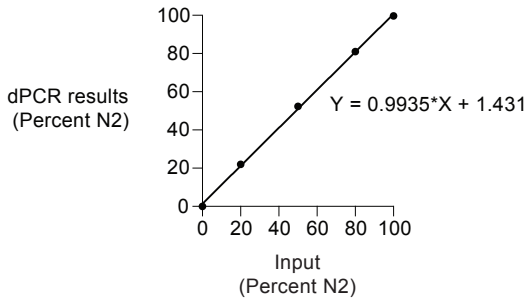
dPCR results
(Percent N2)
100
80
60
40
20
0
0 20 40 60 80 100
Input
(Percent N2)
Y = 0.9935*X + 1.431

Chapter 3:

Alternative foraging strategies arise from combinatorial expression remapping of pheromone receptor genes regulating endocrine signaling

INTRODUCTION

Social communication through signals produced and detected by members of the same species is broadly used throughout nature to organize behavior. Prokaryotes release signaling molecules that can regulate population-wide bacterial behaviors such as biofilm formation[99]; in humans, deficits in the processing of social cues are central features of major neuropsychiatric disorders including schizophrenia and autism. *Caenorhabditis elegans* communicates largely through the secretion of a class of pheromones called ascarosides that can signal an animal's sex[100], developmental stage, and feeding status as well as the population density[92,101]. At least five classes of sensory neurons detect ascarosides, which vary in their ability to induce dauer formation, male attraction, aggregation, or avoidance[48]. We have shown previously that ascarosides influence *C. elegans* foraging behavior - several ascarosides suppress an exploratory foraging state called roaming, favoring the alternative state called dwelling. The ascaroside icas#9 is a particularly potent regulator of foraging behavior in many, but not all, wild *C. elegans* strains. Mapping icas#9 insensitivity of one of the wild strains, MY14, led to the identification of a 43 kb Quantitative Trait Locus (QTL) on chromosome V for density-dependent regulation of roaming. Changes in expression of the icas#9 receptor *srx-43* in the sensory neuron ASI contribute to this QTL. MY14 has reduced *srx-43* expression, which makes it less sensitive to icas#9; indeed null mutants in *srx-43* are also insensitive to icas#9, identifying this gene as an essential icas#9 receptor.

How genes relate to individual differences in behavior is a central question of neuroscience and genetics. It is challenging in part because findings may reflect the methodology being used[102]. For instance, at present classical forward genetic screens have largely identified a set of genes that do not overlap with genes identified by examining natural variation in behavior. Indeed, the very nature of selection may favor distinct genetic architectures in classical genetics and natural trait genetics. Short-term selection may promote many small polymorphisms with additive effects, whereas, longer-duration selection may allow for the occurrence of epistasis, leading to more complicated genetic networks[102]. Most attempts at determining the genetic underpinnings of natural variants suggests that effect size of individual mutations are very small[102]. *srx-43* appeared to represent an exception, in which a single gene has a large effect on a behavioral trait. Here we show that the previously identified QTL regulating *C. elegans* icas#9 response does not reflect a single polymorphism in *srx-43*, but rather multiple changes affecting at least two genes. Changes in expression of *srx-44*, the adjacent gene and close paralog of *srx-43,* contribute this QTL. Reduced icas#9 sensitivity in strains bearing this QTL in part reflects reduced *srx-43* expression in ASI, but also reflects a gain of function in *srx-44* expression in the ASJ sensory neuron,, which antagonizes the pheromone response.

RESULTS

srx-44 increases icas#9 sensitivity in N2 and decreases sensitivity in *roam-1*$_{MY14}$

Despite the compelling results implicating *srx-43* in icas#9 sensitivity, genetic analysis excluded the simple possibility that the *roam-1* QTL (Figure 1A) can be entirely explained by altered *srx-43* expression. The F1 progeny of an N2 *srx-43(lf)* cross with N2 were sensitive to icas#9, indicating that *srx-43(lf)* is recessive. In contrast, the icas#9 insensitivity of a Near Isogenic Line (NIL) with a small introgression from MY14 surrounding *roam-1* in an N2 background was dominant (Figure 1B). This dominant effect is due to alternative alleles of *srx-44* in N2 and MY14, as described below.

Protein-terminating *srx-44(lf)* alleles were generated by CRISPR-cas9 mutagenesis in both N2 and *roam-1*$_{MY14}$ strains. In each genetic background, *srx-44(lf)* resulted in an icas#9 response that was intermediate between those of N2 and *roam-1*$_{MY14}$ (Figure 1C). N2 with an *srx-44(lf)* mutation was less icas#9 sensitive than N2, but *roam-1*$_{MY14}$ *srx-44(lf)* was more icas#9 sensitive than *roam-1*$_{MY14}$ (Figure 1C), indicating that the *srx-44* alleles in N2 and *roam-1*$_{MY14}$ have opposite effects on icas#9 sensitivity. *srx-44* cDNA did not confer icas#9 sensitivity when expressed in ASH neurons whereas *srx-43* cDNA did (Figure S1). The weaker effects of *srx-44(lf)* compared to *srx-43(lf)* suggest that *srx-44* is a modifier gene rather than an essential icas#9 sensor. In agreement with this idea, a *roam-1* $_{MY14}$ *srx-43(lf) srx-44(lf)* strain generated by CRISPR-Cas9 mutagenesis was insensitive to icas#9 (Figure 1C), suggesting that *srx-43* is

essential for icas#9 sensitivity in all genetic backgrounds, while *srx-44* acts to modify its function.

With this information, genetic tests were conducted to assess the contributions of *srx-43* and *srx-44* to the *roam-1* QTL. The F1 progeny of a *roam-1*$_{MY14}$ *srx-44(lf)* cross with N2 resembled N2 (Figure 1D), indicating that *srx-44* is necessary for the dominance of the *roam-1*$_{MY14}$ foraging phenotype and facilitating a complementation experiment testing for a loss of *srx-43* function in *roam-1*$_{MY14}$. The F1 progeny of a cross between *roam-1*$_{MY14}$ *srx-44(lf)* and N2 *srx-43(lf)* remained insensitive to icas#9 (Figure 1D). This failure to complement confirmed reduced *srx-43* function. To test for altered *srx-44* function, a reciprocal hemizygosity test was conducted: The F1 progeny of N2 *srx-44(lf)* crossed with *roam-1*$_{MY14}$ were compared to the F1 progeny of N2 crossed with *roam-1*$_{MY14}$ *srx-44(lf).* Although the resulting hemizygotes differed genetically only in their functional *srx-44* allele, they demonstrated significantly different icas#9 sensitivity (Figure 1E), confirming *srx-44* allele affects foraging behavior.

As *srx-43* and *srx-44* are closely linked, manipulations of *srx-44* may directly impact *srx-43* expression, which has a well-established connection to icas#9 sensitivity (Chapter 2). Therefore in N2 and in a *roam-1*$_{MY14}$ N2 NIL, the endogenous *srx-43* was knocked out and replaced with a WT N2 allele on a separate chromosome using Mos1 Single Copy Insertion. Although the resulting animals had identical *srx-43* alleles, the *roam-1*$_{MY14}$ strain was slightly less sensitive to icas#9 than the N2 strain (Figure 1F). These experiments indicate

that both a loss of *srx-43* function and a gain of *srx-44* function in *roam-1*$_{MY14}$ contribute to icas#9 insensitivity.

Sequence diversity in the promoter accounts for differences in the pheromone response

srx-44 falls within a hypervariable region on chromosome V; sanger sequencing the 2.8 Kb gene and promoter revealed that MY14 and N2 sequences differed by 5.0% (Figure 2A), which is five times the genome-wide average[87]. Transgenes were used to localize the changes responsible for altered *srx-44* activity between N2 and MY14. The *roam-1*$_{MY14}$ allele was dominant in the genomic context, but its defect in pheromone sensitivity was suppressed by high-copy transgenes that expressed the N2 *srx-44* gene(Figure 2B). Niether a N2 *srx-44* gene mutated to contain a nonsense mutation nor a MY14 *srx-44* gene were able to confer pheromone sensitivity on *roam-1*$_{MY14}$ animals (Figure 2B).

To localize the biological difference between the N2 and MY14 *srx-44* gene, transgenes with swapped promoters and coding regions were used. Transgenes with the N2 *srx-44* promoter restored icas#9 sensitivity regardless of the coding region, whereas transgenes with the MY14 promoter did not rescue pheromone sensitivity when driving either N2 or MY14 coding regions (Figure 2B). Therefore, the promoter of *srx-44* accounts for the differential activity of N2 and MY14 genes (Figure 2C).

The N2 and MY14 promoters differ at 35 out of the 515 bases between the start codon of *srx-44* and the 5' adjacent gene. Nine changes cluster in a region

34-72 bp upstream of the start codon of *srx-44* (Figure 2A, red bar). Exchanging JUST this proximal promoter sequence in *srx-44* transgenes was sufficient to alter their effect on icas#9 sensitivity: transgenes with N2 sequence in the proximal promoter restored pheromone response, but transgenes with MY14 proximal promoter sequence and N2 distal promoter and coding region were not active (Figure 2D).

To confirm the biological importance of this potential regulatory site, the sequence 34-72 bp upstream of the *srx-44* start codon were precisely exchanged at the endogenous genomic loci of N2 and *roam-1*$_{MY14}$ using oligonucleotide-templated homologous recombination with CRISPR/Cas9. Introducing the MY14 *srx-44* proximal promoter element into the N2 genome reduced response to icas#9 (Figure 2E). Conversely, the N2 proximal promoter element for *srx-44* enhanced icas#9 sensitivity in a *roam-1*$_{MY14}$ N2 NIL (Figure 2E). These experiments localized altered icas#9 sensitivity to 9 bp in the proximal promoter that vary between N2 and MY14.

srx-44 acts in different neurons to promote or inhibit icas#9 sensitivity

To understand how altered *srx-44* activity was conferred by the promoter sequence, we explored the expression pattern of *srx-44* using N2 and MY14 transgenes. Transgenes with the N2 promoter sequence used in Figures 2C and 2D, drove the green fluorescent protein (GFP) expression selectively in the two ADL sensory neurons (Figure 3A). The same GFP expression pattern was observed with transgenes with the N2 proximal promoter and the MY14 distal

promoter (Figure 3A). In contrast, transgenes with either the full MY14 promoter or a MY14 proximal promoter and a N2 distal promoter drove GFP expression in ADL and ASJ sensory neurons (Figure 3A). These experiments indicate that the functionally significant 9 bp change upstream of *srx-44* regulates the site of *srx-44* expression.

The expression analysis suggests a hypothesis for the opposing functions of *srx-44* in N2 and *roam-1*$_{MY14}$: *srx-44* activity in ADL might inscrease icas#9 sensitivity, whereas *srx-44* activity in ASJ might suppress icas#9 responses. We tested this model directly by expressing *srx-44* in either ASJ or ADL neurons under the control of other promoters. Expression of *srx-44* with an ASJ-specific promoter reduced icas#9 responses in N2 (Figure 3B), consistent with a suppressive activity of ASJ. Overexpression of *srx-44* under an ADL-specific promoter increased icas#9 responses in *roam-1*$_{MY14}$ (Figure 4K), supporting a positive role for ADL, even in the presence of the antagonistic ASJ expression in *roam-1*$_{MY14}$.

Based on our prior discoveries with *srx-43*, a likely mechanism by which ASJ and ADL could affect roaming and dwelling is by releasing neurotransmitters or neuropeptides. The tetanus toxin light chain, which cleaves synaptobrevin, can be used to reduce neurotransmitter and neuropeptide secretion in a cell-selective manner. ADL::tetanus toxin reduced the response to icas#9 in N2 (Figure 3C), supporting the hypothesis that that vesicular release from ADL enhances N2 pheromone sensitivity. ASJ::tetanus toxin restored the icas#9 response in *roam-1*$_{MY14}$ (Figure 3C), supporting the hypothesis that vesicular release from ASJ

antagonizes pheromone sensitivity. Neither ADL::tetanus toxin or ASJ::tetanus toxin had a significant effect in N2 *srx-44*(*lf*) mutants, indicating that these neurons modulate icas#9 responses by coupling *srx-44* expression to vesicular release.

icas#9 influences behavior through *tgf-β* and insulin signaling pathways

Previous work showed that regulation of *daf-7 (*tgf-β) transcription in ASI contributes to the icas#9 foraging response, and that alterations in icas#9 regulation of *daf-7* accounts for part of the difference between N2 and *roam-1*$_{MY14}$ (Chapter 2). The presence of *srx-44* in ASJ led us to consider *daf-28* (insulin) signaling, as *daf-28* is secreted from both ASI and ASJ and operates in parallel to *daf-7* to mediate effects of ascarosides on development.

The commonly used *daf-28(sa191)* loss of function allele is an interfering mutation that is thought to antagonize the activity of several insulin-related peptides that are partly redundant with *daf-28*[103]. These *daf-28(lf)* animals demonstrated significantly less roaming at baseline than WT (Figure S2), which is consistent with the observation that dauer-promoting ascarosides both downregulate *daf-28* and suppress roaming. To quantify the effects of 10 nM icas#9 on *daf-28,* we used integrated *daf-28::*GFP reporters that are expressed in both ASI and ASJ. Animals were treated with icas#9 for the same period used in behavioral assays and then examined using quantitative microscopy. In N2 animals, icas#9 exposure lowered *daf-28::GFP* by 37% in ASI and by 28% in

ASJ (Figure 4A). However in *roam-1*$_{MY14}$, icas#9 failed to suppress *daf-28::GFP* levels (Figure 4A).

N2 and the *roam*-1$_{MY14}$ N2 NIL differ in a 182 kb region encompassing the *roam-1* QTLs and containing a total of 81 genes. To confirm that changes in *srx-43* and *srx-44* could account for altered endocrine signaling in *roam-1*$_{MY14}$, we looked at icas#9 regulation of *daf-28::GFP* in N2 *srx-43(lf)* and in *roam*-1$_{MY14}$ *srx-44(lf).* In N2 *srx-43(lf), icas#9* did not decrease *daf-28::GFP* in either ASI or ASJ (Figure 4A). This result shows that *srx-43* activity in N2 is necessary for icas#9 regulation of *daf-28::GFP,* as well as the effect of this pheromone on behavior. Interestingly, icas#9 reduced *daf-28::GFP* expression in ASI neurons of *roam-1*$_{MY14}$ *srx-44 (lf)* animals, although it did not have this effect on *roam-1* $_{MY14}$ (Figure 4A). This result suggests that *srx-44* activity in *roam-1*$_{MY14}$, most likely in ASJ, non-autonomously suppresses icas#9 regulation of *daf-28* in ASI. Together these experiments indicate that both a loss of *srx-43* function and a gain of *srx-44* function contribute to the attenuated regulation of neuroendocrine factors by icas#9 in *roam-1*$_{MY14}$.

Although dauer-inducing ascaroside pheromones have previously been shown to regulate the expression of the ASI specific *str-3* chemoreceptor, a *str-3::GFP* reporter was not regulated by icas#9 (Figure S3). This result reveals differences in the transcriptional effects of icas#9 and ascarosides such as ascr#5 that more potently regulate dauer formation even though both sets of pheromones act on overlapping neurons.

The above results suggest that ascarosides regulate expression of *daf-28* in addition to *daf-7* to alter foraging behavior. To confirm the importance of *daf-28* regulation for N2 foraging response to pheromone, we examined animals with a loss-of-function mutation in *daf-16,* a transcription factor whose inhibition is a common readout of the insulin pathway that includes *daf-28. daf-16 (lf)* mutants resembled N2 animals in their basal exploration in the absence of pheromones, but responded significantly less strongly to icas#9 than N2 (Figure 4B). This partial suppression was reminscent of the partial suppresion mediated by *daf-3*, the transcription factor that is the target of *daf-7* signaling. *daf-28/daf-16 and daf-7/daf-3* signaling pathways converge upon the transcription factor *daf-12* to induce dauer formation, so we asked whether a similar convergence occurs in foraging response to icas#9. daf-*12 (lf)* animals failed to respond at all to icas#9 (figure 4C). Thus the *daf-7 (tgf*-β*)* and *daf-28 (insulin)* pathways, regulated by *srx-44*, converge upon *daf-12* to mediate the effect of icas#9 on foraging behavior.

DISCUSSION

The genetic underpinnings of natural traits are often complex. Here we show that a previously identified QTL for pheromone response, *roam-1*, reflects changes in at least two genes. Previously we had shown that reduced expression of the icas#9 receptor *srx-43* contributes to decreased pheromone response in wild strains with a MY14 *roam-1* haplotype. We find that changes in *srx-44,* a homologous chemoreceptor, also contributes to *roam-1*. The relation between

srx-44 and behavior is not simple. Depending on its site of expression in either ADL or ASJ, *srx-44* promotes or inhibits pheromone responses, respectively. Naturally occurring icas#9 insensitivity stems in part from increased expression of *srx-44* in ASJ, in addition to reduced *srx-43* expression in ASI.

Sensory receptors evolve rapidly between species based on their ecological needs[2,3]. These families quickly acquire and lose new members by duplication and divergence, and are therefore known to acquire new properties at the level of protein function. For example, the G protein-coupled receptors for sweet taste have been lost several times independently in carnivorous vertebrates such as cats, reptiles, and bats, which lack sugar in their diet; the reappearance of a sugar-rich diet in nectar-feeding birds was accompanied by the elaboration of new sweet taste receptors from an amino acid receptor. Previous studies of *C. elegans* and another species, *C. briggsae,* showed how sensory receptor gene loss can cause a selective advantage in a laboratory environment. Deletions in the C3 ascaroside receptor genes *srg-36* and *srg-37* arose spontaneously in the laboratory on two separate occasions in which *C. elegans* was continuously cultivated at high densities that promote dauer formation[43]. A spontaneous deletion in the *C. briggsae* ortholog of *srg-36/37* arose when it was cultivated in the same conditions. Presumably, the loss of dauer formation allowed these strains to overgrow their wild-type competitors[43].

In the *roam-1* QTL, chemoreceptor genes have undergone a more subtle elaboration. The *srx-43* and *srx-44* genes are present and have detectable activity in both N2 and MY14 strains; the *roam-1* QTL respecifies behaviors by

modifying their levels and sites of expression. It is noteworthy that the *roam-1*$_{MY14}$ *srx-44* that confers icas#9 resistance does so not by losing its site of expression in ADL, but by retaining that site and gaining a new antagonistic site, ASJ. Natural alleles like *roam-1*$_{MY14}$ may be less likely to delete genes outright than artificially-selected alleles like *srg-36/37* because a wider range of natural conditions could maintain selective pressure for gene function.

Figure 3.1 *srx-43* and *srx-44* both influence icas#9 sensitivity

A) The *roam-1* locus. Black bar indicates genomic region used in rescue experiments in figure 2B-D.

B) The icas#9 response expressed as mean ± SEM of parental strains and of the F1 progeny from crosses between N2 and *roam-1*$_{MY14}$ or N2 *srx-43(lf)*. ***P<0.001; ns, not significant by ANOVA with Dunnett correction.

C) *srx-43* and *srx-44* loss-of-function mutants. Bars indicate pheromone response expressed as mean ± SEM. ***P<0.001,*P<0.05 by t test (N2) or by ANOVA with Dunnett correction (*roam-1*$_{MY14}$).

D) *srx-43 c*omplementation test*.* Bars indicate mean icas#9 response ± SEM of parental strains and of F1 progeny from *crosses* between *roam-1*$_{MY14}$ *srx-44(lf)* and N2 or N2 *srx-43(lf)*. ***P<0.001; ns = not significant by ANOVA with Dunnett correction.

E) Reciprocal hemizygosity test for *srx-44*. Bars indicate icas#9 response ± SEM of the F1 progeny from crosses between N2 and *roam-1*$_{MY14}$ *srx-44(lf)* and between N2 *srx-44(lf)* and *roam-1.*

F) The pheromone sensitivity of N2 and r*oam-1*$_{MY14}$ strains with the endogenous *srx-43* replaced with a WT allele on chromosome II through Mos Single Copy Insertion (MosSCI). Bars show icas#9 response expressed as mean ± SEM. *'*genomic *srx-43'* indicates endogenous *srx-43* allele. 'MosSCI *srx-43*' indicates chromosome II MosSCI *srx-43* allele.

For A-E, Bar and letter color indicates genotype at the *roam-1* locus (Red = N2; Blue = MY14; red and blue stripes = heterozygous).

Figure 3.1

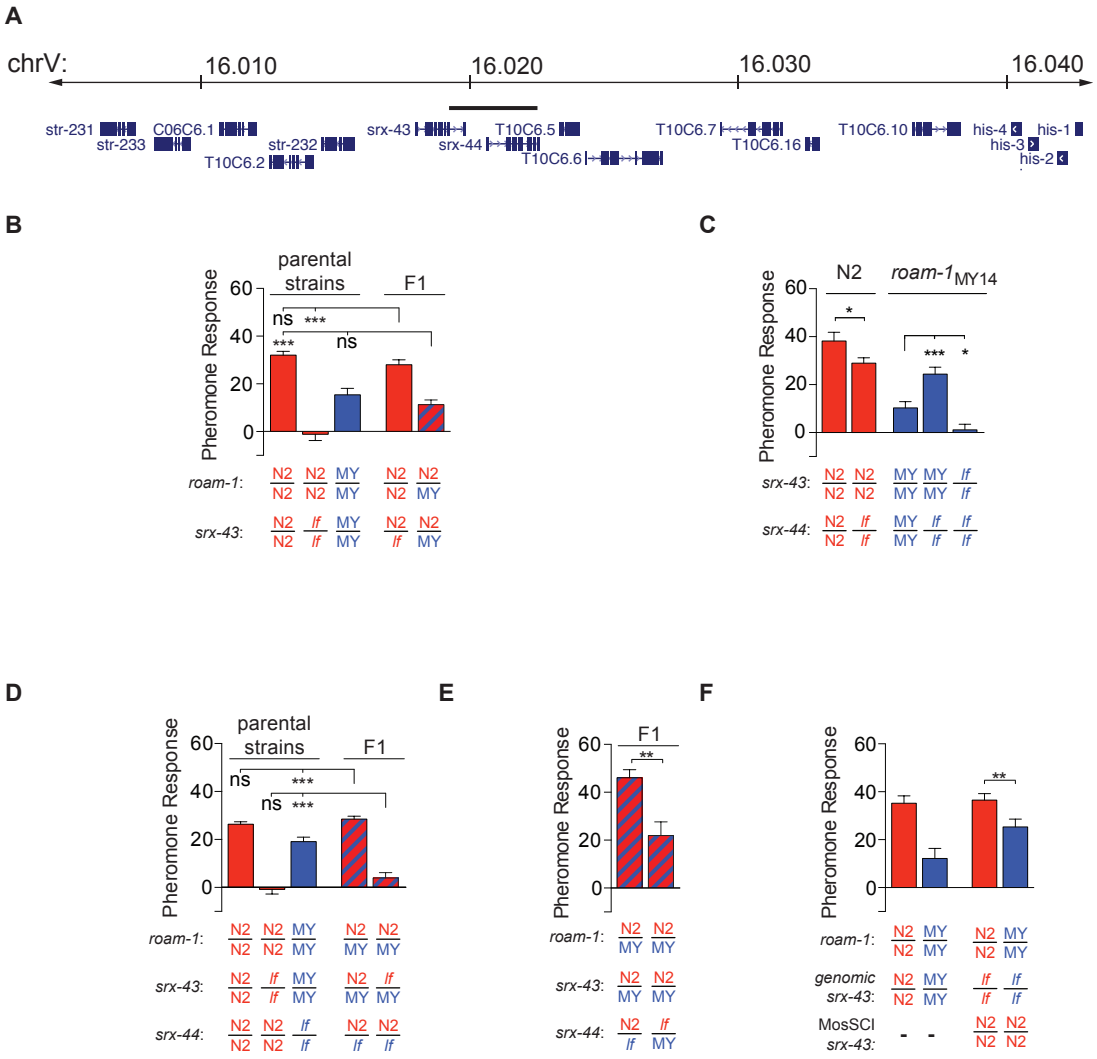
A
chrV:
16.010
16.020
16.030
16.040
str-231
str-233
C06C6.1
str-232
T10C6.2
srx-43
srx-44
T10C6.5
T10C6.6
T10C6.7
T10C6.16
T10C6.10
his-4
his-1
his-3
his-2
B
parental strains
F1
Pheromone Response
ns
***
roam-1:
srx-43:
C
N2
roam-1MY14
srx-43:
srx-44:
D
parental strains
F1
roam-1:
srx-43:
srx-44:
E
F1
roam-1:
srx-43:
srx-44:
F
roam-1:
genomic srx-43:
MosSCI srx-43:

Figure 3.2 Change in the proximal promoter underly altered *srx-44* activity in MY14

A) N2/MY14 polymorphisms in the *srx-44* promoter and coding region as revealed by Sanger sequencing. Red ovals and yellow rectangles indicate single nucleotide polymorphisms (SNPs) and insertion/deletion events respectively. Red bar indicates the cluster of polymorphism in the proximal promoter examined in 2D and 2E and shown bellow.

B) N2 *srx-44* transgenes (depicted with black bar in figure 1A) confer icas#9 sensitivity on *roam-1*$_{MY14}$. A similar transgene bearing a frameshift in the coding region does not, nor does a MY14 *srx-44* transgene. ***P<0.001; ns, not significant by ANOVA with Dunnett correction.

C) *srx-44* transgenes with a N2 promoter confer icas#9 sensitivity on *roam-1* $_{MY14}$, whereas *srx-44* transgenes with a MY14 promoter do not. ***P<0.001; ns, not significant by ANOVA with Dunnett correction.

D) The proximal but not distal promoter accounts for N2 *srx-44* activity. **P<0.001; ns, not significant by ANOVA with Dunnett correction.

E) The icas#9 response of Allele Replacement Lines for the *srx-44* proximal promoter made with CRISPR/Cas9.

For B-D data presented as mean ± SEM. Color shows genotype at the *roam-1* locus (Red = N2; Blue = MY14).

Figure 3.2

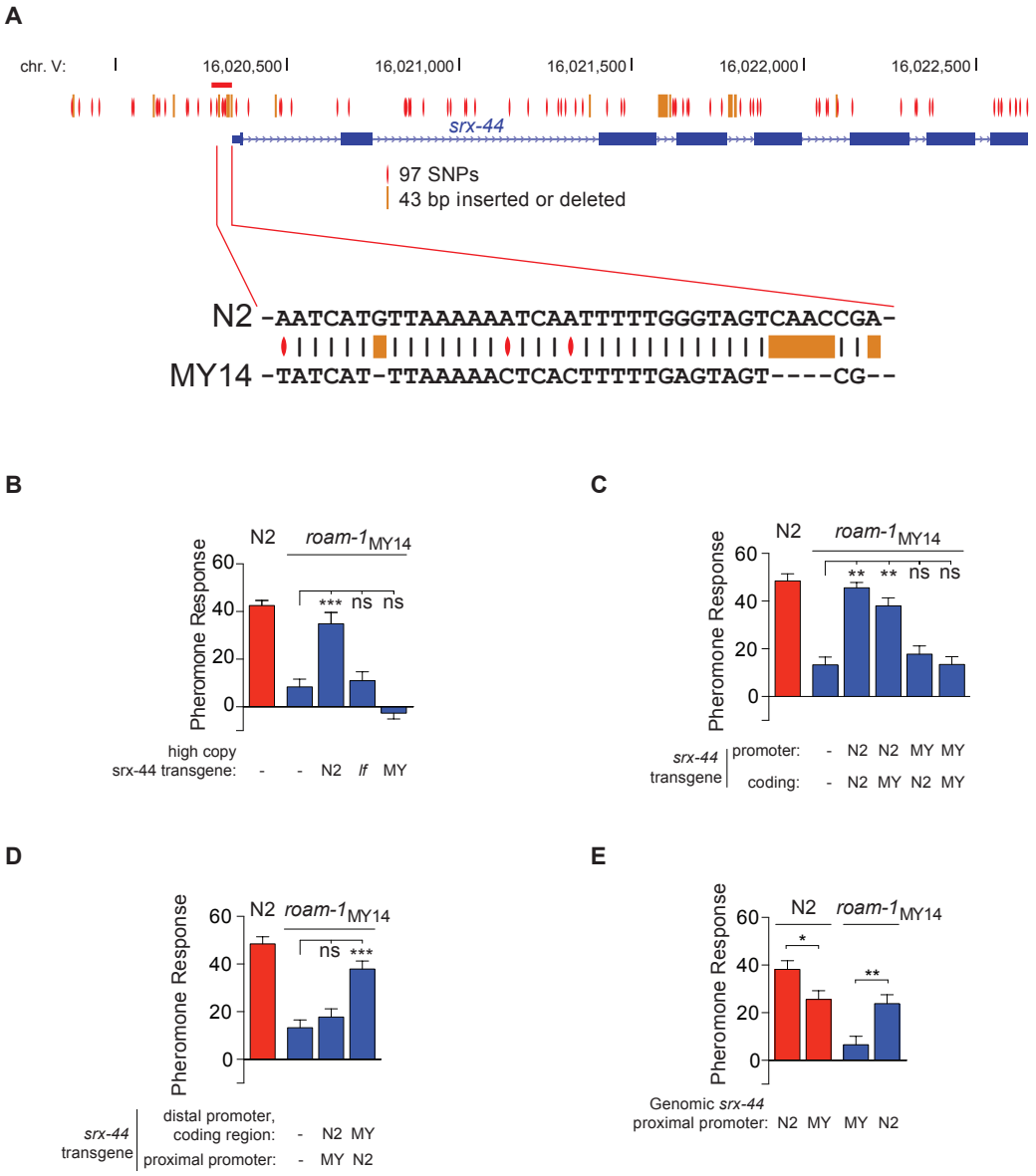
A
chr. V:
16,020,500
16,021,000
16,021,500
16,022,000
16,022,500
srx-44
97 SNPs
43 bp inserted or deleted
N2 -AATCATGTTAAAAAATCAATTTTTGGGTAGTCAACCGA-
MY14 -TATCAT-TTAAAAACTCACTTTTTGAGTAGT----CG--
B
Pheromone Response
N2
roam-1MY14
*** ns ns
high copy
srx-44 transgene: - - N2 lf MY
C
** ** ns ns
srx-44 transgene
promoter: - N2 N2 MY MY
coding: - N2 MY N2 MY
D
ns ***
srx-44 transgene
distal promoter, coding region: - N2 MY
proximal promoter: - MY N2
E
*
**
Genomic srx-44
proximal promoter: N2 MY MY N2

Figure 3.3 *srx-44* site of expression determines whether it potentiates (ADL) or suppresses (ASJ) behavioral response to icas#9

A) GFP driven by *srx-44* promoters. Top left = P*srx-44(N2)::GFP*; Top right = Ps*rx-44(MY14)::GFP.* Bottom left = *Psrx-44(N2 distal promoter/MY14proximal promoter)::GFP;* Bottom right = *Psrx-44(MY14 distal promoter/N2 proximal promoter)::GFP.* Arrowheads indicate ADL, Arrows indicate ASJ.

B) Transgenes expressing *srx-44* under ASJ or ADL specific promoters can influence pheromone response. Bars indicate mean icas#9 response ± SEM. ***P<0.001, **P<0.01 by t test.

C) Tetanus toxin (TeTx) inhibition of release of neurotransmitters and neuropeptides in ASJ or ADL impacts icas#9 sensitivity in an *srx-44* dependent manner. Bars indicate mean icas#9 response ± SEM. ***P<0.001,* P<0.05, ns = not significant by t test (N2 or *roam-1*$_{MY14}$) or by ANOVA with Dunnett correction (N2 *srx-43(lf)*).

Color shows genotype at the *roam-1* locus (Red = N2; Blue = MY14).

Figure 3.3

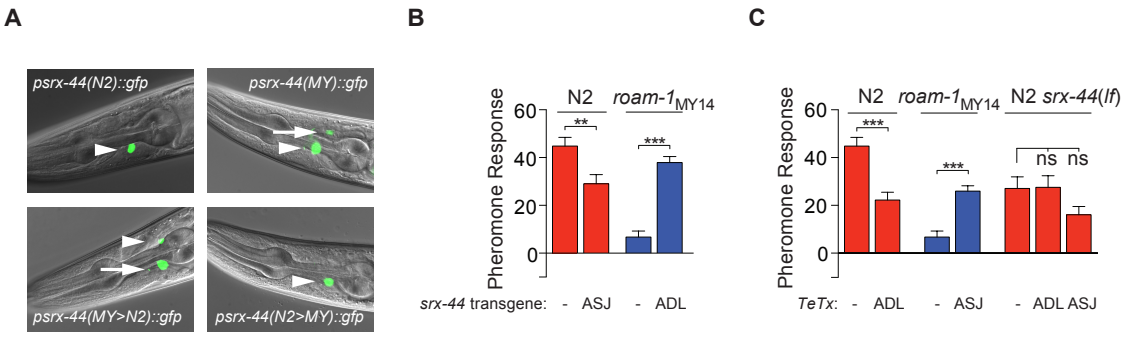
A
psrx-44(N2)::gfp
psrx-44(MY)::gfp
psrx-44(MY>N2)::gfp
psrx-44(N2>MY)::gfp
B
N2
roam-1MY14
Pheromone Response
60
40
20
0
**
***
srx-44 transgene: - ASJ - ADL
C
N2
roam-1MY14
N2 srx-44(lf)
Pheromone Response
60
40
20
0
***
***
ns ns
TeTx: - ADL - ASJ - ADL ASJ

Figure 3.4 *srx-43* and *srx-44* regulate foraging behavior through regulation of endocrine signaling pathways

A) The influence of icas#9 on ASI and ASJ *daf-28::GFP* expression in N2, *roam-1*$_{MY14}$, N2 s*rx-43(lf)*, and *roam-1*$_{MY14}$ *srx-44(lf)* animals. Bars indicate mean fluorescence intensity ± SEM. ***P<0.001,** P<0.01, ns = not significant by ANOVA with Dunnett correction (baseline comparisons) or by t-test (pheromone effects)

B) Pheromone response of mutant animals expressed as mean ± SEM. **P<0.01, *P<0.05 by ANOVA with Dunnett correction.

C) *daf-12*, a necessary mediator of *daf-7* and *daf-28* influence on development, is also necessary for icas#9 modulation of foraging behavior. Bars indicate icas#9 response expressed as mean ± SEM.

Color indicates genotype at *roam-1* locus (red = N2, blue = MY14).

Figure 3.4

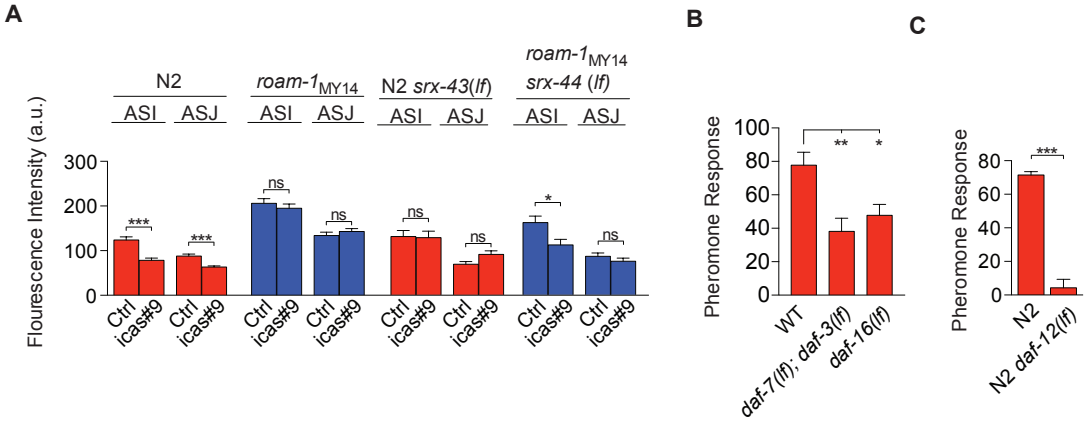
A
B
C
N2
roam-1MY14
N2 srx-43(lf)
roam-1MY14 srx-44 (lf)
ASI
ASJ
Flourescence Intensity (a.u.)
300
200
100
0
***
ns
*
Ctrl
icas#9
Pheromone Response
100
80
60
40
20
0
**
WT
daf-7(lf); daf-3(lf)
daf-16(lf)
N2
N2 daf-12(lf)

Figure 3.S1 *srx-44* does not act as an icas#9 receptor when expressed in ASH

Whereas *srx-43* expressed in ASH confers a selective calcium response to icas#9, *srx-44* failed to induce a calcium response in ASH to icas#9 or other ascarosides. Ascarosides tested at 10 nM.

Figure 3.S1

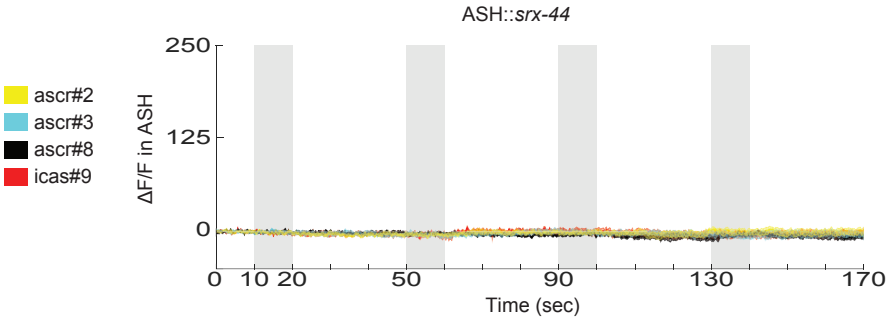
ASH::srx-44
ascr#2
ascr#3
ascr#8
icas#9
ΔF/F in ASH
250
125
0
0 10 20 50 90 130 170
Time (sec)

Figure 3.S2 Exploratory foraging behavior in *daf-7* and *daf-28* mutants

daf-7 (lf) and daf-28 (lf) in an N2 background enter fewer squares than N2 during an exploration assay in the absence of added pheromones.

***P<0.001 by ANOVA with Dunnett correction.

Figure 3.S2

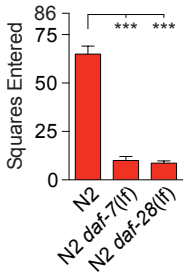

Figure 3.S3 *str-3::GFP* reporter lines

10 nM icas#9 does not alter *str-3::GFP* levels in ASI sensory neurons in N2 animals.

Figure 3.S3

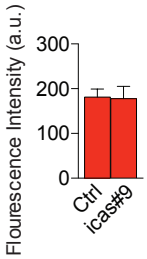

Chapter 4:

GABA release from the neuron AVL is necessary for ascaroside regulation of foraging behavior.

INTRODUCTION

Social cues exert a profound impact on development and behavior in species ranging from microbes to humans[104]. C*aenorhabidits elegans* is an ideal model organism to study social communication, as *C. elegans* has a well characterized nervous system[105] and is influenced by social cues in many ways. For instance, social isolation in *C. elegans* induces wide-ranging deficits, including slower development, altered neuronal connectivity, and reduced response to touch[106]. *C. elegans* communicates principally through a class of pheromones called ascarosides, which at high concentrations can influence entry into the dauer developmental stage[107] and at lower concentrations can influence several behaviors including social aggregation[78], male attraction to hermaphrodites[88], and foraging (Chapter 2 and 3). To take advantage of the well characterized nervous system in *C. elegans*, we examined pheromone sensitive behaviors in animals lacking specific neurotransmitters or neurotransmitter receptors. This led to the identification of GABA as a necessary mediator of a behavioral pheromone response, the suppression of exploration on food. Follow-up experiments involving cell-specific rescue and inhibition showed that the GABAergic neuron AVL is required for ascaroside regulation of foraging behavior.

RESULTS

To study the mechanism by which population density impacts foraging behavior, we used exploration assays to search for altered ascaroside-supression of roaming in mutants with deficits in specific neurotransmitter systems. This screen included animals deficient for essential enzymes in the synthesis of dopamine (*cat-2),* octopamine (*tbh-1),* octopamine and tyramine *(tdc-1),* and GABA (*unc-25).* As ablating serotonin or glutamate leads to large changes in roaming in the absence of ascarosides, animals lacking individual receptors for these neurotransmitters were examined instead (Glutamate: *nmr-1, nmr-1, glr-1, glr-3, glr-6, mgl-1, mgl-2, mgl-3;* Serotonin: *ser-1, ser-4, ser-7, mod-1)*. *unc-25(lf)* and *nmr-1(lf)* animals showed attenuated responses to 10 nm icas#9 and ascr#8 (Figure 1A). The 14 other mutant strains respond to one or both ascarosides similarly to WT. Reduced pheromone response of *nmr-1(lf)* were associated with decreased exploration in the absence of ascarosides, potentially indicating a nonspecific effect. Therefore, further experiments focused on GABA; in the absence of ascarosides, *unc-25(lf)* animals explored only slightly more than WT animals.

To confirm that the reduced pheromone response of *unc-25(lf)* stemmed from the absence of GABA, we examined two other *unc-25(lf)* alleles as well as two loss-of-function alleles for *unc-47,* which encodes a transporter essential for loading GABA into synaptic vesicles[108-110]. All *unc-25(lf)* and *unc-47(lf)* alleles failed to respond to the either icas#9 or ascr#8 (Figure 1B). *unc-46* also facilitates the loading of GABA into vesicles but is less important than *unc-47*[111]*;*

unc-46(lf) animals had a similar but milder defect in their pheromone response (Figure 1B). Although icas#9 and ascr#8 are particularly potent regulators of foraging, other ascarosides can suppress exploration. Further experiments indicated that *unc-25(lf)* also failed to respond to 100 nm ascr#2 or ascr#3 (Figure 1C). These results show that GABA is necessary for foraging response to multiple ascaroside pheromones.

One well established function of GABA in *C. elegans* is the regulation of locomotion[112]. The 19 type D GABAergic neurons in the ventral and dorsal cord inhibit the body-wall muscles on the opposite side of contraction, thereby facilitating body bends during sinusoidal locomotion[113]. We tested pheromone response of animals deficient in *unc-30,* a transcription factor necessary for all 19 type D GABAergic neurons to undergo terminal differentiation and express GABA[114,115]. *unc-30(lf)* animals responded normally to both icas#9 and ascr#8 (Figure 2A), indicating that GABAergic activity in the 19 VD and DD motorneurons is not necessary for the response to ascarosides.

Only 26 of the 302 neurons in *C. elegans* hermaphrodites are GABAergic. In addition to the 19 VD and DD motorneurons, there are four RME neurons as well as unique RIS, AVL and DVB neurons[113]. To determine which GABAergic neurons are involved in ascaroside responses, intersectional genetics were used to rescue *unc-25* in individual classes of GABAergic neurons. First, we generated transgenic *unc-25(lf)* animals with an extrachromosomal array containing an inverted *unc-25* coding region that was *LoxP* flanked (floxed) and driven by the endogenous *unc-25* promoter. GFP was bicistronically expressed with *unc-25* to

facilitate identification of cells in which *Cre* recombination of *LoxP* restored proper *unc-25* orientation and therefore expression. In animals with the extrachromosomal *unc-25* array but no *Cre* recombinase, there was no GFP signal nor rescue of pheromone response, indicating that the transgene was not expressed (Figure 2B). To confirm the efficacy of this approach, a pan-neuronal *Cre* was used to recombine the transgene in all neurons. The combination of the pan-neuronal::*Cre* with the floxed *unc-25* transgenes should result in GFP expression in all 26 GABAergic neurons and a rescued response to pheromones, which was in fact observed (Figure 2B). Next, *Cre* drivers that intersected with the *unc-25* promoter in a single class of GABAergic neuron were tested. Whereas rescuing *unc-25* expression specifically in the GABAergic neuron AVL rescued pheromone response, rescuing *unc-25* in DVB, RIS or the four RME neurons had no effect (Figure 2B). These results show that GABAergic activity in AVL is sufficient for an ascaroside response. As DVB and AVL have largely redundant functions regulating the defecation cycle, the inability of DVB::*unc-25* to rescue pheromone response disassociates pheromone insensitivity from defecation cycle defects; a secondary analysis of EMC coupling to expulsion events indicated that DVB::*unc-25* indeed restores mostly normal defecation (data not shown).

As tetanus toxin light chain (TeTx) cleaves synaptobrevin and thereby blocks neurotransmitter release, TeTx can be used to inhibit individual GABAergic neurons. Intersectional genetics was used to target TeTx expression to the AVL neurons. Successful targeting of TeTx to AVL was confirmed through

bicistronic GFP expression. Wild-type animals with TeTx in AVL failed to respond to ascarosides (Figure 2C), whereas animals with only the floxed inverted *TeTx* or the AVL::*Cre* transgenes responded normally. These results indicate that neurotransmitter release from AVL is necessary for ascaroside response, complementing the result that GABA release from AVL is sufficient for ascaroside response.

To interrogate downstream effectors of GABAergic signaling from AVL we examined animals lacking individual GABA receptors. *C. elegans* possess nine known GABA receptor genes, including 7 ligand-gated channels with homology to mammalian $GABA_A$ channels (chloride channels: *unc-49, gab-1, lgc-36, lgc-37, lgc-38*[116,117]*;* cation channels: *exp-1, lgc-35*[118,119]*)*. The other two receptor genes, *gbb-1* and *gbb-2,* form a heterodimer that is homologous to mammalian metabotropic $GABA_B$ receptors[120,121]. All receptor mutants responded to pheromones similarly to WT (Figure 3B), indicating that no known GABA receptor is individually necessary for pheromone response.

The *exp-1(lf)* allele tested, *ox276,* is a null allele as it consists of a large deletion spanning several exons. A recent report suggests that *exp-1(sa6)* exerts dominant negative effects, and can better recapitulate certain *unc-25(lf)* phenotypes presumably in part by inhibiting the closely homologous *lgc-35* receptor[119]. *exp-1(sa6)* animals roamed substantially more than *exp-1(ox276)* or wild-type, confounding exploration assays on standard size plates, and therefore 10 cm plates were used to quantify exploration in the presence and absence of ascarosides. In contrast to *unc-25(lf)*, which did not respond at all to pheromone

on 10 cm plates, *exp-1(sa6)* responded moderately. The substantial baseline shift in exploration limits interpretation of the difference in pheromone response between *exp-1(sa6)* and N2. However, *exp-1(sa6)* has a clear influence on baseline locomotion and likely exerts at least a moderate influence on pheromone response. As these results were not observed with *exp-1(ox276)*, this suggests that the inhibition of receptors in addition to *exp-1* are necessary to influence exploration or pheromone response.

DISCUSSION

In mammals, GABA is the principle inhibitory neurotransmitter in the central nervous system. GABAergic dysfunction contributes to a spectrum of diseases including epilepsy, anxiety, schizophrenia, and autism spectrum disorders. In *C. elegans*, there are just 26 GABAergic neurons: 13 VD, 6 DD, 4 RME, RIS, AVL, and DVB. RIS is an interneuron, whereas AVL and DVB possess both interneuron and motorneuron properties. The other 23 neurons are all motorneurons[113]. Several behavioral functions of these neurons have been characterized: the VD and DD neurons innervate the body wall muscles to produce contralateral inhibition facilitating coordinated locomotion, the RME neurons inhibit head muscles to limit head movements during foraging, and AVL and DVB innervate and contract enteric muscles to induce defecation[113]. The results here extend our knowledge of the function of GABA in *C. elegans* to the regulation of behavioral state and the processing of social cues: We show that the neuron AVL is a necessary source of GABA, facilitating foraging-response to

multiple ascaroside pheromones.

None of the identified GABA receptors in *C. elegans* can account for the influence of GABA on foraging behavior. The dominant negative *exp-1(sa6)* allele comes closest to recapitulating *unc-25(lf)*, as *exp-1(sa6)* only suppress exploration moderately in response to ascarosides, but interpretation of this finding is limited by *exp-1(sa6)* animals roaming excessively in the absence of pheromones. The effect of *exp-1(sa6)* does not stem simply from the loss of *exp-1* function, but also that of at least one additional receptor, as *exp-1(ox276)* resembles WT. One additional receptor is likely to be *lgc-35,* as *exp-1(sa6)* has been shown previously to inhibit *lgc-35* in the gut. Interestingly, *exp-1* has been previously implicated in regulating social behavior as well as *daf-7* expression[122]*,* an important mediator of ascaroside-suppression of roaming. Changes in *exp-1* expression between N2 and CB4856 accounts for some of the differences in their propensity to aggregate[122]. Our study provides another example of GABAergic involvement in *C. elegans* social behavior, and opens directions for future investigation of this topic.

Figure 4.1 GABA is necessary for ascaroside suppression of exploratory foraging

A) Response to icas#9 and ascr#8 in 16 mutants with deficits in specific neurotransmitter systems. Bars indicate ascaroside response expressed as mean ± SEM. *** P<0.001, ** P<0.01, * P<0.05; ns, not significant by ANOVA with Dunnett correction (*roam-1*$_{MY14}$). Green indicates response to icas#9; Turquoise indicates ascr#8.

B) The icas#9 and ascr#8 response expressed as mean ± SEM of strains with deficits in GABAergic neurotransmission. *** P<0.001, ** P<0.01; ns, not significant by ANOVA with Dunnett correction.

C) GABA is required for response to ascr#2 and ascr#3 in addition to icas#9 and ascr#8. Bars indicate pheromone response expressed as mean ± SEM. ***P<0.001,* P<0.05 by t test. Orange indicates ascr#2, brown indicates ascr#3.

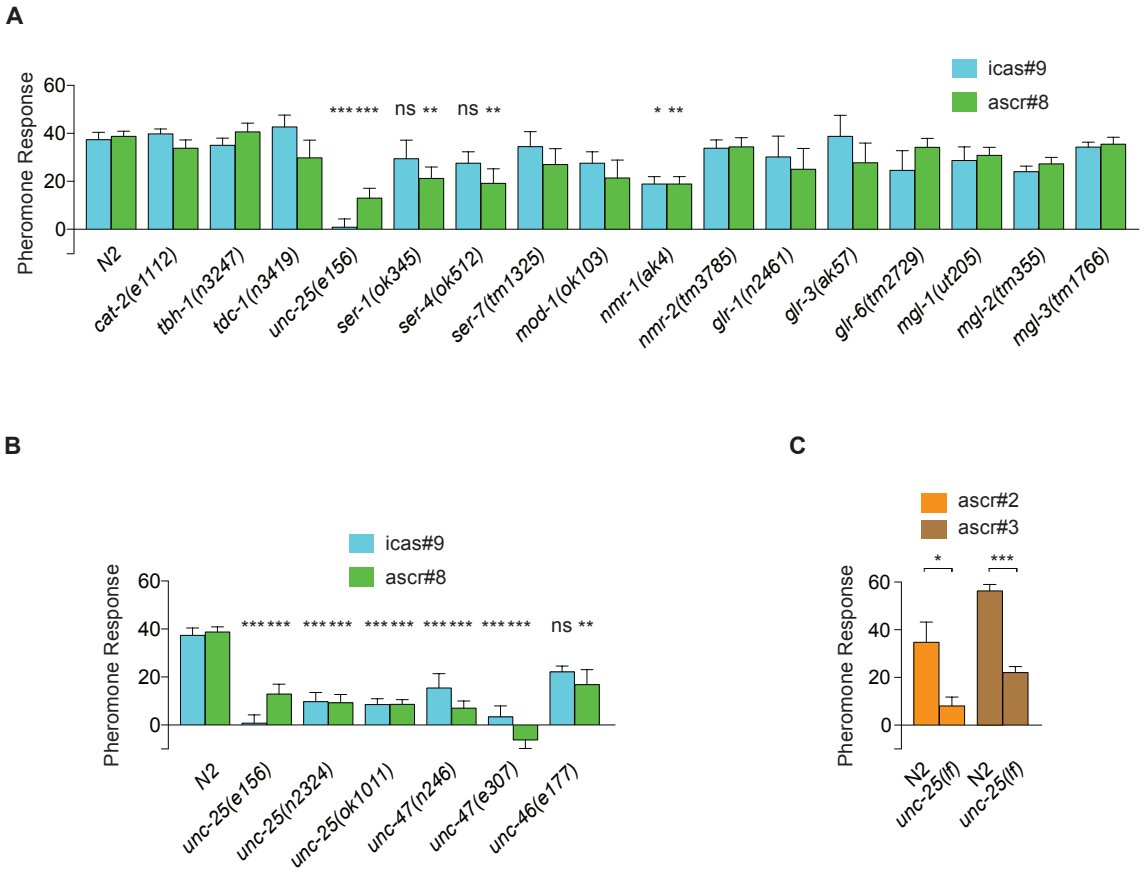
A
Pheromone Response
60
40
20
0
icas#9
ascr#8
****** ns ** ns **
* **
N2
cat-2(e1112)
tbh-1(n3247)
tdc-1(n3419)
unc-25(e156)
ser-1(ok345)
ser-4(ok512)
ser-7(tm1325)
mod-1(ok103)
nmr-1(ak4)
nmr-2(tm3785)
glr-1(n2461)
glr-3(ak57)
glr-6(tm2729)
mgl-1(ut205)
mgl-2(tm355)
mgl-3(tm1766)
B
Pheromone Response
60
40
20
0
icas#9
ascr#8
****** ****** ****** ****** ****** ns **
N2
unc-25(e156)
unc-25(n2324)
unc-25(ok1011)
unc-47(n246)
unc-47(e307)
unc-46(e177)
C
Pheromone Response
60
40
20
0
ascr#2
ascr#3
*
***
N2
unc-25(lf)
N2
unc-25(lf)

Figure 4.2 The GABAergic neuron AVL is involved in pheromone response

A) Response to icas#9 and ascr#8 in *unc-30(lf)* mutants. ns, not significant by t test. Green indicates response to icas#9; Turquoise indicates response to ascr#8.

B) Rescuing *unc*-25 in AVL but not in other GABAergic neurons restores response to ascarosides. Bars indicate icas#9 response expressed as mean ± SEM. Bellow the bars, presence (+) or absence (-) of the *LoxP flanked (floxed) inverted unc-25* transgene, and the GABAergic cell class expressing *Cre*. *** P<0.001, * P<0.05; ns, not significant by ANOVA with Dunnett correction.

C) AVL is necessary for pheromone response. Bars indicate icas#9 response expressed as mean ± SEM. Bellow the bars, *floxed inverted TeTx* presence (+) or absence (-) is indicated, as well as the location of *Cre* expression. *** P<0.001, * P<0.05; ns, not significant by ANOVA with Dunnett correction.

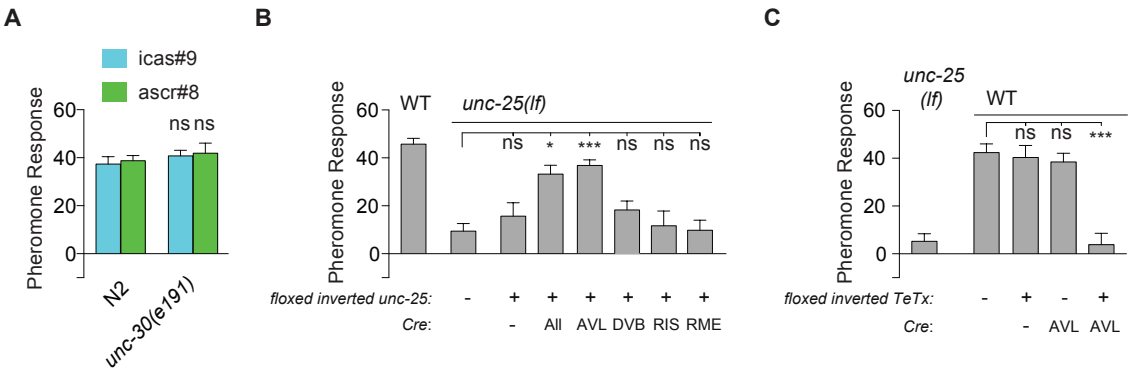
A
icas#9
ascr#8
Pheromone Response
60
40
20
0
ns ns
N2
unc-30(e191)
B
Pheromone Response
WT
unc-25(lf)
ns * *** ns ns ns
floxed inverted unc-25:
Cre:
- + + + + + +
- All AVL DVB RIS RME
C
unc-25 (lf)
WT
ns ns ***
floxed inverted TeTx:
Cre:
- + - +
- AVL AVL

Figure 4.3 No known GABA receptor is necessary for pheromone response

A) Icas#9 response of animals deficient for individual GABA receptors expressed as mean ± SEM. Above the bars, category of receptor is indicated ($GABA_{A,}$ ligand-gated ion channel; $GABA_{B,}$ GPCR). No mutants were significantly different from N2 by ANOVA with Dunnett correction.

B) Exploration assays conducted on 10 cm plates with *exp-1 (sa6)* animals. Bars indicate mean squares entered (out of 175) ± SEM. Condition (Control or icas#9) indicated below the bars. ***P<0.001, ns, not significant by t test.

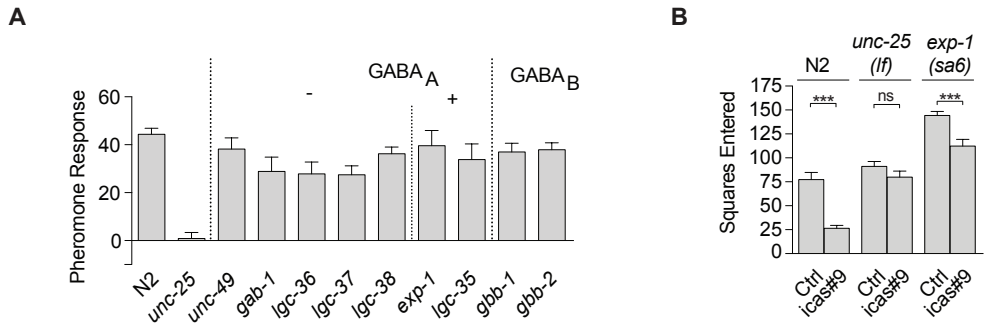
A
Pheromone Response
60
40
20
0
GABA A
-
+
GABA B
N2
unc-25
unc-49
gab-1
lgc-36
lgc-37
lgc-38
exp-1
lgc-35
gbb-1
gbb-2
B
Squares Entered
175
150
125
100
75
50
25
0
N2
unc-25 (lf)
exp-1 (sa6)
***
ns
***
Ctrl
icas#9
Ctrl
icas#9
Ctrl
icas#9

Chapter 5:
Future Directions

In my thesis work, I explored the genetic basis of natural variation in social foraging behavior. Studying natural variation informs our understanding of what makes us different as individuals, and in addition, the information learned can be leveraged to better understand the genetic regulation of nervous system function. To date, this project has primarily focused on precisely determining the the genetic changes underlying natural variation in pheromone response. In the future, the most fruitful experiments may be those that broaden the scope of study to explore the interaction between icas#9 signaling and innate neural circuitry.

One promising future direction would expand upon the preliminary studies looking at downstream effectors of *srx-43,* in particular, those showing the importance of the TGF-β and insulin-related peptides encoded by *daf-7* and *daf-28*. One simple question is to ask which neurons detect these peptides to regulate roaming and dwelling. The peptides are released and diffuse nonsynaptically so the wiring diagram provides little insight to their potential targets. However, the cellular targets of *daf-7* and *daf-28* could be identified through rescue experiments with their receptors or necessary mediators. Previous work by Dr. Evan Macosko showed that knocking out *daf-1,* the receptor for *daf-7* had similar effects to *daf-7(lf)* on exploration in the absence of ascarosides. Moreover, restoring *daf-1* in RIM, RIC, and UV1 cells partially rescued foraging behavior. This work raises the possibility that reduced *daf-7* signaling through the *daf-1* receptor in RIM, RIC, and/or UV1 may contribute to

icas#9 effect. These finding could be expanded using intersectional genetics to determine the precise cellular targets of *daf-7*. It should be noted that while RIM and RIC are the principle neuronal sources of tyramine and octopamine, respectively, in *C. elegans* these monoaminergic neurotransmitters seem unimportant for foraging response to ascarosides (Chapter 4). Of course, RIM or RIC may be involved in foraging behavior through other mechanisms. In addition to these experiments with *daf-1,* a similar set could be conducted with d*af-2,* the receptor for *daf-28* and other insulins*. daf-7* and *daf-28* may be acting in the same or distinct populations of neurons to mediate ascaroside effect.

One goal of this line of research would be to connect our understanding of *srx-43* and *srx-44* to the networks previously identified as promoting and maintaining the behavioral states of roaming and dwelling. Dr. Steven Flavell identified a flip-flop switch consisting of opposing serotonergic and *pdf-1* neuropetidergic systems that prolong dwelling or roaming states, respectively. How does this respond to increasing population density? Our initial characterization of the effects of icas#9 and ascr#8 led to a hypothesis: both ascarosides suppressed exploration by shortening roaming state duration without impacting dwelling state duration. This resembles what happens in animals lacking serotonin, suggesting that ascarosides could operate by reducing serotonergic signaling. In accordance with this hypothesis, the work of Dr. Andy Chang showed that *daf-7* signaling increases expression of *tph-1*, the rate limiting enzyme in serotonin synthesis[45]. Therefore, ascaroside suppression of *daf-7* expression could lower serotonin production and shorten roam state

duration. A preliminary characterization of *tph-1::GFP* failed to identify regulation by icas#9 in N2. This reporter may not be sufficient to detect the relevant changes in serotonergic signaling - down-regulation can be particularly hard to observe with GFP, a stable protein, and moreover *tph-1* levels and serotonin can be somewhat distinct, at least in the short term. An alternative approach to exploring this hypothesis would be looking at double mutants of *tph-1* with *daf-7* or *daf-28.* One possible outcome is that these animals would resemble the hyper-roaming phenotype of *tph-1(lf)* animals, not the hyper-dwelling phenotype of the *daf-7(lf) or daf-28(lf)* animals. Such an epistatic relationship would suggest that ascaroside suppression of *daf-7* and *daf-28* signaling regulates foraging behavior solely through the modulation of serotonergic signaling. However, in the likely case that the double mutants are intermediate in phenotype, interpretation would be less straightforward.

Over the last few years several members of the Bargmann lab have successfully sequenced the transcriptomes of individual cell types by isolating RNA associated with tagged ribosomes expressed under cell-specific promoters. This technology might be employed to ask two questions relating to this project: first, what *srx-43*-dependent changes occur in the ASI transcriptome in response to icas#9, and second, what *daf-7* and *daf-28*-dependent changes occur in downstream effector cells. *daf-7* and *daf-28* are likely to influence foraging behavior through transcriptional changes, as a downstream effector of both of these signaling pathways, *daf-12* encodes a transcription factor[123]. This approach

could help identify other effectors released by ASI or changes produced by *daf-7* and *daf-28* signaling that mediate the effect of ascarosides on foraging.

Social cues are not the only regulator of foraging behavior. Roaming and dwelling rates also change in response to the quality of the food and in response to past food experience. Interestingly, when worms are shifted to a different quality food, their foraging behavior changes and gradually returns to baseline over the course of hours. How do past and present food experiences impinge upon foraging? Evidence indicates that both *daf-7* and *daf-28* expression levels change in response to food[124,125], so these TGF-β and insulin signals are strong candidates to mediate the effect of food on foraging. A similar set of experiments to those conducted with icas#9 could be conducted to explore the dependence of food history effects on *daf-7* and *daf-28*.

In addition to these studies aimed at understanding how experience impacts innate foraging circuits, it would be valuable to extend our understanding of the *roam-1* locus. Is balancing selection acting on *roam-1* because of its effect on foraging? Changing the distribution of food altered the direction of selection in the predicted way, as the scattered food environment favored the strain that was more inclined to roam. This result supports but does not prove that selection is acting on foraging and not some other icas#9 response. One starting point would be to examine *roam-1* influence on other icas#9-behavioral and developmental effects. Icas#9 is not a particularly efficacious inducer of dauer formation, but does exerts a moderate effect. Does *roam-1* influence this activity of icas#9?

Icas#9 also can induce aggregation; does this behavior have anything to do with the observed selection? Although it is clearly impossible to determine all possible actions of icas#9 in a laboratory environment, we could look at a few candidates and determine the influence of *roam-1* genotype. One interesting possibility is that *roam-1* exerts a relatively selective effect on foraging behavior. The receptors necessary for ascr#9 to induce dauer formation, are unimportant for behavioral actions of this pheromone[43]. Given the large repertoire of chemoreceptors and ascaroside pheromones, *C. elegans* has the genomic potential to intepret a rich and specific chemical language.

Relating to this line of experiments is the question of why selection of the *roam-1* locus produced the particular mutations that it did? For instance, the effect of *roam-1*$_{MY14}$ on foraging behavior could largely be replicated by a loss of *srx-43* function. Yet while a simple nonsense mutation in *srx-43* would quickly lead to a foraging phenotype quite similar to *roam-1*$_{MY14}$, no such mutation was found in the wild. Moreover, there is strong evidence for purifying selection maintaining functional *srx-43* activity in MY14. Why is this receptor conserved in MY14? What function does it serve? MY14 worms retain a moderate foraging response to icas#9, more so than *srx-43(lf)* worms, and perhaps retaining a moderate response is optimal for MY14. Another interesting possibility is that *srx-43* serves other functions besides regulating foraging behavior, and that in altering *srx-43* and *srx-44* expression, foraging behavior can be changed without adversely affecting the other functions of these chemoreceptors. Having a better

sense of what these genes do in addition to regulate foraging might help us craft better testable hypotheses.

The creation and genotyping of 94 MY14-CX12311 RILs has created a resource that could be used to ask many other questions about natural variation in *C. elegans*. Until now, work characterizing the genetic basis of behavioral differences in wild *C. elegans* strains has largely focused on differences between HW and N2. MY14 is genetically distinct from both of these strains, and thereby the MY14-CX12311 RILs may allow access to a new set of behavioral variants. One exciting possible set of experiments would be to examine CX12311 and MY14 in the behavioral chambers designed by Dr. Shay Stern, which records behavior of individual worms from egg hatching to adulthood. These long-term behavioral experiments may allow identification of stage-specific changes in foraging behaviors or general locomotor characteristics among individuals with different genetic backgrounds. In addition to examining differences between average behavior of different strains, the single-animal design of these chambers can be used to examine individual variability within a strain. I suspect that strains could be behavioral generalists and others specialists. The generalists could have evolved greater behavioral diversity to assure that some animals take appropriate advantage of a variable environment, while the specialists may have evolved minimal variation in pursuit of an optimal strategy for a constant environment.

During my thesis work, I identified GABA as a necessary mediator of ascaroside-suppression of roaming. However, the exact function of GABA in these behavior remains largely unknown. Are changes in GABAergic signaling directly influencing roaming and dwelling rates, or alternatively, is GABA necessary to facilitate the detection of ascarosides? This question could be explored through optogenetic stimulation of AVL neurons, to ask if they can acutely influence roaming and dwelling states. An effect of AVL stimulation would be compelling evidence of the importance of AVL activity, but negative results could be uninformative. A complementary approach would be an observational study involving AVL::GCaMP: do changes in AVL activity follow ascaroside exposure? Do changes in AVL activity accompany transitions between roaming and dwelling? As AVL is presumed to have a semi-periodic signaling pattern determined by a pacemaker in the gut[126], it is unclear what sort of changes we might anticipate. We might observe changes in the magnitude of periodic AVL activation, the chance of AVL missing a cycle, or activations that are not coupled to the gut pacemaker.

Another question the GABA project raises is the identity of the downstream effectors of AVL. The relevant GABAergic receptors have proven elusive, but the *exp-1(sa6)* dominant negative allele may provide an approach to determine neurons acting downstream of AVL. An *exp-1(sa6)* transgene could be expressed in neurons and muscle downstream of AVL to determine where this gene is acting to regulate foraging. Following identification of downstream

effector cells, single-cell RNAseq could be conducted to identify candidate GABA receptors in these cells.

In conclusion, the findings of my thesis could be extended in several directions. Our understanding of *roam-1* can be leveraged to better understand how neural circuits operate and incorporate information about the environment. We can also seek a deeper understanding of the nature of the *roam-1* mutation, specifically its other effects and why *roam-1* has arisen in this particular form. Finally, we can expand on findings showing a necessary role of GABA in ascaroside response by asking how GABA impinges on pheromone-to-behavior signaling. Studying density-dependent foraging behavior has provided an exciting window to explore the evolution of behavior and the functioning of neural circuits, and has the potential to uncover new discoveries as well.

Experimental procedures

Nematode Culture:

All strains were grown at 21-22°C on nematode growth medium plates seeded with *Escherichia coli* OP50 bacteria[127]. For OP50 cultures a single colony was inoculated into 100 ml of LB and grown for 48 hours at 21-22°C. Transgenic lines were generated by standard injection methods, and included the desired transgene, a fluorescent co-injection marker, and empty vector bringing the total DNA concentration up to 100 ng/ul. For each transgene, three independent extrachromosomal lines that propagated the transgene at high rates were tested in parallel to account for variability typical of such strains. For CRISPR/Cas9 mediated mutagenesis, we used the coCRISPR protocol developed in Arribere *et al* 2014[128]. Young adults were injected with a mix of plasmids containing Cas9, guideRNA targeting *rol-6,* or guideRNA targeting the location of the desired mutation, as well as a ssDNA template for inducing a dominant *rol-6(su1006)* mutation. F1 animals with a roller phenotype were isolated and allowed to lay eggs before secondary screening for the target mutation by Sanger sequencing. All mutagenized strains were backcrossed 5-7 times before characterization.

Strains :

Chapter 2

Natural isolates and WT strains	Origin
N2	Bristol, UK

CX12311 *kyIR1* [V,CB4856>N2] V; *qqIR1* [X, CB4856>N2]	(N2/CB4856)
CB4856 (“HW”)	Hawaii, USA
JU258	Riberio Frio, Madeira
MY1	Lingen, Germany
MY14	Mecklenbeck, Germany
JU775	Lisbon, Portugal
JU1400	Sevilla, Spain
JU1652	Montevideo, Uruguay
AB1	Adelaide, Australia
MY16	Mecklenbeck, Germany
JU1171	Concepcion, Chile
MY6	Roxel, Germany
JU360	Franconville, France
ED3021	Edinburgh,Scotland
MY2	Roxel, Germany

MY14-CX12311 RILs:

CX14697-CX14712, CX14731-CX14748, CX14750-CX14757, CX14783, CX14784, CX14786-CX14820, CX14822-CX14839.

Near-isogenic Lines

CX15881 *kyIR142 [V:~14.3-~16.8Mb, CX12311>MY14]*

CX15878 *kyIR139 [V:~14.3-~16.8Mb, MY14>CX12311]*

CX15883 *kyIR144 [V:~14.3-~16.8Mb, MY14>N2]*

CX16075 *kyIR147 [V:~15.861-~16.8Mb, MY14>N2]*

CX16140 *kyIR153 [V:~16.043-~16.8Mb, MY14>N2]*

CX16300 *kyIR163 [roam-1$_{MY14}$ V:~15.861-~16.043Mb, MY14>N2]*

CX16294 *kyIR157 [V:~15.861-~16.006Mb, MY14>N2]*

Transgenic Lines

CX16884 *kyIR163 V, kyEx5851 [Psrx-43::srx-43::sl2::GFP @ 2.5 ng/ul, Pmyo3::mcherry @ 5 ng/ul]*

CX17202 *kyIR163 V, kyEx6012 [Psrx-43::srx-43(nonsense)::sl2::GFP @ 2.5 ng/ul, Pmyo3::mcherry @ 5 ng/ul]*

CX16881 *srx-43(gk922634)*, *kyEx5848 [srx-43 @ 2.5 ng/ul, Pmyo3::mcherry @ 5 ng/ul]; gk922634* changes R160 to an opal stop codon.

CX17204 *kyEx6013 [Psrx-43(N2)::srx-43(N2)-GFP translational fusion @ 50 ng/ul, Pelt-2::GFP @ 5 ng/ul]*

CX16943 *kyIR163 V; kyEx5894 [Psrx-43(MY14)::srx-43(MY14)::sl2::GFP @ 2.5 ng/ul, Pmyo3::mcherry @ 5 ng/ul]*

CX16425 *kyIs602 [Psra-6::GCaMP3.0 @ 75ng/uL; Pcoel::GFP @ 10 ng/uL]; kyEx5594 [Psra-6::srx-43(N2) @ 50 ng/ul, Pmyo3::mcherry @ 5 ng/ul]*

CX16931 *kyIs602*; *kyEx5885 [Psra-6::srx-43(MY14) @ 50 ng/ul, Pmyo3::mcherry @ 5 ng/ul]*

CX17196 *srx-43(gk922634); kySi66 [MosSCI Psrx-43(N2)::srx-43(N2)] II*, outcrossed 4X

CX17198 *srx-43(gk922634)*; *kySi68 [MosSCI Psrx-43(MY14)::srx-43(MY14)] II*, outcrossed 4X

CX17201 *srx-43(gk922634); kySi71 [MosSCI Psrx-43(N2)::srx-43(MY14)] II,* outcrossed 4X

CX17203 *srx-43(gk922634)*; *kySi72 [MosSCI Psrx-43(MY14)::srx-43(N2)] II*, outcrossed 4X

FK181 ksIs2 [Pdaf-7::GFP + rol-6(su1006)]

Loss-Of-Function Alleles

CX16849 *srx-43(gk922634) V* outcrossed 5X to N2. *gk922634* is R160opal.

CX16935 *srx-43(ky1019) V*; *kyIR163 V*. *ky1019* is an indel that causes a frameshift mutation after the first transmembrane domain (insertion (tcactgagttcgaat), deletion (CCCCG), final sequence TCGCAGCTCTCAAGTtcactgagttcgaatTTCGGAATTCTC)

CX13846 *daf-22(ok693) II*

CX17082 *daf-22(ok693) II*; *kyIR163 V*

Chapter 3

Loss-Of-Function Alleles

CX16490 *srx-44(ky1009) V* backcrossed 6X to N2. *ky1009* is a two bp deletion (TACCCTTC—GTTCTTGATA) leading to a frameshift after amino acid #57.

CX16934 *kyIR163 V; srx-44(ky1013) V. backcrossed 7X. ky1013* is a two bp deletion (TATGCGCCGG—ACAACGACAGATT) leading to a frameshift after amino acid #49.

CX16936 *kyIR163 V; srx-43(ky1013) V; srx-44(ky1023) V; ky1023* is 3 bp deletion, 7 bp insertion (CTCTCAAGTCCggaattcTTCGGA) leading to a frameshift after amino acid #98.

CX13568 *daf-28 (sa191) V*

DR26 *daf-16 (m26) I*

DR20 *daf-12(m20) X*

MosSCI strains

CX17196 *srx-43 (gk922634) V; kySi66 [MosSCI II:srx-43(N2)]*

CX17260 *kyIR163 V; srx-43 (ky1013) V; kySi66 II*

CRISPR allele replacement strains

CX16800 *ky982 V [38 bp in the N2 promoter of srx-44 changed from (AATCATGTTAAAAAATCAATTTTTGGGTAGTCAACGGA) to the 32 bp in MY14 (TATCATTTAAAAACTCACTTTTTGAGTAGTCG) using CRISPR/Cas9], b*ackcrossed to N2 4X.

CX16799 *kyIR163 V; ky1015 V [32 bp in the MY14 proximal promoter changed to the 38 bp in N2 using CRISPR/Cas9],* backcrossed 4X

Transgenic Lines

CX16350 *kyIR163 V, kyEx5577 [Psrx-44::srx-44(N2) @ 5 ng/ul, Pmyo-3:: mcherry @ 5 ng/ul.]*

CX16350 *kyIR163 V, kyEx5577 [Psrx-44::srx-44(N2) @ 5 ng/ul, Pmyo-3:: mcherry @ 5 ng/ul.]*

CX16431 *kyIR163 V, kyEx5600 [Psrx44(N2)::srx44(N2)::sl2::GFP @ 2.5 ng/ul, Pmyo-3::mcherry @ 5 ng/ul.]*

CX16480 *kyIR163 V, kyEx5626 [Psrx44(MY14)::srx44(MY14)::sl2::GFP @ 2.5 ng/ul, Pmyo-3::mcherry @ 5 ng/ul.]*

CX16477 *kyIR163 V, kyEx5623 [Psrx44(MY14)::srx44(N2)::sl2::GFP @ 2.5 ng/ul, Pmyo-3::mcherry @ 5 ng/ul.]*

CX16483 *kyIR163 V, kyEx5629 [Psrx44(N2)::srx44(MY14)::sl2::GFP @ 2.5 ng/ul, Pmyo-3::mcherry @ 5 ng/ul.]*

CX16624 *kyIR163 V, kyEx5698 [Psrx44(N2)::GFP @ 2.5 ng/ul, Pmyo-3::mcherry @ 5 ng/ul.]*

CX16627 *kyIR163 V, kyEx5701 [Psrx44(MY14)::GFP @ 2.5 ng/ul, Pmyo-3::mcherry @ 5 ng/ul.]*

CX16752 *kyIR163 V, kyEx5775 [Psrx44(N2 proximal, MY14 distal)::GFP @ 2.5 ng/ul, Pmyo-3::mcherry @ 5 ng/ul.]*

CX16735 *kyIR163 V, kyEx5759 [Psrx44(N2 proximal, MY14 distal)::GFP @ 2.5 ng/ul, Pmyo-3::mcherry @ 5 ng/ul.]*

CX16425 *KyIs602 [Psra-6:GCaMP3.0 @ 75ng/uL, coel:GFP @ 10ng/uL, integrated], KyEx5594 [Psra-6::srx-44(N2) @ 50 ng/ul, Pmyo-3::mcherry @ 5 ng/ul]*

CX16428 *KyIs602, KyEx5597 [Psra-6::srx-44(MY14) @ 50 ng/ul, Pmyo-3::mcherry @ 5 ng/ul]*

CX16533 *kyIR163 V, KyEx5646 [Psrh-11(ASJ)::srx-44::sl2::GFP 50 ng/ul, Pmyo-3::mcherry @ 5 ng/ul]*

CX16530 *kyIR163 V, kyEx5643 [Psrh-220(ADL)::srx-44::sl2::GFP @ 50 ng/ul, Pmyo-3::cherry @ 5 ng/ul]*

CX16611 kyEx5688 [Psre-1(ADL)::TeTx @ 50 ng/ul, myo-3::cherry @ 5 ng/ul]

CX16611 kyIR163 V, kyEx5688 [Psrh-11(ASJ)::TeTx @ 50 ng/ul, myo-3::cherry @ 5 ng/ul]

Reporter lines

GR1455 *mgIs40 [Pdaf-28::GFP],* outcrossed 5X

CX16956 kyIR163 V, mgIs40

CX16957 srx-43(gk922634) V, mgIs40

CX15046 lin-15(n765) X, kyIs128 [lin-15, Pstr-3::GFP]

Chapter 4

Loss-Of-Function Alleles

CX11078 *cat-2(e1112) II*

MT9455 *tbh-1(n3247) X*

MT10548 *tdc-1(n3420) II*

CX13851 *unc-25(e156) III*

DA1814 *ser-1(ok345) X*

AQ866 *ser-4(ok512) III*

DA2100 *ser-7(tm1325) X*

MT9668 *mod-1(ok103) V*

VW4509 *nmr-1(ak4) II*

FX03785 *nmr-2(tm3785) V*

KP4 *glr-1(n2461) III*

VM1846 *glr-3(ak57) I*

CX14904 *glr-6(tm2729) X*

JC1762 *mgl-1(ut205) X*

CX12797 mgl-2(tm355)

CX13156 mgl-3(tm1766)

CX14453 *unc-25(n2324) III*

CX14454 *unc-25(ok1901) III*

MT6201 *unc-47(n2409) III*

CX13976 *unc-47(e307) III*

BC356 *unc-46 (e177) V*

CX15250 *unc-30(e191) IV*

CX15785 *unc-49(e382) III*

CX12723 *gab-1(tm3577) III*

CX15902 *lgc-36(gk247083) V*

CX15900 *lgc-37(tm0864) III*

CX15901 *lgc-38(gk177664) III*

EG276 *exp-1(ox276) II*

CX15784 *lgc-35(tm1444) II*

CX15899 *gbb-1(tm1406)* X

CX14520 *exp-1(sa6) II*

Transgenic Lines

CX15598 *unc-25(e156) III; KyEx5250(unc-25::inverted[unc-25::sl2::GFP] @ 15 ng/ul; myo-3::mCherry @ 5 ng/ul)*

CX15601 unc-25(e156) III; KyEx5250; KyEx5253(Pan-neuronal::nCre @ 10 ng/ul; myo-2::mCherry @ 5 ng/ul)

CX15636 *unc-25(e156) III; KyEx5250; KyEx5263(AVL::nCre @ 10 ng/ul; myo-2::mCherry @ 5 ng/ul)*

CX15782 *unc-25 e156) III; KyEx5250; KyEx5317(DVB::nCre @ 10 ng/ul; myo-2::mCherry @ 5 ng/ul)*

CX15639 *unc-25(e156) III; KyEx5250; KyEx5266(RIS::nCre @ 10 ng/ul; myo-2::mCherry @ 5 ng/ul)*

CX15644 *unc-25(e156) III; KyEx5250; KyEx5271(RME::nCre @ 10 ng/ul; myo-2::mCherry @ 5 ng/ul)*

CX15603 KyEx5256(snf-11::inverted[TeTx::sl2::GFP] @ 15 ng/ul; myo-2::mCherry @ 2 ng/ul)

CX15603 KyEx5256; kyEx5420(AVL::nCre @ 25 ng/ul; myo-3::mCherry @ 5 ng/ul)

Behavioral Analysis:

Exploration assays were conducted on 35 mm Petri dishes evenly seeded with 100 µl of OP50 bacteria 24 hours before the start of the assay. Individual two-day old L4 hermaphrodites were picked to the center of the plate. After 16 hours, plates were placed on a grid containing 35 mm squares, and the number of full or partial squares containing tracks were quantified by an investigator blind to the genotype. Pheromones or control solvent were mixed into the agar, and a pheromone response was calculated by determining the mean squares entered in control conditions for a genotype each test day, and subtracting from the mean the squares entered for pheromone plates. N2 strains were tested in 21% oxygen; natural isolates and strains bearing ancestral alleles of *npr-1* and *glb-5* were conducted in 8% oxygen to suppress the oxygen-dependent roaming of ancestral *npr-1* alleles[16,38].

Direct examination of roaming and dwelling was modified from *Flavell et al* 2013[9]. 14.5 hours before testing, 25 L4 larvae were picked to 150 mm test plates thinly seeded with 1.5 mL of OP50 bacteria with or without synthetic pheromone. Video

recording was conducted under red light to minimize behavioral response to imaging conditions. 1.5 hour-long videos were recorded at 3 frames/s using Streampix software (Norpix Inc., Montreal, CA) and a 6.6MP PL-B781F CMOS camera (PixeLINK, Ottawa, CA). Custom Matlab scripts[75] were employed to determine worm trajectories and conduct a two-state hidden Markov model determining the most probable state path for each animal and thereby measure state durations.

Statistics:

Most statistical comparisons were done by ANOVA with Dunnett correction for multiple comparisons or t test, as noted in the figure legends.

Ascaroside Quantification:

150 mL unsynchronized worm cultures were grown for 9 d and fed *E. coli* (HB101 or OP50), as described[92]. Extracts were generated from the culture medium and analyzed by LC-MS/MS, as described[92], and analyzed on a Thermo Scientific TSQ Quantum Access MAX, with the collision gas pressure set to 1 mTorr. Ascaroside concentrations present in the culture were quantified using the corresponding synthetic standards, except that synthetic ascr#18 was used to quantify ascr#22 and ascr#26, and synthetic icas#3 was used to quantify icas#1 and icas#10.

Recombinant inbred lines:

The MY14-CX12311 recombinant inbred lines were generated by crossing MY14 males to CX12311 hermaphrodites and CX12311 males to MY14 hermaphrodites, to ensure the mitochondrial DNA from both strains were equally represented in the RILs. 94 F2 were individually picked to plates and inbred through self-fertilization for 10 generations. RIL genotyping was conducted by low-coverage shotgun sequencing[82], Genomic DNA was fragmented and attached to sequencing adapters with a Nextera DNA Library Prep Kit (Illumina, San Diego, USA). Samples were pooled and sequenced on an Illumina HiSeq 2000. Sequencing reads from each strain were mapped to the WS235 release of the *C. elegans* genome using bwa to create bamfiles for further analysis[129]. The set of MY14/N2 SNVs identified in the Million Mutation project were used for genotyping purposes[86]. Each genetic variant was genotyped in each strain. Due to the low coverage, the majority of SNVs were not genotyped. To improve the data coverage, we grouped 200 neighboring SNV genotypes together to create a consensus genotype for 540 bins (either N2, MY14 or heterozygous). These genotypes were used for QTL mapping.

QTL mapping:

The pheromone response index was used as the phenotype in combination with the 540 genotype bins from above. R/qtl was used to perform a one-dimensional scan using marker regression on all 540 markers. The significance threshold was determined using 1000 permutation tests. The effect-size of the *roam-1* locus was estimated using the fitqtl function with a single QTL. The peak of the *roam-1*

locus (Chromosome V: 16451686-16579457) was used as an additive and interactive covariate for additional one-dimensional scans, assuming a normal model. The significance threshold for these two tests was also determined using 1000 permutation tests.

NIL Mapping:

kyIR142 was made by backcrossing the RIL CX14816 nine times to MY14, maintaining N2 alleles at V:14.3 and V:16.8 Mb at each generation.
kyIR139 was made by backcrossing the RIL CX14708 nine times to CX12311, maintaining MY14 alleles at V:14.3 and V:16.8 Mb.
kyIR144 was made by crossing *kyIR139* with N2 and isolating recombinants with the N2 allele of *glb-5* (V:5.56 Mb) and the MY14 alleles at V:14.3 and 16.8 Mb. In addition, animals were selected for the N2 allele of *npr-1.*
kyIR147 and *kyIR153* were created by crossing *kyIR144* with N2 and identifying progeny with the N2 allele at V:14.3 Mb and the MY14 allele at V:16.8 Mb.

High Density Recombination Mapping:

kyIR147 was crossed with males from CX16290, a N2 strain with an integrated fluorescent marker at V:15.83 Mb. F1 progeny were identified by fluorescence, picked to growth plates, and allowed to lay eggs for 12 hours. Following 3 days of growth, ~2600 nonfluorescent F2 were sorted individually into wells of 96-well plates by a worm sorter (COPAS biosort systems; Union Biometrica). These F2 were grown in 200 ul of S-basal buffer + cholesterol supplemented with OP50

bacteria. A fraction of the F3 progeny from each isolate were lysed and genotyped at V:16.043 Mb. Those with a N2 allele at V:16.043 Mb were genotyped at V:15.861 Mb. Twelve recombinants with a N2 allele at V:16.043 Mb and a MY14 allele at V:15.861 Mb were isolated and characterized behaviorally, among which were kyIR163 and kyIR157 (Figure 2.2Diii).

Calcium Imaging:

Calcium imaging experiments were performed and analyzed as described[130]. Briefly, young adult animals were placed into custom-made 3x3 mm microfluidic polydimethylsiloxane devices that permit rapid changes in stimulus solution. Each device contains two arenas, allowing for simultaneous imaging of two genotypes with approximately ten animals each. Animals were transferred to the arenas in S-Basal buffer and paralyzed for 80-100 minutes in 1 mM (-)-tetramisole hydrochloride. Experiments consisted of four 10 s pulses of stimulus separated by 30 seconds of buffer, with 60 additional seconds between stimulus types. Tiff stacks were acquired at 10 frames/second at 5x magnification (Hamamatsu Orca Flash 4 sCMOS), with 10 ms pulsed illumination every 100 ms (Sola, Lumencor; 470/40 nm excitation).

Fluorescence levels were analyzed using a custom ImageJ script that integrates and background-subtracts fluorescence levels of the ASH cell body (4x4 pixel ROI). Using MATLAB, the calcium responses were normalized for each stimulus type by dividing fluorescence levels by the baseline fluorescence, defined as the

average fluorescence of the 10 s preceding the first pulse of the stimulus. Each experiment was performed a total of four times over two separate days. Animals of a given strain were pooled together to calculate population mean and standard error (N2 *srx-43* allele: 23 animals; MY14 *srx-43* allele: 30 animals; array negative control: 19 animals).

GFP reporter line Studies:

Live adult animals were mounted on 2% agarose pads containing 5 mM sodium azide. Images were collected with a 100X objective on a Zeiss Axioplan2 imaging system with a Hamamatsu Photonics C24200 CCD camera, a Zeiss Axio Imager.Z1 with Apotome with a Zeiss AxioCam MRm CCD camera. For *daf-7* reporter studies, expression was quantified 16-24 hours after L4 animals were placed on exploration assay plates. Images were processed in Metamorph and imageJ. A maximum intensity Z-projection was conducted. Reporter values were assessed as the the mean gray value for a 16-pixel-radius circle centered over the cell body minus the mean background intensity.

Digital PCR:

Digital PCR was conducted on a QuantStudio™ 3D digital PCR platform (Thermo Fisher Scientific Inc., New York, USA), and analyzed on the QuantStudio™ 3D AnalysisSuite Cloud.

Expression studies were conducted on synchronized L4 worms 48 hours after laying. RNA was collected on RNeasy Mini columns (Qiagen, Hilden, DE) and treated with DNAse (Qiagen). SuperScript III First-Strand Synthesis System (Thermo Fisher Scientific) was used to create cDNA libraries. Custom TaqMan Expression Assays (Thermo Fisher Scientific) were used for *srx-43* quantification, and the tubulin gene, *tbb-1*, was used for normalization.

For quantitative analysis of the competition experiments, DNA was extracted with a standard phenol-chloroform protocol. Custom TaqMan SNP Genotyping Assays (Thermo Fisher Scientific) were used to determine the relative ratio of N2 versus *roam-1*$_{MY14}$ DNA. The assay was validated with known ratios of N2 to *roam-1*$_{MY14}$ DNA (Figure S9).

Gene and strain trees:

To create the gene and organism phylogenies, we used SNV data downloaded from the Million Mutation project (http://genome.sfu.ca/mmp/). Software was written in Python using the Biopython module to create a neighbor joining tree. For the *roam-1* locus, SNVs on Chromosome V between 16,010,000 and 16,030,000 were used. For the *glc-1* locus, SNVs on Chromosome between 16,181,000 and 16,222,000 were used. All SNVs were used to construct the whole genome strain tree.

Fitness Assays:

Competition experiments consisted of three boom-bust cycles. During the boom phase, population growth led to rapid depletion of food, initiating the bust phase, which lasted for two days. Simple lawn competition experiments were conducted on 100 mm NGM agar plates with a single lawn formed from 800 µl OP50. Patchy lawn competition experiments were conducted on 150 mm NGM agar plates with a 200 µl OP50 central lawn surrounded by 15 small 40 µl lawns (Figure 2.5A).

Populations were initiated from 20 N2-type and 20 *roam-1*$_{MY14}$-type age-synchronized young adult animals. The initial population depleted food within 4 days, and on day 6 animals were washed into M9 media, 20% of the suspension was transferred to a new plate, and the remainder was lysed for quantitative DNA analysis. For the second and third boom bust cycle, food resources were depleted in 2 days and the plates were kept starved for 2 additional days. Following the second bust phase 20% of the animals were transferred to a new plate, and following the third bust phase the entire population was harvested for DNA extraction.

References

1. Feuda, R., Hamilton, S. C., McInerney, J. O. & Pisani, D. Metazoan opsin evolution reveals a simple route to animal vision. *Proc. Natl. Acad. Sci. U.S.A.* **109,** 18868–18872 (2012).

2. Bargmann, C. I. Comparative chemosensation from receptors to ecology. *Nature* **444,** 295–301 (2006).

3. Nei, M., Niimura, Y. & Nozawa, M. The evolution of animal chemosensory receptor gene repertoires: roles of chance and necessity. *Nat. Rev. Genet.* **9,** 951–963 (2008).

4. Greer, P. L. *et al.* A Family of non-GPCR Chemosensors Defines an Alternative Logic for Mammalian Olfaction. *Cell* (2016). doi:10.1016/j.cell.2016.05.001

5. Gray, J. M. *et al.* Oxygen sensation and social feeding mediated by a C. elegans guanylate cyclase homologue. *Nature* **430,** 317–322 (2004).

6. Troemel, E. R., Chou, J. H., Dwyer, N. D., Colbert, H. A. & Bargmann, C. I. Divergent seven transmembrane receptors are candidate chemosensory receptors in C. elegans. *Cell* **83,** 207–218 (1995).

7. Colosimo, M. E. *et al.* Identification of thermosensory and olfactory neuron-specific genes via expression profiling of single neuron types. *Curr. Biol.* **14,** 2245–2251 (2004).

8. McCarroll, S. A., Li, H. & Bargmann, C. I. Identification of transcriptional regulatory elements in chemosensory receptor genes by probabilistic segmentation. *Curr. Biol.* **15,** 347–352 (2005).

9. Chen, N. *et al.* Identification of a nematode chemosensory gene family. *Proc. Natl. Acad. Sci. U.S.A.* **102,** 146–151 (2005).

10. Rozengurt, E. & Sternini, C. Taste receptor signaling in the mammalian gut. *Curr Opin Pharmacol* **7,** 557–562 (2007).

11. Niimura, Y. & Nei, M. Comparative evolutionary analysis of olfactory receptor

gene clusters between humans and mice. *Gene* **346,** 13–21 (2005).

12. Liman, E. R. & Innan, H. Relaxed selective pressure on an essential component of pheromone transduction in primate evolution. *Proc. Natl. Acad. Sci. U.S.A.* **100,** 3328–3332 (2003).

13. Laska, M., Seibt, A. & Weber, A. 'Microsmatic' primates revisited: olfactory sensitivity in the squirrel monkey. *Chem. Senses* **25,** 47–53 (2000).

14. Freitag, J., Ludwig, G., Andreini, I., Rössler, P. & Breer, H. Olfactory receptors in aquatic and terrestrial vertebrates. *J. Comp. Physiol. A* **183,** 635–650 (1998).

15. Feng, P., Zheng, J., Rossiter, S. J., Wang, D. & Zhao, H. Massive losses of taste receptor genes in toothed and baleen whales. *Genome Biol Evol* **6,** 1254–1265 (2014).

16. Kishida, T., Kubota, S., Shirayama, Y. & Fukami, H. The olfactory receptor gene repertoires in secondary-adapted marine vertebrates: evidence for reduction of the functional proportions in cetaceans. *Biol. Lett.* **3,** 428–430 (2007).

17. McGowen, M. R., Clark, C. & Gatesy, J. The vestigial olfactory receptor subgenome of odontocete whales: phylogenetic congruence between gene-tree reconciliation and supermatrix methods. *Syst. Biol.* **57,** 574–590 (2008).

18. Niimura, Y. & Nei, M. Extensive gains and losses of olfactory receptor genes in mammalian evolution. *PLoS ONE* **2,** e708 (2007).

19. Pettigrew, J. D. Electroreception in monotremes. *J. Exp. Biol.* **202,** 1447–1454 (1999).

20. Thomas, J. H. & Robertson, H. M. The Caenorhabditis chemoreceptor gene families. *BMC Biol.* **6,** 42 (2008).

21. Stewart, M. K., Clark, N. L., Merrihew, G., Galloway, E. M. & Thomas, J. H. High genetic diversity in the chemoreceptor superfamily of Caenorhabditis elegans. *Genetics* **169,** 1985–1996 (2005).

22. Robertson, H. M. & Thomas, J. H. The putative chemoreceptor families of C. elegans. *WormBook* 1–12 (2006). doi:10.1895/wormbook.1.66.1

23. Beauchamp, G. K., Maller, O. & Rogers, J. G. Flavor preferences in cats (Felis catus and Panthera sp.). *Journal of Comparative and Physiological Psychology* **91,** 1118–1127 (1977).

24. Li, X. *et al.* Pseudogenization of a sweet-receptor gene accounts for cats' indifference toward sugar. *PLoS Genet.* **1,** 27–35 (2005).

25. Jiang, P. *et al.* Major taste loss in carnivorous mammals. *Proc. Natl. Acad. Sci. U.S.A.* **109,** 4956–4961 (2012).

26. Zhao, H. *et al.* Evolution of the sweet taste receptor gene Tas1r2 in bats. *Mol. Biol. Evol.* **27,** 2642–2650 (2010).

27. Zhao, H., Xu, D., Zhang, S. & Zhang, J. Genomic and genetic evidence for the loss of umami taste in bats. *Genome Biol Evol* **4,** 73–79 (2012).

28. Zhao, H., Yang, J.-R., Xu, H. & Zhang, J. Pseudogenization of the umami taste receptor gene Tas1r1 in the giant panda coincided with its dietary switch to bamboo. *Mol. Biol. Evol.* **27,** 2669–2673 (2010).

29. Zhao, H., Li, J. & Zhang, J. Molecular evidence for the loss of three basic tastes in penguins. *Current Biology* **25,** R141–R142 (2015).

30. Baldwin, M. W. *et al.* Sensory biology. Evolution of sweet taste perception in hummingbirds by transformation of the ancestral umami receptor. *Science* **345,** 929–933 (2014).

31. Shi, P. & Zhang, J. Contrasting modes of evolution between vertebrate sweet/umami receptor genes and bitter receptor genes. *Mol. Biol. Evol.* **23,** 292–300 (2006).

32. Ganchrow, J. R., Steiner, J. E. & Bartana, A. Behavioral reactions to gustatory stimuli in young chicks (Gallus gallus domesticus). *Developmental*

Psychobiology **23,** 103–117 (1990).

33. FISHER, R. A., FORD, E. B. & HUXLEY, J. Taste-testing the Anthropoid Apes. *Nature* **144,** 750–750 (1939).

34. Wooding, S. *et al.* Independent evolution of bitter-taste sensitivity in humans and chimpanzees. *Nature* **440,** 930–934 (2006).

35. Gilad, Y., Bustamante, C. D., Lancet, D. & Pääbo, S. Natural Selection on the Olfactory Receptor Gene Family in Humans and Chimpanzees. *The American Journal of Human Genetics* **73,** 489–501 (2003).

36. Wooding, S. *et al.* Natural selection and molecular evolution in PTC, a bitter-taste receptor gene. *Am. J. Hum. Genet.* **74,** 637–646 (2004).

37. Drewnowski, A. & Rock, C. L. The influence of genetic taste markers on food acceptance. *Am. J. Clin. Nutr.* **62,** 506–511 (1995).

38. Barrett, R. D. H. & Hoekstra, H. E. Molecular spandrels: tests of adaptation at the genetic level. *Nat. Rev. Genet.* **12,** 767–780 (2011).

39. Gould, S. J. & Lewontin, R. C. The spandrels of San Marco and the Panglossian paradigm: a critique of the adaptationist programme. *Proc. R. Soc. Lond., B, Biol. Sci.* **205,** 581–598 (1979).

40. Gracheva, E. O. *et al.* Molecular basis of infrared detection by snakes. *Nature* **464,** 1006–1011 (2010).

41. Kang, K. Exceptionally high thermal sensitivity of rattlesnake TRPA1 correlates with peak current amplitude. *Biochim. Biophys. Acta* **1858,** 318–325 (2016).

42. Gracheva, E. O. *et al.* Ganglion-specific splicing of TRPV1 underlies infrared sensation in vampire bats. *Nature* **476,** 88–91 (2011).

43. McGrath, P. T. *et al.* Parallel evolution of domesticated Caenorhabditis species targets pheromone receptor genes. *Nature* **477,** 321–325 (2011).

44. McGrath, P. T. *et al.* Quantitative mapping of a digenic behavioral trait implicates

globin variation in C. elegans sensory behaviors. *Neuron* **61,** 692–699 (2009).

45. Chang, A. J., Chronis, N., Karow, D. S., Marletta, M. A. & Bargmann, C. I. A distributed chemosensory circuit for oxygen preference in C. elegans. *PLoS Biol.* **4,** e274 (2006).

46. de Bono, M. & Bargmann, C. I. Natural variation in a neuropeptide Y receptor homolog modifies social behavior and food response in C. elegans. *Cell* **94,** 679–689 (1998).

47. Bendesky, A., Tsunozaki, M., Rockman, M. V., Kruglyak, L. & Bargmann, C. I. Catecholamine receptor polymorphisms affect decision-making in C. elegans. *Nature* **472,** 313–318 (2011).

48. Bargmann, C. I. Chemosensation in C. elegans. *WormBook* 1–29 (2006). doi:10.1895/wormbook.1.123.1

49. Sengupta, P., Chou, J. H. & Bargmann, C. I. odr-10 encodes a seven transmembrane domain olfactory receptor required for responses to the odorant diacetyl. *Cell* **84,** 899–909 (1996).

50. Robertson, H. M. Two large families of chemoreceptor genes in the nematodes Caenorhabditis elegans and Caenorhabditis briggsae reveal extensive gene duplication, diversification, movement, and intron loss. *Genome Res.* **8,** 449–463 (1998).

51. Robertson, H. M. Updating the str and srj (stl) families of chemoreceptors in Caenorhabditis nematodes reveals frequent gene movement within and between chromosomes. *Chem. Senses* **26,** 151–159 (2001).

52. Robertson, H. M. The large srh family of chemoreceptor genes in Caenorhabditis nematodes reveals processes of genome evolution involving large duplications and deletions and intron gains and losses. *Genome Res.* **10,** 192–203 (2000).

53. Thomas, J. H., Kelley, J. L., Robertson, H. M., Ly, K. & Swanson, W. J. Adaptive evolution in the SRZ chemoreceptor families of Caenorhabditis elegans and Caenorhabditis briggsae. *Proceedings of the National Academy of Sciences* **102,** 4476–4481 (2005).

54. Thomas, J. H. Analysis of homologous gene clusters in Caenorhabditis elegans reveals striking regional cluster domains. *Genetics* **172,** 127–143 (2006).

55. Silbering, A. F. & Benton, R. Ionotropic and metabotropic mechanisms in chemoreception: 'chance or design'? *EMBO Rep.* **11,** 173–179 (2010).

56. Barnes, T. M., Kohara, Y., Coulson, A. & Hekimi, S. Meiotic recombination, noncoding DNA and genomic organization in Caenorhabditis elegans. *Genetics* **141,** 159–179 (1995).

57. Katju, V. & Lynch, M. The structure and early evolution of recently arisen gene duplicates in the Caenorhabditis elegans genome. *Genetics* **165,** 1793–1803 (2003).

58. Rane, H. S., Smith, J. M., Bergthorsson, U. & Katju, V. Gene conversion and DNA sequence polymorphism in the sex-determination gene fog-2 and its paralog ftr-1 in Caenorhabditis elegans. *Mol. Biol. Evol.* **27,** 1561–1569 (2010).

59. Miller, M. A., Cutter, A. D., Yamamoto, I., Ward, S. & Greenstein, D. Clustered organization of reproductive genes in the C. elegans genome. *Curr. Biol.* **14,** 1284–1290 (2004).

60. Bargmann, C. I., Thomas, J. H. & Horvitz, H. R. Chemosensory cell function in the behavior and development of Caenorhabditis elegans. *Cold Spring Harb. Symp. Quant. Biol.* **55,** 529–538 (1990).

61. Hilliard, M. A., Bargmann, C. I. & Bazzicalupo, P. C. elegans responds to chemical repellents by integrating sensory inputs from the head and the tail. *Curr. Biol.* **12,** 730–734 (2002).

62. Hilliard, M. A., Bergamasco, C., Arbucci, S., Plasterk, R. H. A. & Bazzicalupo, P. Worms taste bitter: ASH neurons, QUI-1, GPA-3 and ODR-3 mediate quinine avoidance in Caenorhabditis elegans. *EMBO J.* **23,** 1101–1111 (2004).

63. Kaplan, J. M. & Horvitz, H. R. A dual mechanosensory and chemosensory neuron in Caenorhabditis elegans. *Proceedings of the National Academy of Sciences* **90,** 2227–2231 (1993).

64. Sambongi, Y. *et al.* Sensing of cadmium and copper ions by externally exposed ADL, ASE, and ASH neurons elicits avoidance response in Caenorhabditis elegans. *Neuroreport* **10,** 753–757 (1999).

65. Hilliard, M. A. *et al.* In vivo imaging of C. elegans ASH neurons: cellular response and adaptation to chemical repellents. *EMBO J.* **24,** 63–72 (2005).

66. de Bono, M., Tobin, D. M., Davis, M. W., Avery, L. & Bargmann, C. I. Social feeding in Caenorhabditis elegans is induced by neurons that detect aversive stimuli. *Nature* **419,** 899–903 (2002).

67. Smith, J. M. The theory of games and the evolution of animal conflicts. *J. Theor. Biol.* **47,** 209–221 (1974).

68. Dugatkin, L. A. & Reeve, H. K. *Game Theory and Animal Behavior*. (Oxford University Press, 1998).

69. Sokolowski, M. B. Foraging strategies of Drosophila melanogaster: a chromosomal analysis. *Behav. Genet.* **10,** 291–302 (1980).

70. Sokolowski, M. B., Pereira, H. S. & Hughes, K. Evolution of foraging behavior in Drosophila by density-dependent selection. *Proc. Natl. Acad. Sci. U.S.A.* **94,** 7373–7377 (1997).

71. You, Y.-J., Kim, J., Raizen, D. M. & Avery, L. Insulin, cGMP, and TGF-beta signals regulate food intake and quiescence in C. elegans: a model for satiety. *Cell Metab.* **7,** 249–257 (2008).

72. Fitzpatrick, M. J., Feder, E., Rowe, L. & Sokolowski, M. B. Maintaining a behaviour polymorphism by frequency-dependent selection on a single gene. *Nature* **447,** 210–212 (2007).

73. Fujiwara, M., Sengupta, P. & McIntire, S. L. Regulation of body size and behavioral state of C. elegans by sensory perception and the EGL-4 cGMP-dependent protein kinase. *Neuron* **36,** 1091–1102 (2002).

74. Ben Arous, J., Laffont, S. & Chatenay, D. Molecular and sensory basis of a food related two-state behavior in C. elegans. **4,** e7584 (2009).

75. Flavell, S. W. *et al.* Serotonin and the neuropeptide PDF initiate and extend opposing behavioral states in C. elegans. *Cell* **154,** 1023–1035 (2013).

76. Jeong, P.-Y. *et al.* Chemical structure and biological activity of the Caenorhabditis elegans dauer-inducing pheromone. *Nature* **433,** 541–545 (2005).

77. Srinivasan, J. *et al.* A modular library of small molecule signals regulates social behaviors in Caenorhabditis elegans. *PLoS Biol.* **10,** e1001237 (2012).

78. Macosko, E. Z. *et al.* A hub-and-spoke circuit drives pheromone attraction and social behaviour in C. elegans. *Nature* **458,** 1171–1175 (2009).

79. Kim, K. *et al.* Two chemoreceptors mediate developmental effects of dauer pheromone in C. elegans. *Science* **326,** 994–998 (2009).

80. Park, D. *et al.* Interaction of structure-specific and promiscuous G-protein-coupled receptors mediates small-molecule signaling in Caenorhabditis elegans. *Proc. Natl. Acad. Sci. U.S.A.* **109,** 9917–9922 (2012).

81. Greenberg, A. J., Moran, J. R., Coyne, J. A. & Wu, C.-I. Ecological adaptation during incipient speciation revealed by precise gene replacement. *Science* **302,** 1754–1757 (2003).

82. Andolfatto, P. *et al.* Multiplexed shotgun genotyping for rapid and efficient

genetic mapping. *Genome Res.* **21,** 610–617 (2011).

83. Schackwitz, W. S., Inoue, T. & Thomas, J. H. Chemosensory neurons function in parallel to mediate a pheromone response in C. elegans. *Neuron* **17,** 719–728 (1996).

84. Ren, P. *et al.* Control of C. elegans larval development by neuronal expression of a TGF-beta homolog. *Science* **274,** 1389–1391 (1996).

85. Akerboom, J. *et al.* Optimization of a GCaMP calcium indicator for neural activity imaging. *J. Neurosci.* **32,** 13819–13840 (2012).

86. Thompson, O. *et al.* The million mutation project: a new approach to genetics in Caenorhabditis elegans. *Genome Res.* **23,** 1749–1762 (2013).

87. Thompson, O. A. *et al.* Remarkably Divergent Regions Punctuate the Genome Assembly of the Caenorhabditis elegans Hawaiian Strain CB4856. *Genetics* **200,** 975–989 (2015).

88. Srinivasan, J. *et al.* A blend of small molecules regulates both mating and development in Caenorhabditis elegans. *Nature* **454,** 1115–1118 (2008).

89. Edison, A. S. Caenorhabditis elegans pheromones regulate multiple complex behaviors. *Curr. Opin. Neurobiol.* **19,** 378–388 (2009).

90. Félix, M.-A. & Duveau, F. Population dynamics and habitat sharing of natural populations of Caenorhabditis elegans and C. briggsae. *BMC Biol.* **10,** 59 (2012).

91. Yamada, K. *et al.* Olfactory plasticity is regulated by pheromonal signaling in Caenorhabditis elegans. *Science* **329,** 1647–1650 (2010).

92. Zhang, X. *et al.* Acyl-CoA oxidase complexes control the chemical message produced by Caenorhabditis elegans. *Proc. Natl. Acad. Sci. U.S.A.* **112,** 3955–3960 (2015).

93. Artyukhin, A. B. *et al.* Succinylated octopamine ascarosides and a new pathway

of biogenic amine metabolism in Caenorhabditis elegans. *J. Biol. Chem.* **288,** 18778–18783 (2013).

94. Seidel, H. S., Rockman, M. V. & Kruglyak, L. Widespread genetic incompatibility in C. elegans maintained by balancing selection. *Science* **319,** 589–594 (2008).

95. Charlesworth, D. Balancing selection and its effects on sequences in nearby genome regions. *PLoS Genet.* **2,** e64 (2006).

96. Ghosh, R., Andersen, E. C., Shapiro, J. A., Gerke, J. P. & Kruglyak, L. Natural variation in a chloride channel subunit confers avermectin resistance in C. elegans. *Science* **335,** 574–578 (2012).

97. Bendesky, A. & Bargmann, C. I. Genetic contributions to behavioural diversity at the gene-environment interface. *Nat. Rev. Genet.* **12,** 809–820 (2011).

98. Kendler, K. S. *et al.* Stressful life events, genetic liability, and onset of an episode of major depression in women. *Am J Psychiatry* **152,** 833–842 (1995).

99. Miller, M. B. & Bassler, B. L. Quorum sensing in bacteria. *Annu. Rev. Microbiol.* **55,** 165–199 (2001).

100. Izrayelit, Y. *et al.* Targeted Metabolomics Reveals a Male Pheromone and Sex-Specific Ascaroside Biosynthesis in Caenorhabditis elegans. *ACS Chemical Biology* **7,** 1321–1325 (2012).

101. Kaplan, F. *et al.* Ascaroside Expression in Caenorhabditis elegans Is Strongly Dependent on Diet and Developmental Stage. *PLoS ONE* **6,** e17804 (2011).

102. Greenspan, R. J. Selection, gene interaction, and flexible gene networks. *Cold Spring Harb. Symp. Quant. Biol.* **74,** 131–138 (2009).

103. Li, W., Kennedy, S. G. & Ruvkun, G. daf-28 encodes a C. elegans insulin superfamily member that is regulated by environmental cues and acts in the DAF-2 signaling pathway. *Genes Dev.* **17,** 844–858 (2003).

104. Sokolowski, M. B. Social interactions in ‘simple’ model systems. *Neuron* **65,**

780–794 (2010).

105. White, J. G., Southgate, E., Thomson, J. N. & Brenner, S. The structure of the nervous system of the nematode Caenorhabditis elegans. *Philos. Trans. R. Soc. Lond., B, Biol. Sci.* **314,** 1–340 (1986).

106. Rose, J. K., Sangha, S., Rai, S., Norman, K. R. & Rankin, C. H. Decreased sensory stimulation reduces behavioral responding, retards development, and alters neuronal connectivity in Caenorhabditis elegans. *J. Neurosci.* **25,** 7159–7168 (2005).

107. Ludewig, A. H. & Schroeder, F. C. Ascaroside signaling in C. elegans. *WormBook* 1–22 (2013). doi:10.1895/wormbook.1.155.1

108. McIntire, S. L., Reimer, R. J., Schuske, K., Edwards, R. H. & Jorgensen, E. M. Identification and characterization of the vesicular GABA transporter. *Nature* **389,** 870–876 (1997).

109. McIntire, S. L., Jorgensen, E. & Horvitz, H. R. Genes required for GABA function in Caenorhabditis elegans. *Nature* **364,** 334–337 (1993).

110. Sagné, C. *et al.* Cloning of a functional vesicular GABA and glycine transporter by screening of genome databases. *FEBS Lett.* **417,** 177–183 (1997).

111. Schuske, K., Palfreyman, M. T., Watanabe, S. & Jorgensen, E. M. UNC-46 is required for trafficking of the vesicular GABA transporter. *Nat. Neurosci.* **10,** 846–853 (2007).

112. Jorgensen, E. M. GABA. *WormBook* 1–13 (2005). doi:10.1895/wormbook.1.14.1

113. McIntire, S. L., Jorgensen, E., Kaplan, J. & Horvitz, H. R. The GABAergic nervous system of Caenorhabditis elegans. *Nature* **364,** 337–341 (1993).

114. Jin, Y., Hoskins, R. & Horvitz, H. R. Control of type-D GABAergic neuron differentiation by C. elegans UNC-30 homeodomain protein. *Nature* **372,** 780–783 (1994).

115. Eastman, C., Horvitz, H. R. & Jin, Y. Coordinated transcriptional regulation of the unc-25 glutamic acid decarboxylase and the unc-47 GABA vesicular transporter by the Caenorhabditis elegans UNC-30 homeodomain protein. *J. Neurosci.* **19,** 6225–6234 (1999).

116. Ringstad, N., Abe, N. & Horvitz, H. R. Ligand-gated chloride channels are receptors for biogenic amines in C. elegans. *Science* **325,** 96–100 (2009).

117. Feng, X.-P., Hayashi, J., Beech, R. N. & Prichard, R. K. Study of the nematode putative GABA type-A receptor subunits: evidence for modulation by ivermectin. *J. Neurochem.* **83,** 870–878 (2002).

118. Beg, A. A. & Jorgensen, E. M. EXP-1 is an excitatory GABA-gated cation channel. *Nat. Neurosci.* **6,** 1145–1152 (2003).

119. Jobson, M. A. *et al.* Spillover transmission is mediated by the excitatory GABA receptor LGC-35 in C. elegans. *J. Neurosci.* **35,** 2803–2816 (2015).

120. Dittman, J. S. & Kaplan, J. M. Behavioral impact of neurotransmitter-activated G-protein-coupled receptors: muscarinic and GABAB receptors regulate Caenorhabditis elegans locomotion. *J. Neurosci.* **28,** 7104–7112 (2008).

121. Schultheis, C., Brauner, M., Liewald, J. F. & Gottschalk, A. Optogenetic analysis of GABAB receptor signaling in Caenorhabditis elegans motor neurons. *J. Neurophysiol.* **106,** 817–827 (2011).

122. Bendesky, A. *et al.* Long-range regulatory polymorphisms affecting a GABA receptor constitute a quantitative trait locus (QTL) for social behavior in Caenorhabditis elegans. *PLoS Genet.* **8,** e1003157 (2012).

123. Mahanti, P. *et al.* Comparative metabolomics reveals endogenous ligands of DAF-12, a nuclear hormone receptor, regulating C. elegans development and lifespan. *Cell Metab.* **19,** 73–83 (2014).

124. Murphy, C. T. & Hu, P. J. Insulin/insulin-like growth factor signaling in C.

elegans. *WormBook* 1–43 (2013). doi:10.1895/wormbook.1.164.1

125. Gumienny, T. L. & Savage-Dunn, C. TGF-β signaling in C. elegans. *WormBook* 1–34 (2013). doi:10.1895/wormbook.1.22.2

126. Wang, H. *et al.* Neuropeptide secreted from a pacemaker activates neurons to control a rhythmic behavior. *Curr. Biol.* **23,** 746–754 (2013).

127. Sulston, J. E. & Brenner, S. The DNA of Caenorhabditis elegans. *Genetics* **77,** 95–104 (1974).

128. Arribere, J. A. *et al.* Efficient marker-free recovery of custom genetic modifications with CRISPR/Cas9 in Caenorhabditis elegans. *Genetics* **198,** 837–846 (2014).

129. Li, H. & Durbin, R. Fast and accurate long-read alignment with Burrows-Wheeler transform. *Bioinformatics* **26,** 589–595 (2010).

130. Larsch, J., Ventimiglia, D., Bargmann, C. I. & Albrecht, D. R. High-throughput imaging of neuronal activity in Caenorhabditis elegans. *Proc. Natl. Acad. Sci. U.S.A.* **110,** E4266–73 (2013).